TRANSVERSAL FILTER DESIGN AND APPLICATION IN SATELLITE COMMUNICATIONS

Remigio de Cristofaro

A Thesis

in

The Department

of

Electrical Engineering

Presented in Partial Fulfillment of the Requirement
for the degree of Master of Engineering at
Concordia University
Montréal, Québec, Canada

April, 1976

ABSTRACT

R. DE CRISTOFARO

TRANSVERSAL FILTER DESIGN AND
APPLICATION IN SATELLITE COMMUNICATIONS

In narrow-band digital communications systems, it is essential to generate precisely shaped pulses in order to avoid intersymbol interference. This can be accomplished by the use of filters satisfying Nyquist criterions. However, current Nyquist type analog filters are difficult to synthesise and to implement. An alternative solution to this problem found in a class of Transversal Filters (TF's) called Binary Transversal Filters (BTF's) is the subject of this thesis.

Simulation studies on the BTF's energy ratio performance, discrete eye diagram, power spectrum density and filter's coefficient sensitivity are employed to demonstrate the practicality and limitations of such filters. The increase in energy ratio performance of a BTF followed by an analog low pass filter is also evaluated.

The design and evaluation of a BTF for the Single Channel per Carrier pre-modulation filter is undertaken. The BTF constructed consisted of COS/MOS shift registers, a-weighting resistors network and a summing amplifier. The practical results are shown to compare favourable with the theoretical expectations.

ACKNOWLEDGEMENT

The author wishes to thank Dr. Kamilo Feher for having suggested such an interesting research subject and for his guidance during the preparation of this work.

He is especially endebted to Mr. Mark Heath for the careful revision of the English version. Many thanks to Miss Lucie Bastien for the typing and to Miss Michèle Tremblay for the drawings.

Finally he wishes to thank his wife for all her encouragement and patience during seemingly endless hours spent in the preparation of this report.

TABLE OF CONTENTS

LIST OF FIGURES

LIST OF TABLES

LIST OF SYMBOLS AND ABBREVIATIONS

$A(\omega)$	Real part of $H(\omega)$
BER	Bit Error Rate
BM	Measured Noise Bandwidth
$B(\omega)$	Imaginary part of $H(\omega)$
br	Bit Rate
BTF	Binary Transversal Filter
c(i)	ith BTF or TF coefficients
D	Time delay between coefficients c(i)
DASS	Demand Assignment Singaling and Switching
e	Lease square discrete error
E	Least square continuous error
E_b	Energy per bit
E(h)	Energy above excess Nyquist frequency (ω_o)
$E(\infty)$	Total energy
E_w	Energy of the function w(t)
$E(\omega_o)$	Energy below excess Nyquist frequency (ω_o)
F{ }	Fourier Transform
f_c	Cut off frequency
FDM	Frequency Division Multiplex
f_N	Nyquist frequency
f_o	Excess Nyquist frequency
f_s	Signaling frequency or bit rate

$G(f)$	Power spectrum density function of a random binary signal
$G(\omega)$	Weighting function
$h(t)$	Network impulse response
$H(\omega)$	Network transfer function
HPF	High Pass Filter
ITF	Ideal Transversal Filter
j	$\sqrt{-1}$
K	Number of samples per baud interval (T)
L	Number of lobes in the BTF impulse response
LPF	Low Pass Filter
LPTI	Linear Passive Time Invariant
N	Noise Power
N_o	Noise Power density
NRZ	Non Return to Zero
N_t	Total number of coefficients c(i)
p	a priory probability
$p(t)$	rectangular pulse function
P(e)	Probability of error
PRBS	Pseudo Random Binary Sequence
Q	Positive definite Matrix
QPSK	Quarternary Phase Shift Keying
R_i	ith weighting resistor

$R(\omega)$	Magnitude of $H(\omega)$
RZ	Return to Zero
S	Signal power
SCPC	Single Channel Per Carrier
SPADE	Single channel per carrier Pulse code modulation multiple Access Demand assignment Equipment
T	Baud interval
TF	Transversal Filter
$w(t)$	Weighting function
$W(\omega)$	$F\{w(t)\}$
$\bar{X}$	Mean value of samples x_i
$y_i(t)$	Binary waveform function
$Y_i(f)$	$F\{y(t)\}$
z_i	$\exp\{j\omega D\}$
α	Excess Nyquist bandwidth
γ	f_c/f_N
$\delta(\cdot)$	Unit impulse function
λ	$E(\omega_o)/E(\infty) \equiv$ max. eigenvalue of Q matrix
σ	Standard deviation
$\phi(\omega)$	Phase of $H(\omega)$
ω	$2\pi f$
ω_p	Periodicity of the function $H(\omega) \equiv 2\pi/D$

CHAPTER 1

INTRODUCTION

1.1 Principle of Digital Communications

Binary Transversal Filters are a comparatively recent development in Transversal Filter theory. These filters can be more economically constructed for use in digital transmission systems than can their analog counterparts and, as a result, there exists much interest in their development. This thesis will carry out the design and implementation of a Binary Transversal Filter and will investigate the practicality of its use in digital transmission.

To begin our introduction to the Binary Transversal Filter, it is worthwhile to review some of the basic ideas governing the digital communication field. The three essential building blocks, required in establishing a communication system, are shown in figure 1.1.1.

Figure 1.1.1: Basic Communication Model

In digital communication, the information input to the first of these blocks (the transmitter) is represented by bits. This term is coined from the contraction of the words Binary and Digits and implies signals consisting of two levels only. Another term often encountered is the "Baud", which

represents the unit of signaling speed, or the number of symbols transmitted per second. If the format of the transmitted symbols is binary then bits and bauds are equivalent. At present, binary digits are generated by many types of equipment. The telegraph is the oldest one. The teletypewriter which encodes alphanumeric characters into bits, the digital computer with its peripherals and terminals, and analog signals encoded into bits by means of Pulse Code Modulation (PCM) or Delta Modulation are other binary sources.

The bits generated by the data sources are transformed by the transmitter into electrical waveforms which are more appropirate for transmission through the channel. The channel is the physical liaison interconnecting the receiver to the transmitter. It may consist of a simple pair of wires as in telephone circuits or coaxial cable, microwave radio links, satellite transponders and other sophisticated carrier systems. The channel distorts, attenuates and introduces various types of noise into the transmitted information. The receiver at the other end must reestablish the transmitted information from the output of this channel. Unfortunately, due to channel impairments, some of the received bits are unrecognizable, and errors are introduced.

In analog communications, there are many parameters which characterize the performance of a system, whereas in

digital communications the main decisional parameter is the Bit Error Rate (BER), or Probability of Error P(e).
This Bit Error Rate has been defined by the International Telecommunication Union [34] as the ratio of the number of bits incorrectly received to the total number of bits transmitted.

1.2 Power Spectrum Density of Random Binary Pulses and the Nyquist Filter.

In digital transmission systems, the data source generates random sequences of bits. Each bit, in synchronous communication, has a time slot of T-sec allocated for its transmission. A one is usually represented by a square pulse of amplitude A and duration t_p-sec while the absence of a pulse denotes a zero.

If the pulse of t_p-sec (Figure 1.2.1) is equal to the bit interval T-sec, then such signal is called Non Return to Zero (NRZ) [12, p. 27].

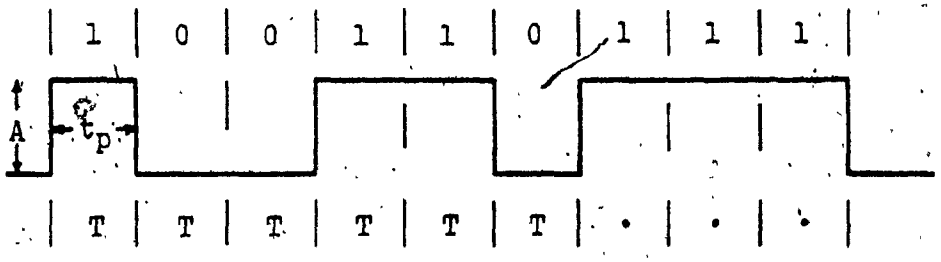

Figure 1.2.1 - Non Return to Zero Type Pulses

If the pulse duration t_p (Figure 1.2.2) is less than the bit interval T, then the signal is referred as Return to Zero (RZ) [12, p. 27].

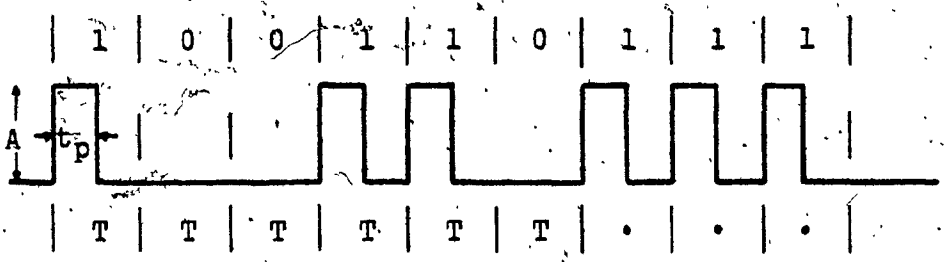

Figure 1.2.2 - Return to Zero Type Pulses

The duty factor or duration cycle of an RZ signal is defined [12] by the ratio of the pulse width (t_p) to the bit interval (T). Usually, RZ type pulses have a 50% duty cycle (figure 1.2.2).

The Power Spectrum Density of random sequences of RZ, NRZ and various other binary formats are given by W. R. Bennet [12, ch. 19]. In his study he has shown that the RZ pulses have a broader spectrum when compared with the NRZ ones, and require, for identical bit rates, a greater bandwidth. For this reason, they are seldom used in digital transmission, and they will not be considered here.

The Power Spectrum of the NRZ pulses given in [12] is:

$$G(f) = \frac{AT}{2}\left\{\frac{\sin(\pi fT)}{\pi fT}\right\}^2$$

where A and T are the pulse amplitude and the bit interval respectively.

Figure 1.2.3 represents on a logarithmic basis $\{10 \log_{10}(G(f)/G(0))\}$ the measured Power Spectrum of NRZ random signals. Unfortunately, we notice that, due to the relatively slowly decaying lobes of the function G(f), the bandwidth required to transmit such signals undistorted is still extended. However, by passing the NRZ data through a Nyquist Filter [12, Ch. 5] it is possible to reduce the required

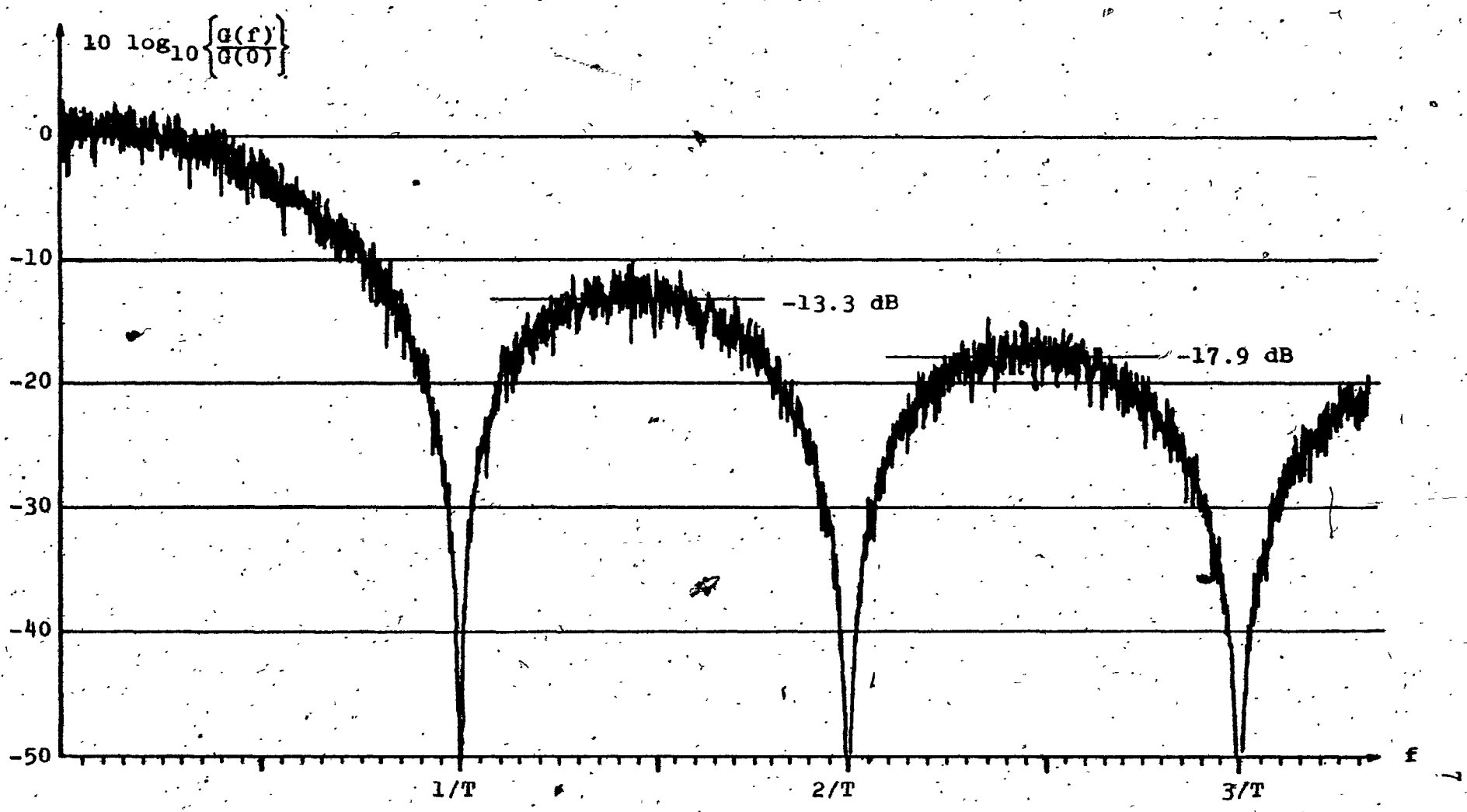

Figure 1.2.3: Measured Power Spectrum Density of random NRZ Binary data (T=1=60 kbps)

bandwidth to acceptable limits.

Fundamental to the understanding of the Nyquist Filter is the concept of intersymbol interference (ISI). Intersymbol interference is one of the possible system impairements due to the waveform distortion of the transmitted pulses. In this process, the pulses get dispersed in time, occupying more then a single time slot of T-sec. Depending on the degree of dispersion, the receiver may no longer distinguish some of the transmitted symbols and in consequence errors are introduced. An elementary digital receiver for a noiseless channel would consist essentially of a sampling device which would sample the incoming signal at regularly spaced intervals of T-sec. The intersymbol interference is a measure of the degradation in the amplitude of these received samples caused by the time dispersion of the other symbols. Nyquist has shown that a maximum of 1/T symbols per second can be transmitted through an ideal low pass filter having a cut off frequency of $(2T)^{-1}$ - Hz, without intersymbol interference. This frequency of $(2T)^{-1}$ - Hz is also known as Nyquist frequency abbreviated f_N. The transfer function of an ideal low pass filter is depicted in figure 1.2.4.

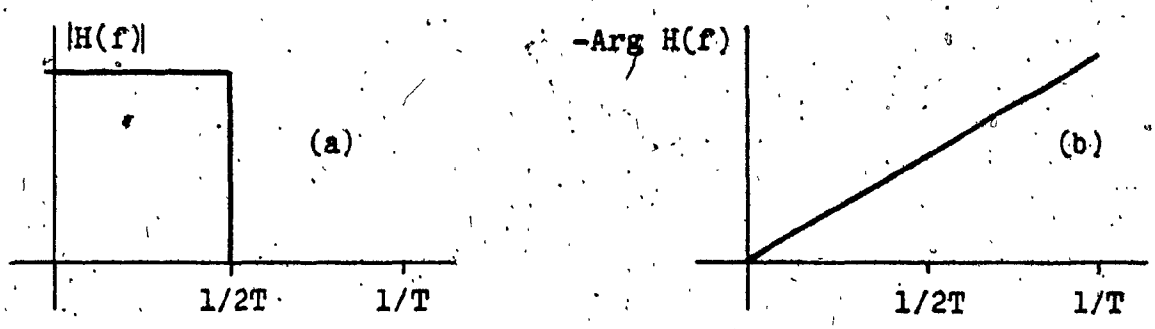

Figure 1.2.4 - Ideal Nyquist Filter; a - Attenuation, b - Phase

Unfortunately, due to amplitude discontinuities at $(2T)^{-1}$ - Hz [19, ch. 2], this filter is not realizable, but can only be approximated. However, by employing equivalent Nyquist Filters, the minimum ISI feature of ideal filters is retained.

Equivalent Nyquist filters have a gradual roll-off and are a combination of the Ideal Filter transfer function and a transfer function having an odd amplitude characteristic about $(2T)^{-1}$ - Hz. For this filter as for the Ideal Nyquist Filter, phase linearity exists. A class of Nyquist filters of this type, but relatively simple to approximate in practice, is the raised cosine filter. Its frequency characteristic is given by [25, ch. 4].

$$|H(f)| = \begin{cases} T & ; \quad 0 \le f \le \frac{1}{2T}(1-\alpha) \\ \frac{T}{2}\left\{1-\sin\left[\frac{\pi T}{\alpha}\left(f-\frac{1}{2T}\right)\right]\right\} & ; \quad \frac{1}{2T}(1-\alpha) \le f \le \frac{1}{2T}(1+\alpha) \end{cases}$$

where α represents the bandwidth used in excess of the theoretical minimum Nyquist Bandwidth, and T, the symbol interval.

Figure 1.2.5 represents the filter transfer function $|H(f)|$ and the associated impulse response.

Observing in figure 1.2.5-a, the filter's transfer function we notice that:

i) α lies between 0 and 1.

ii) The ideal Nyquist filter is represented by $\alpha=0$.

iii) As much as twice the Nyquist bandwidth is required for $\alpha=1$.

Since α represents the filter roll-off about the Nyquist frequency, it is common to express this parameter in percent. Thus 50% roll-off is equivalent to .5 excess Nyquist bandwidth, or $\alpha=.5$. Observing in figure 1.2.5-b - the filter impulse response - it is important to notice that, at the time origin, the waveform amplitude is maximum and, independently of the filter roll-off, the response crosses zero at regularly spaced T-sec intervals. As a result, no inter-symbol interference exists at these time instants.

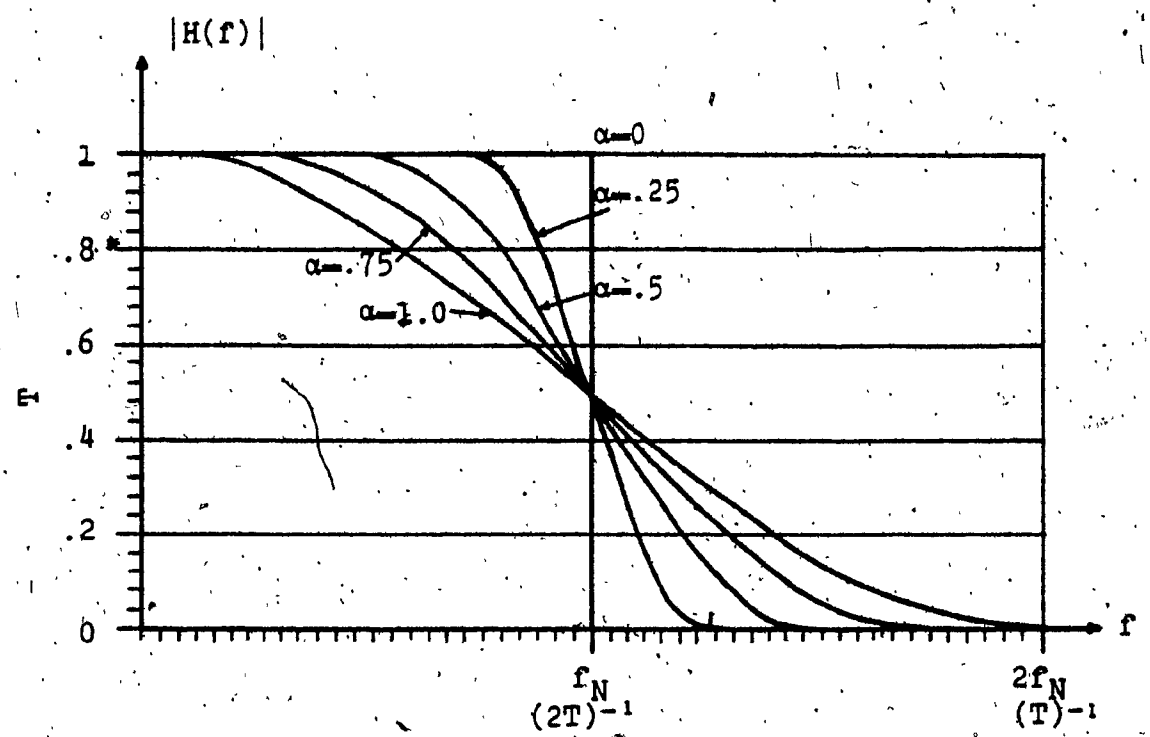

Fig. 1.2.5-a - Raised Cosine Filter Transfer function

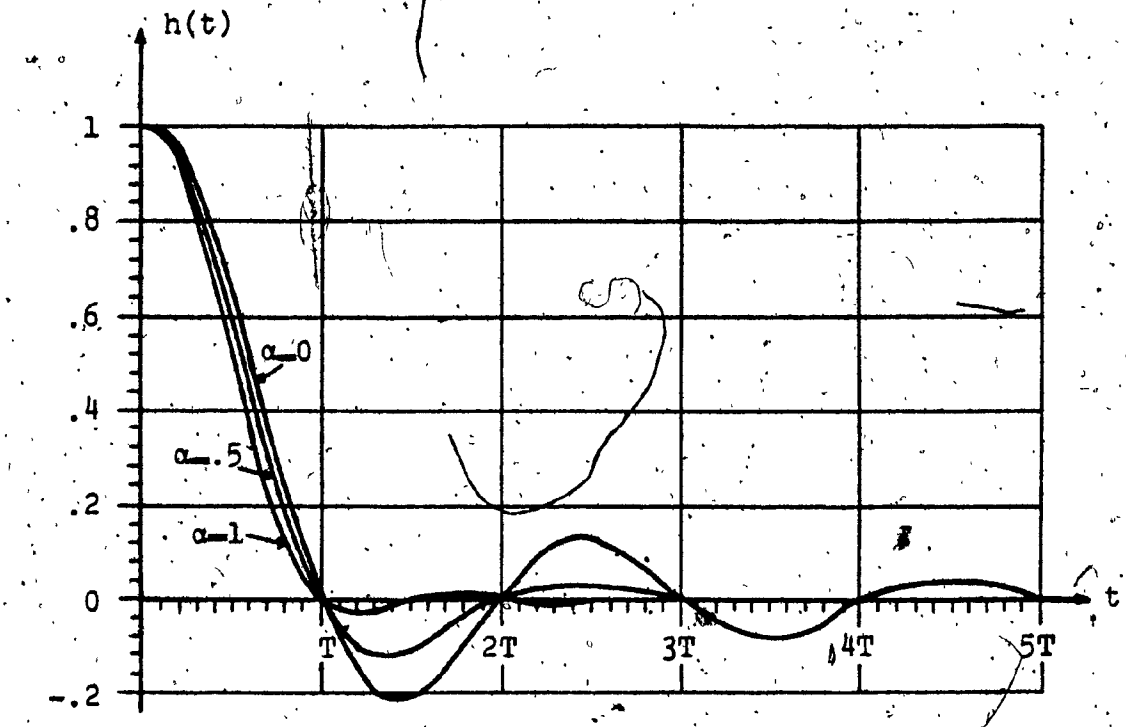

Fig. 1.2.5-b - Raised Cosine filter Impulse Response

1.3 Implementation of Equivalent Nyquist Filters

Previously, we have seen that the filter employed to band limit the spectrum of a binary signal should have an equivalent Nyquist type response in order to minimize the intersymbol interference. With presently known filter techniques, both passive and active analog and, more recently, Binary Transversal Filters are practical and economical Nyquist type filters which may be used in digital transmission systems. When we consider that, at present, filters alone might represent 30% of the total cost of communications equipment it is apparent that great savings can be realized by developing a filter which can achieve acceptable performance at a low cost. Transversal Filters appear to achieve this goal in digital communication systems.

Using conventional frequency domain synthesis techniques, it is possible to realize analog filters having excellent band limiting properties, but usually such filters are not appropriate for data transmission purposes due to their poor intersymbol interference performance. However, Spaulding [24] using 7th and 11th order filter transfer functions was able to achieve almost Nyquist pulses. In his development, the magnitude of the filter frequency response was approximated by carefully positioning the zeros of the network transfer function, while the transfer function poles were optimized with a computer to achieve almost Nyquist pulses. The final

filter was implemented by active filtering techniques and successful results were reported. This filter is however relatively costly.

The second filter's design choice, which is gaining wide popularity, utilizes a class of Transversal Filters (TF's) [2], [6], [19] called Binary Transversal Filters (BTF's) [1], [4], [8], [26]. The reasons for this popularity lie in the fact that BTF's can easily be implemented in practice without encountering stability problems [19]. This filter can be realized using mainly digital integrated circuits (Shift Registers), weighting resistors and a summing operational amplifier. Stability is assured as these filters do not have any feedback path - the main source of instabilities. In addition to these factors, the Binary Transversal Filter has the following advantages:

i) Because of the digital circuitry employed, they are usually self-adaptive to a wide range of data bit rates. Analog filters, by contrast, have optimum performances at a single data rate.

ii) BTF's in general, do not require element trimming, and in most situations standard 1% resistors are sufficient.

In fact, the only disadvantage of BTF's lies in the fact that they are limited to synchronous binary pulses, whereas analog filters can accept almost any sort of waveform.

When we consider all these advantages, we immediately conclude that Binary Transversal Filters are the best choice for application in binary data transmission.

The following chapters will investigate in detail by means of computer simulations and practical realization, the applicability of such filters when employed in digital transmission systems. To begin, the second chapter gives the Transversal Filter fundamentals and analyses two methods of Transversal Filter Synthesis.

Following this, in chapter three, Mueller's method of Transversal Filter synthesis [8] is reviewed in detail, this being the best method for data transmission. An analysis of the in to out of band energy ratio obtained using Mueller's coefficients and a simulated eye pattern of the signal at the output of the BTF are developed. In section 3.4- a study of the sensitivity of the energy ratio to changes in the coefficients is given and in section 3.5 the BTF power spectrum density is obtained by computer simulation. Finally, chapter 3 concludes with a study of the energy ratio performance of the BTF when followed by a simple low pass filter (LPF).

Chapter 4 begins with the design of a hybrid BTF - a BTF followed by a simple LPF - intended for use as a pre-modulation filter in the Single Channel per Carrier (SCPC) [28] system. A section of this chapter describes the test

results obtained from the Binary Transversal Filter.

The Binary Transversal Filter developed here was able to meet all SCPC specifications at a lower cost than analog type filters. RCA Limited intends to employ this filter in their SCPC thin route satellite communication systems.

CHAPTER 2

A SURVEY OF TRANSVERSAL FILTERS SYNTHESIS METHODS

2.1 Transversal Filter Fundamentals

This chapter will cover the principle of operation of the Transversal Filter and also the Fourier Series method of synthesis for such filters. The principle of operation described here was originally given by Leuthold [1] and his derivation is followed as it begins at the convolution integral - a tool which is extensively utilized in controls, networks and communication. Consider the linear passive time invariant network (LPTI) represented by fig. 2.1.1.

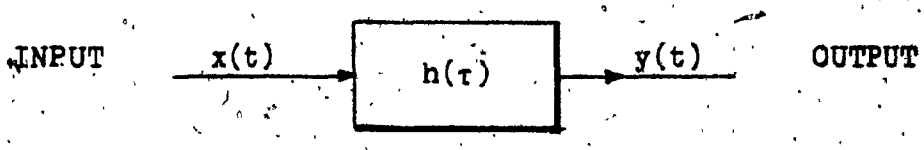

Figure 2.1.1–Linear Passive Time Invariant Network

In the time domain the output y(t) can be expressed in terms of the network input signal x(t) by means of the convolution integral [4, p. 440], given by:

$$y(t) = \int_{-\infty}^{\infty} h(\tau)\, x(t-\tau)\, d\tau \qquad (2.1.1)$$

where h(t) is the network impulse response.

An electrical network having a specified impulse response h(τ) can in most cases be synthetized using conventional techniques, i.e. active or passive filter design [7].

Equation 2.1.1 could be implemented directly in the time domain if it would be possible to realize the device

shown in figure 2.1.2.

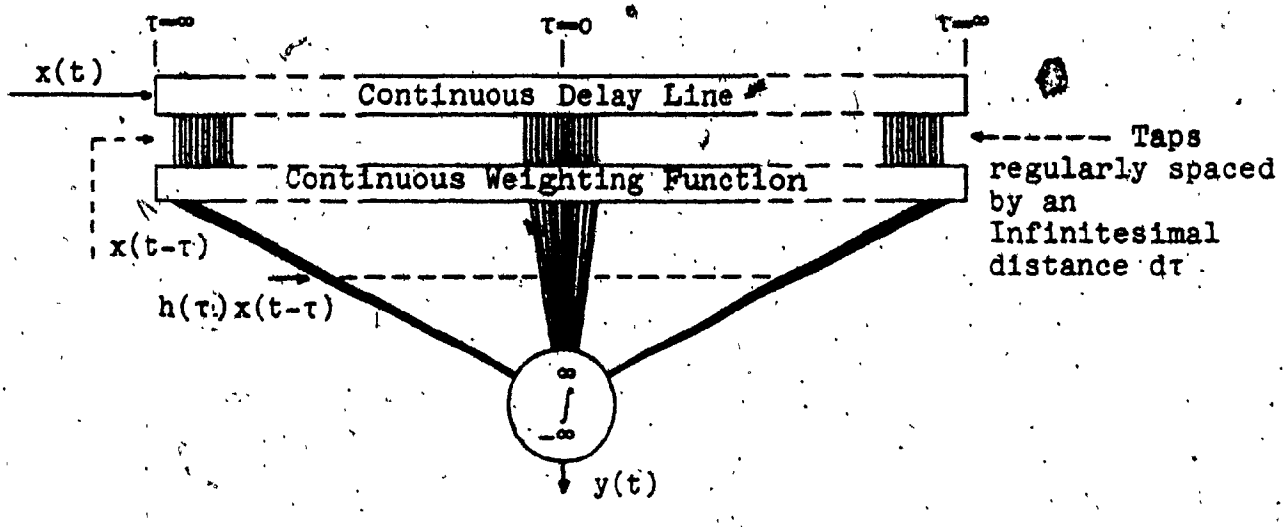

Figure 2.1.2-A model for the convolution integral

The input signal x(t) is delayed by a delay line infinite in length and continuously tapped. The delayed signal generated at the output of each hypothetical tap is multiplied by the weighting function h(τ). Finally, the output y(t) is obtained summing the delayed and weighted signals through the entire length of the line.

A device capable of performing such operation is called an Ideal Transversal Filter (ITF). The term Transversal Filter was introduced by H. E. Kallman in 1940 [6].

The major characteristic of the ITF is that the input signal x(t) propagates through the delaying device without being deformed, with the output y(t) being obtained by processing the signal x(t) in the sense "Transversal" to that of propagation. A conventional filter by constrast will distort the signal.

Practical TF are limited by two major restrictions:

i) The delay line is not infinite in length.

ii) Only past values of the input x(t) are known.

The consequences to these restrictions are:

i) The impulse response h(τ) has to be truncated at τ = ±a.

ii) A time delay "a" is present at the output y(t).

To clarify the consequence to the second restriction assume a truncated impulse response h(t) of the form:

$$h(t) = \text{sinc}(t) = \frac{\sin(t)}{t} \qquad \text{For } -a \leq t \leq a$$

$$h(t) = 0 \qquad \text{Elsewhere} \qquad (2.1.2)$$

Also assume that the network is excited by a Dirac type impulse δ(t). Replacing 2.1.2 into 2.1.1 and x(t) by δ(t), we obtain the output:

$$y(t) = \int_{-a}^{a} \frac{\sin(t)}{t} \cdot \delta(t-\tau)\, d\tau$$

By definition the impulse δ(t) exists only at t = 0. Hence, the maximum of y(t) is attained at t = 0, which implies that the leading tail of the function sinc(t) has preceeded the impulse δ(t) by a time interval "a".

If we now consider a real Transversal Filter, then the maximum of y(t) is reached at t = a indicating that the

output is delayed with respect to the input.

In order to represent these practical restrictions, equation 2.1.1 has been modified:

$$y(t) = \int_{-a}^{a} h(\tau)\, x(t'-\tau)\, d\tau \qquad t' = t-a \qquad (2.1.3)$$

However, equation 2.1.3 still cannot be realized in practice because it is difficult to obtain continuously tapped delay lines [10]. The practical model which best approximates the continuously tapped delay line is one tapped at fixed intervals "D". Using this concept the final structure of the TF is obtained and is shown in figure 2.1.3.

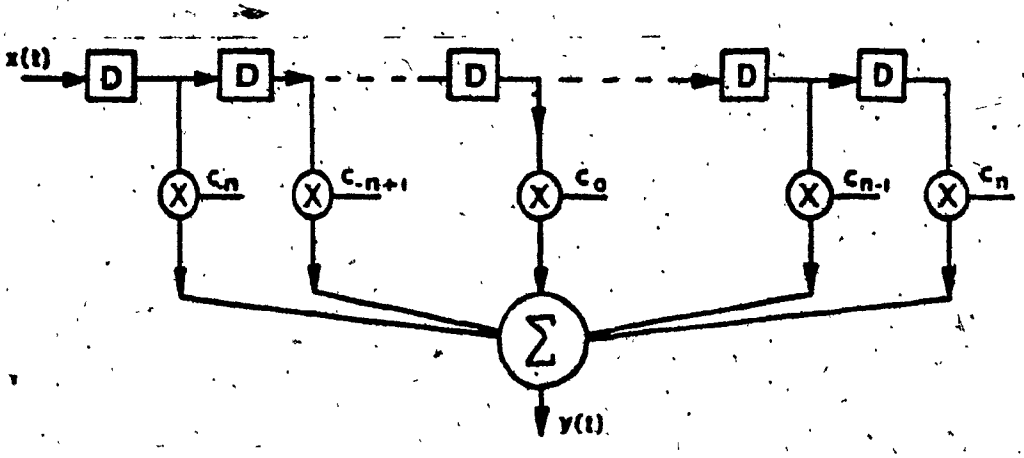

Figure 2.1.3-Transversal Filter Structure

Equation 2.1.3 is further modified to better represent the final structure of the TF, and the integral is replaced by a discrete sum:

$$y(t) = \sum_{i=-n}^{n} D\, h(iD)\, x(t'-iD), \qquad nD = a \qquad (2.1.4)$$

The replacement of the integral by a discrete sum introduces an additional error, inversely proportional to the total number of summation terms (2n+1). Since the impulse response is truncated at ±a, the error is also directly related to the delay D. An extensive study on this approximation error was given by Vaelcker [4].

Continuing with Leuthold's approach, the impulse response h(t) degenerates into a set of discrete weighting coefficients.

$$c_i = D\, h(iD) \qquad (2.1.5)$$

The final equation for the TF is obtained:

$$y(t) = \sum_{i=-n}^{n} c_i\, x(t'-iD) \qquad (2.1.6)$$

The impulse response of this filter is given by:

$$h(t) = \sum_{i=-n}^{n} c_i\, \delta(t'-iD) \qquad (2.1.7)$$

Substituting in 2.1.7 t' by t-a and taking the Fourier transform, the frequency response of the TF is obtained:

$$H(\omega) = e^{-j\omega a} \sum_{i=-n}^{n} c_i\, e^{-j\omega iD} \qquad (2.1.8a)$$

where $j = \sqrt{-1}$.

The term $e^{-j\omega a}$ represents a constant delay which can, in most cases, be compensated for at the receiver end. Hence, this term will be neglected in this study, therefore:

$$H(\omega) = \sum_{i=-n}^{n} c_i \, e^{-j\omega iD} \qquad (2.1.8b)$$

Splitting $H(\omega)$ into the real and imaginary parts, we obtain:

$$H(\omega) = A(\omega) + jB(\omega) \qquad (2.1.9)$$

Expanding $A(\omega)$ and $B(\omega)$ in Fourier series:

$$A(\omega) = a_0 + 2 \sum_{i=1}^{n} a_i \cos(i\omega D) \qquad (2.1.10)$$

$$B(\omega) = 2 \sum_{i=1}^{n} b_i \sin(i\omega D) \qquad (2.1.11)$$

Expanding equation 2.1.8b into a cosine and a sine series, rearranging the terms and then comparing with equations 2.1.10 and 2.1.11, it can be shown that the coefficients a_i and b_i are related to the coefficients c_i in the following manner:

$$\begin{aligned} c_i &= a_i - b_i \quad ; \quad a_i = \tfrac{1}{2}(c_{-i} + c_i) \\ c_{-i} &= a_i + b_i \quad ; \quad b_i = \tfrac{1}{2}(c_{-i} - c_i) \end{aligned} \qquad (2.1.12)$$

In general, the transfer function $H(\omega)$ is complex. It becomes real if the coefficients b_i are set to zero i.e., $c_{-i} = c_i$; or imaginary if the a_i's are set to zero i.e., $c_{-i} = -c_i$. In the first case the filter is said to have absolute linear phase because the only delay existent is introduced by the term $\exp(-j\omega a)$ which is linear with frequency. In the second case the real terms disappear and a frequency independent 90° phase shift is obtained.

Assuming that $A(\omega)$ and $B(\omega)$ are some given functions that we wish to approximate then, from equations 2.1.10, 2.1.11, and 2.1.12, it is not difficult to recognize that the coefficients a_i and b_i are the Fourier series coefficients of such functions.

$$a_i = \frac{2}{\omega_p} \int_0^{\omega_p/2} \tilde{A}(\omega) \cos(i\omega D)\, d\omega \qquad (2.1.13)$$

$$b_i = \frac{2}{\omega_p} \int_0^{\omega_p/2} \tilde{B}(\omega) \sin(i\omega D)\, d\omega \qquad (2.1.14)$$

ω_p is the periodicity of the function $H(\omega)$ and is given by the reciprocal of the time delay "D".

$$\omega_p = \frac{2\pi}{D} \qquad (2.1.15)$$

The functions $\tilde{A}(\omega)$ and $\tilde{B}(\omega)$ have to be specified in the interval $0 \le \omega \le \omega_p/2$. The Fourier sums $A(\omega)$ and $B(\omega)$ will converge to $\tilde{A}(\omega)$ and $\tilde{B}(\omega)$ respectively if these functions

satisfy the strong Dirichlet conditions [3, p. 687]. The method just described, also known as Fourier series method [2], is the simplest method for transversal filter synthesis.

The summary of this method is:

i) Split the specified function $\tilde{H}(\omega)$ into the real and imaginary parts $\tilde{A}(\omega)$ and $\tilde{B}(\omega)$.

ii) Using relations 2.1.13 and 2.1.14, obtain the coefficients a_i and b_i.

iii) Obtain the coefficients c_i by substituting a_i and b_i in 2.1.12.

2.2 The Least Squares Method of TF Synthesis

In the previous section, the fundamentals of transversal filters and the Fourier Series method of synthesis were studied. In this section, a method of TF synthesis proposed by A. Vincent Carrefour et. al. [5] is introduced. The TF coefficients "c_i" obtained using this method are such that the error "E" between the specified transfer function $\tilde{H}(\omega)$ and the actual filter transfer function $H(\omega)$ is minimum in the least square sense.

The error E is defined by:

$$E = E(c_{-n},\ldots,c_0,\ldots,c_n) = \int_0^{\omega_p/2} |\tilde{H}(\omega) - H(\omega)|^2 \, G(\omega) \, d\omega \qquad (2.2.1)$$

where $G(\omega)$ is the weighting function used in the least square technique.

This function is positive, even, and of the same periodicity as $\tilde{H}(\omega)$. We assume that g(t) - the inverse Fourier transform of $G(\omega)$ - exists. To simplify the mathematical derivations, the transfer function $H(\omega)$ will be expressed in the exponential form.

$$\tilde{H}(\omega) = \tilde{R}(\omega)\, e^{j\tilde{\phi}(\omega)} \tag{2.2.2}$$

where

$$\tilde{R}(\omega) = (\tilde{A}^2(\omega) + \tilde{B}^2(\omega))^{\frac{1}{2}} \tag{2.2.3}$$

and

$$\tilde{\phi}(\omega) = \tan^{-1}\left[\frac{\tilde{B}(\omega)}{\tilde{A}(\omega)}\right] \tag{2.2.4}$$

Returning to equation 2.2.1, this can be expanded into:

$$E = \int_0^{\omega_p/2} \{H(\omega)H^*(\omega)+H(\omega)\tilde{H}^*(\omega)-[\tilde{H}(\omega)H(\omega)+\tilde{H}^*(\omega)H(\omega)]\}\, G(\omega)\, d\omega \tag{2.2.5}$$

where the asterisk (*) indicates complex conjugate.

The first step towards minimizing the error E will be to take the partial derivative of E with respect to the coefficients c_i.

$$\frac{\partial E}{\partial c_i} = \int_0^{\omega_p/2} \{H^*(\omega)\frac{\partial H(\omega)}{\partial c_I}+H(\omega)\frac{\partial H^*(\omega)}{\partial c_i}-[\tilde{H}(\omega)\frac{\partial H^*(\omega)}{\partial c_i}+\tilde{H}^*(\omega)\frac{\partial H(\omega)}{\partial c_i}]\}\, G(\omega)\, d\omega \tag{2.2.6}$$

Taking the partial derivative of 2.1.8b with respect to c_i, we obtain:

$$\frac{\partial H(\omega)}{\partial c_i} = e^{-j\omega iD} \qquad (2.2.7a)$$

and

$$\frac{\partial H^*(\omega)}{\partial c_i} = e^{j\omega iD} \qquad (2.2.7b)$$

Substituting 2.2.7 and 2.2.2 into 2.2.6, this equation can be rewritten:

$$\frac{\partial E}{\partial c_i} = \int_0^{\omega_p/2} \sum_{k=-n}^{n} c_k \left[e^{j\omega(k-i)D} + e^{-j\omega(k-i)D}\right] - \tilde{R}(\omega) \left[e^{j(\omega iD \mp \phi(\omega))} + e^{-j(\omega iD \mp \phi(\omega))}\right] G(\omega)\, d\omega \qquad (2.2.8)$$

Using Eulers identities, equation 2.2.8 takes the form:

$$\frac{\partial E}{\partial c_i} = 2 \sum_{k=-n}^{n} \int_0^{\omega_p/2} \cos[\omega(k-i)D]\, G(\omega)\, d\omega - 2 \int_0^{\omega_p/2} R(\omega) \cos[\omega iD \mp \phi(\omega)]\, G(\omega)\, d\omega \qquad (2.2.9)$$

The second step in minimizing the error E is to equalize the partial derivative to zero, thus equation 2.2.9 becomes:

$$\sum_{k=-n}^{n} c_k \, 2 \int_0^{\omega_p/2} \cos[\omega(k-i)D] \, G(\omega) \, d\omega$$

$$= 2 \int_0^{\omega_p/2} R(\omega) \cos[\omega iD + \phi(\omega)] \, G(\omega) \, d\omega \qquad (2.2.10)$$

This equation can be represented in a matrix form:

$$Q \, \hat{c} = \hat{b} \qquad (2.2.11)$$

where the elements of the matrix Q are given by:

$$q_{ki} = \int_0^{\omega_p/2} \cos[\omega(k-i)D] \, G(\omega) \, d\omega \qquad (2.2.12)$$

the coefficients c_i are the elements of the vector $\hat{c}$:

$$\hat{c}^T = (c_{-n}, \ldots, c_o, \ldots, c_n) \qquad (2.2.13)$$

and the elements of the vector $\hat{b}$ are:

$$b_i = \int_0^{\omega_p/2} R(\omega) \cos[\omega iD + \phi(\omega)] \, G(\omega) \, d\omega \qquad (2.2.14)$$

In order to obtain the coefficients c_i which minimize the error E we have to obtain the inverse of Q, this is then multiplied by the vector $\hat{b}$.

$$\hat{c} = Q^{-1} \hat{b} \qquad (2.2.15)$$

The inverse of the matrix Q can be obtained using standard computer subroutines.

Depending on the nature of the functions $R(\omega)$, $\phi(\omega)$, and $G(\omega)$ it is difficult to find a closed form solution for equations 2.2.12 and 2.2.14. In such cases numerical integration is an effective tool.

2.3 Least Square Approximation when the Function $H(\omega)$ is Given by Points

In some occasions the functions $R(\omega)$ and $\phi(\omega)$ are known only at certain frequencies ω_i throughout the interval $[o, \omega_p/2]$. The usual approach to this problem uses a curve fitting algorithm to obtain the coefficients of an orthogonal polynomial that approximates the functions $R(\omega)$ and $\phi(\omega)$ individually. The least square method just described is then applied, obtaining the TF coefficients c_i. This method has the disadvantage that two approximations are made to obtain the coefficients, resulting in a larger error.

A second approach to this problem was given once again by A. Vincent Carrefour et. al.: The functions $R(\omega)$, $\phi(\omega)$, and $G(\omega)$ are defined at m points in the interval $[o, \omega_p/2]$.

	ω_o	ω_1	ω_2	-	-	-	ω_m
$R(\omega)$	R_o	R_1	R_2	-	-	-	R_m
$\phi(\omega)$	ϕ_o	ϕ_1	ϕ_2	-	-	-	ϕ_m
$G(\omega)$	G_o	G_1	G_2	-	-	-	G_m

The mean square error (2.2.1) is expressed in the discrete form:

$$e = \sum_{\ell=0}^{m} |H_\ell - \tilde{H}_\ell|^2 \, G_\ell \qquad (2.3.1)$$

Following the same reasoning as in the previous section the elements of the matrix Q (2.2.2) are given by:

$$q_{ki} = 2 \sum_{\ell=0}^{m} \cos[\omega(k-i)D] \, G_\ell \qquad (2.3.2)$$

and the elements of the vector $\hat{b}$ are:

$$b_i = 2 \sum_{\ell=0}^{m} R_\ell \cos[\omega i D + \phi_i] \, G_i \qquad (2.3.3)$$

Finally following the previous section, the coefficients c_i are obtained.

A. Vincent Carrefour has also derived a method of synthesis for the case when the phase $\phi(\omega)$ is not given. We will not consider here this method for the following reasons. In the first chapter we have seen that there are two main applications of Transversal Filters in digital transmitters:

i) To limit the power spectrum occupancy of binary signals.

ii) Predistort the signal to compensate for the phase distortion introduced by the channel.

For the first application we will see that the method given by Mueller described in the next chapter is the most

appropriate for this purpose. For the second application where the phase is given, the method just described is suitable. As a result, no other means of synthesis are required.

CHAPTER 3

BINARY TRANSVERSAL FILTERS

3.1 Transversal Filter Synthesis using Mueller's Method

In the previous chapter, two methods of TF synthesis have been introduced: The Fourier Series Method and the least squares method.

Many other methods can be found in the literature on Digital Filters [9] where often "TF's" are called Non Recursive Digital Filters.

The first step in synthesizing a TF, using any of the known techniques, is to specify the filter transfer function $H(\omega)$. In data transmission, the equivalent Nyquist type filter transfer function is frequently utilized, although, some care must be taken to minimize the Intersymbol Interference.

For the specific problem of filtering binary pulses, we will now introduce the method proposed by K. H. Mueller [8] in his paper; "A new approach to optimum pulse shaping in sampled systems using time domain filtering". The advantages in utilizing Mueller's technique are:

i) The filter transfer function does not have to be specified.

ii) The coefficients c_1 are optimum in the sense that the transmitted energy in the excess Nyquist bandwidth is maximized.

iii) The Intersymbol interference is minimized.

Considering all these advantages, it is not difficult to recognize that for our particular application, Mueller's technique is the best among the methods available at present.

A description of this method will follow. The impulse response of a Nyquist type TF can be obtained using equation 2.1.7 and is represented in figure 3.1.1.

The TF coefficients "c_i" are the samples of the truncated impulse response of the ideal Nyquist filter. These samples are taken at equally spaced time intervals D corresponding to the delay between the TF's multipliers. (See figure 2.1.3.

To assure minimum Intersymbol Interference - the first Nyquist criterion [12] states that the filter impulse response h(t) crosses the zero axis at regularly spaced intervals of T-sec, except for the central peak (figure 3.1.1); where T-sec is the baud interval. In section 2.1, we have seen that a TF has linear phase or constant time delay if the coefficients c_i have even symmetry. Based on these two requirements and on the practical limitations of a TF, a set of constraints on the coefficients c_i were established:

$$c_o = \max\{c_i\} \tag{3.1.1a}$$

$$c_{-i} = c_i \tag{3.1.1b}$$

$$c_{NK} = 0 \quad , \text{ for } N = \pm 1, \pm 2, \ldots, \pm L \tag{3.1.1c}$$

$$c_i = 0 \quad , \text{ for } |i| \geq KL \tag{3.1.1d}$$

where K represents the number of samples per baud interval (T).

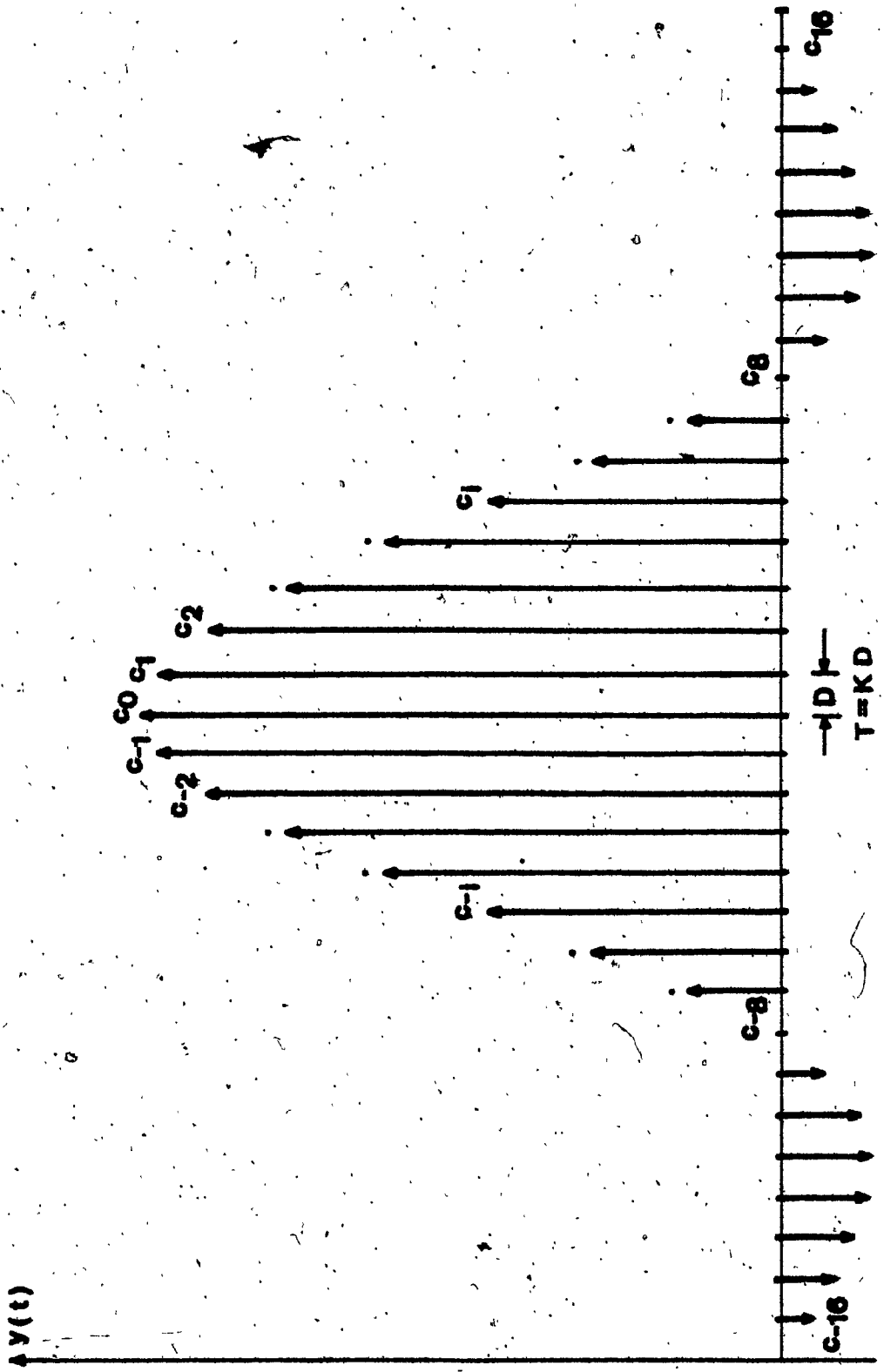

FIG.3.1.1 – Transversal filter impulse response (impulse type samples)

To satisfy equation 3.1.1c, K has to be an integer and since D is the delay between the multipliers c_i, then:

$$K = \frac{T}{D} \quad , \quad K = 1,2,3,\ldots \tag{3.1.2}$$

The symbol L in equations 3.1.1-c and -d represents the number of lobes in the impulse response, and for convenience the sampled impulse response has been truncated at an integer number of lobes. (equation 3.1.1d)

It is important to notice that in data transmission each lobe of the impulse response usually extends through exactly one baud interval i.e. T-sec. This statement is not true when α the excess Nyquist bandwidth exceeds 50% [20, p. 51]. Obviously, since the objective is to approach the Nyquist frequency, usually α is less than 50%.

The TF transfer function $H(\omega)$ given by equation 2.1.8b can be expressed in the vector form:

$$H(\omega) = \hat{c}^T \hat{z} \tag{3.1.3}$$

where $\hat{c}^T$ has been defined in 2.2.13, and

$$\hat{z}^T = (z_{-n},\ldots,z_0,\ldots,z_n), \text{ with } z_i = e^{-ji\omega D} \tag{3.1.4}$$

Until now we have assumed that the samples at the output of the TF are represented by impulses. In practice, it

is quite difficult to obtain this type of signal, and the samples are as a result, usually represented by pulses of finite width.

Let's assume that $W(\omega)$ the Fourier transform of $w(t)$, is a weighting function which converts impulses into pulses or some other waveform. The complex spectrum at the output of the filter is then given by:

$$S(\omega) = W(\omega) \cdot H(\omega) \qquad (3.1.5)$$

replacing $H(\omega)$ by 3.1.3, we obtain:

$$S(\omega) = W(\omega) \cdot \hat{c}^T \hat{z} \qquad (3.1.6)$$

and the power spectrum density is:

$$|S(\omega)|^2 = |W(\omega)|^2 \, \hat{c}^T \, \hat{z} \, \hat{\bar{z}} \, \hat{c} \qquad (3.1.7)$$

where $\hat{\bar{z}}$ is the complex conjugate of the transposed $\hat{z}$ vector.

Let E_W be the energy of the function $w(t)$. Then using Parseval's theorem [3, p. 850], we have:

$$E_W = \int_{-\infty}^{\infty} w(t)^2 \, dt = \frac{1}{2\pi} \int_{-\infty}^{\infty} |W(\omega)|^2 \, d\omega \qquad (3.1.8)$$

The total energy at the TF output is then from Mueller:

$$E(\infty) = \hat{c}^T \hat{c}\, E_w \qquad (3.1.9)$$

and the energy below a frequency ω_o is:

$$E(\omega_o) = \frac{1}{2\pi} \int_{-\omega_o}^{\omega_o} |W(\omega)|^2\, \hat{c}^T \hat{z}\, \hat{\bar{z}}\, \hat{c}\, d\omega \qquad (3.1.10)$$

As said at the beginning of this chapter, our aim is to maximize the energy in the excess Nyquist Bandwidth. To achieve this goal, the frequency ω_o will represent the excess Nyquist Bandwidth and we will define the normalized energy ratio as:

$$\lambda = \frac{E(\omega_o)}{E(\infty)} = \max \qquad (3.1.11)$$

Replacing equations 3.1.9 and 3.1.10 into 3.1.11 and rearranging we obtain:

$$\lambda \hat{c}^T \hat{c} = \hat{c}^T \left\{ \frac{1}{2\pi E_w} \int_{-\omega_o}^{\omega_o} |W(\omega)|^2\, \hat{z}\, \hat{\bar{z}}\, d\omega \right\} \hat{c} \qquad (3.1.12)$$

The product of the vectors $\hat{z}$ by $\hat{\bar{z}}$ generates a symmetric matrix. Using relation 3.1.4, the elements of this matrix are:

$$z_i\, z_k^* = e^{-j\omega(i-k)D} \qquad (3.1.13)$$

where * means complex conjugate.

Equation 3.1.12 can be put in a matrix form

$$\lambda \hat{c}^T \hat{c} = \hat{c}^T Q \hat{c} \qquad (3.1.14)$$

and using 3.1.13, the elements of the symmetric matrix Q are given by:

$$q_{ik} = \frac{1}{2\pi E_W} \int_{-\omega_o}^{\omega_o} |W(\omega)|^2 \, e^{-j\omega(i-k)D} \, d\omega \qquad (3.1.15)$$

Expanding the exponential term into $\cos[\omega(i-k)D] - j \sin[\omega(i-k)D]$ and considering the even nature of the function $|W(\omega)|^2$ the complex terms will cancel and equation 3.1.13 will become:

$$q_{ik} = \frac{1}{\pi E_W} \int_{0}^{\omega_o} |W(\omega)|^2 \cos[\omega(i-k)D] \, d\omega \qquad (3.1.16)$$

Before proceeding with the analysis of equation 3.1.14, in order to alleviate our task, a change will be introduced in the indexing of the elements of the $\hat{c}$ vector and on those of the Q matrix.

The elements of the $\hat{c}$ vector will become:

$$c_m = c_{i+n+1} \quad ; \quad m = 1,2,\ldots,2n+1 \qquad (3.1.17a)$$

and those of the symmetric matrix Q:

$$q_{ik} = q_{ki} = q_{\ell} \qquad (3.1.17b)$$

where

$$\ell = |i-k| + 1 \quad ; \quad \ell = 1,2,\ldots,2n+1 \qquad (3.1.17c)$$

This last relation is valid because the cosine function, in the integral 3.1.16 depends only on the absolute value of its argument. With this new indexed equation, 3.1.16 becomes:

$$q_\ell = \frac{1}{\pi E_w} \int_0^{\omega_o} |W(\omega)|^2 \cos[\omega D(\ell-1)]\, d\omega \qquad (3.1.18)$$

Returning to the analysis of 3.1.14 and expanding the right hand side using the new indexes, we obtain:

$$\lambda\, \hat{c}^T \hat{c} =$$

$$-\begin{bmatrix} c_1 & c_2 \cdots c_m \cdots c_{2n} & c_{2n+1} \end{bmatrix} \begin{bmatrix} q_1 & q_2 \cdots q_\ell \cdots q_{2n} & q_{2n+1} \\ q_2 & q_1 \cdots q_{\ell+1} \cdots q_{2n-1} & q_{2n} \\ \vdots & \vdots & \vdots \\ q_\ell & q_{\ell+1} \quad q_1 \quad \cdots \quad q_{\ell-1} & \\ \vdots & \vdots & \vdots \\ q_{2n} & q_{2n+1} \quad q_{\ell-1} \quad q_1 & q_2 \\ q_{2n+1} & q_{2n} \cdots q_\ell \cdots q_2 & q_1 \end{bmatrix} \begin{bmatrix} c_1 \\ c_2 \\ \vdots \\ c_m \\ \vdots \\ c_n \\ c_{2n+1} \end{bmatrix}$$

(3.1.19)

To assure minimum Intersymbol Interference, the vector $\hat{c}$ should satisfy constraint (3.1.1c). To clarify this point, let us take the example where the number of lobes (L) in the impulse response is 2 and the number of samples (K) per baud interval is 3, then the $\hat{c}$ vector should have the form:

$$\hat{c}^T = [0\ c_2\ c_3\ 0\ c_5\ c_6\ c_7\ c_8\ c_9\ 0\ c_{11}\ c_{12}\ 0]$$

Due to the quadratic form of equation 3.1.14, a vector satisfiying (3.1.1c) can be obtained by setting to zero the rows and colums of Q for which the first element corresponds to a zero element of the vector $\hat{c}$.

In our example, the matrix Q would be:

$$Q = \begin{bmatrix}
0 & & 0 & & & & & 0 & & 0 \\
 & q_1 & q_2 & & q_4 & q_5 & q_6 & q_7 & q_8 & q_{10} & q_{11} \\
 & q_2 & q_1 & & q_3 & q_4 & q_5 & q_6 & q_7 & q_9 & q_{10} \\
0 & & & & & & & & & & \\
 & q_4 & q_3 & & q_1 & q_2 & q_3 & q_4 & q_5 & q_7 & q_9 \\
 & q_5 & & & & q_1 & & & & & \\
 & q_6 & & & & & q_1 & & & & \\
 & q_7 & & & & & & q_1 & & & \\
 & q_8 & & & & & & & q_1 & & \\
0 & & & & & & & & & & \\
 & q_{10} & & & & & & & & q_1 & \\
 & q_{11} & & & & & & & & & q_1 \\
0 & & & & & & & & & &
\end{bmatrix}$$

From matrix theory, we know that when all the elements of a row or a column are equal to zero then the rank of the matrix can be reduced. And the Q matrix of our example becomes:

$$\underline{Q} = \begin{bmatrix} q_1 & q_2 & q_4 & q_5 & q_6 & q_7 & q_8 & q_{10} & q_{11} \\ q_2 & q_1 & q_3 & q_4 & q_5 & & & & \\ q_4 & q_3 & q_1 & & & & & & \\ q_5 & q_4 & q_3 & q_1 & & & & & \\ q_6 & & & & q_1 & & & & \\ q_7 & & & & & q_1 & & & \\ q_8 & & & & & & q_1 & & \\ q_{10} & & & & & & & q_1 & \\ q_{11} & & & & & & & & q_1 \end{bmatrix}$$

where the $\underline{\ }$ Sign under the Q indicates that this matrix is of reduced size.

Applying this shrinking principle to equation 3.1.16, the equation can be written as:

$$\lambda\, \hat{\underline{c}}^T\, \hat{\underline{c}} = \hat{\underline{c}}^T\, \underline{Q}\, \hat{\underline{c}} \qquad (3.1.20)$$

Considering that Q is the only known, it is not difficult to realize that the final solution is given simply

by the eigenvector $\hat{c}$ of Q corresponding to the largest eigenvalue λ_{max}. The final vector $\hat{c}$ containing the optimum coefficients is obtained by reinserting the zero elements in the positions from which they have been previously deleted.

In the next section, we will study the behavior of the energy ratio versus the number of TF coefficients. In this study, it is shown that to achieve energy ratio of the order of 20 dB (λ=.99) a vector $\hat{c}$ containing 30 coefficients is required.

We recognize immediately that finding the maximum eigenvalue and the corresponding eigenvector of a 30×30 matrix cannot be takled manually. The computer program BTF1 has been developed to solve this problem and is given in the appendix (A1).

Until now, our main concern was in finding an optimum solution for equation 3.1.14. Our present concern is to study a solution for the integral 3.1.18 knowing the weighting function w(t).

Two forms of w(t) are of particular interest in Transversal Filters:

i) In the first case, the samples are represented by impulses, then, (figure 3.1.1).

$$w_1(t) = \delta(t) \qquad (3.1.21)$$

ii) In the second, the samples are represented by pulses

of finite width and unit amplitude (figure 3.1.2).

$$w_2(t) \begin{cases} = 1 & \text{for } -\frac{D}{2} < t < \frac{D}{2} \\ = 0 & \text{elsewhere} \end{cases} \qquad (3.1.22)$$

It is worthwhile to note that in this second case, the end of a pulse coincides with the beginning of next. The result is that the signal ressembles a staircase (figure 3.1.2), and hence, will be referred to as staircase in the following pages.

The first case is purely academic, while the second is a good approximation of the signal present at the output of a realizable TF.

It is known that the spectrum generated by impulses is flat and is given by:

$$W_1(\omega) = \mathcal{F}[\delta(t)] = 1 \qquad (3.1.23)$$

while the spectrum generated by pulses is:

$$W_2(\omega) = \mathcal{F}[w_2(t)] = D \operatorname{sinc}(\omega \tfrac{D}{2}) \qquad (3.1.24)$$

where $\operatorname{sinc} x = \sin(x)/x$

Replacing equations 3.1.2 and 3.1.23 into 3.1.18, we obtain:

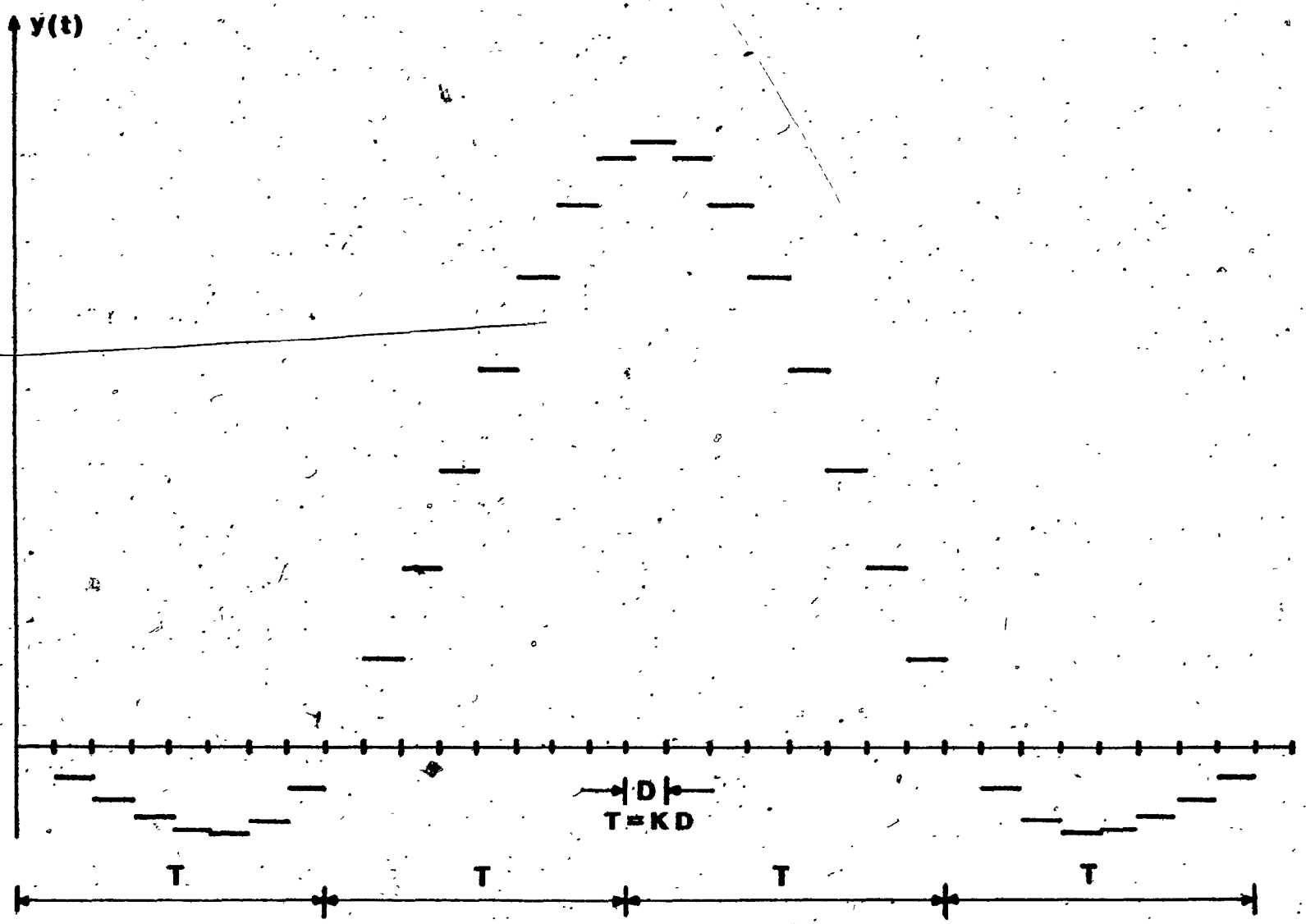

FIG. 3.1.2 – Transversal filter impulse response (Pulse type samples)

$$q_\ell = \frac{1}{\pi E_w} \int_0^{\omega_o} \cos\left[\omega \frac{T}{K}(\ell-1)\right] d\omega \qquad (3.1.25)$$

If T is the baud interval, then the Nyquist frequency is given by:

$$f_N = \frac{1}{2T} \qquad (3.1.26)$$

and if α is the excess Nyquist bandwidth, then the equivalent excess Nyquist frequency is:

$$f_o = f_N(1+\alpha) = \frac{1}{2T}(1+\alpha) \qquad (3.1.27)$$

Expressing ω_o in terms of the excess Nyquist frequency, we have:

$$\omega_o = 2\pi f_o = \frac{\pi}{T}(1+\alpha) \qquad (3.1.28)$$

Setting $\omega T = x$ and $d\omega = dx/T$, equation 3.1.25 becomes:

$$q_\ell = \frac{1}{\pi TEw} \int_0^{\pi(1+\alpha)} \cos\left[\frac{x}{K}(\ell-1)\right] dx \qquad (3.1.29)$$

for this integral, a closed form solution can be easily obtained, and is given by:

$$q_o = \frac{1+\alpha}{TE_w}$$
$$q_\ell = \frac{1+\alpha}{TE_w} \operatorname{sinc}\left[\pi(1+\alpha)\,(\ell-1)\right] \quad , \quad \text{for } \ell > 1 \qquad (3.1.30)$$

For the case of impulses, the elements of the Q matrix are simply given by regularly spaced samples of the function sin(x)/x.

In the second case where the weighting function represents pulses (3.1.24), a similar development is followed. Following the same reasoning as in the first case, equation 3.1.25 becomes:

$$q_\ell = \frac{D}{\pi K E_w} \int_0^{\pi(1+\alpha)} \operatorname{sinc}^2\left(\frac{x}{2K}\right) \cos\left[\frac{x}{K}(\ell-1)\right] dx \qquad (3.1.31)$$

A closed form solution for this integral cannot be found. A computer subroutine based on Romberg algorithm [11] has been developed to evaluate the integral 3.1.31. This subroutine is called by the main program BTF1 and is also given in the appendix.

3.2 In to Out of Band Energy Ratio

Continuing our study of Mueller's method, the next step is to establish the relation between the total number of transversal filter coefficients and the in to out of band energy ratio. The total number of TF coefficients (N_t) deduced from equation 3.1.17 is:

$$N_t = 2n+1 \qquad (3.2.1)$$

Considering that the filter impulse response is

truncated at an integer number of lobes (L) (equation 3.1.1d) and that K is the number of samples per baud interval (3.1.2), equation 3.2.1 becomes:

$$N_t = 2KL+1 \qquad (3.2.2)$$

We notice that different combinations of K's and L's will lead to the same total number of TF coefficients, N_t.

At this stage two questions can be raised:

i) Given the in to out of band energy ratio, what is the minimum number (N_t) of coefficients required?

ii) Which combination of K and L will simultaneously achieve the specified energy ratio and minimize the total number of coefficients (N_t)?

It is obvious that the answer to the second question is the optimum solution to the first one.

Before considering the problem, we will express the energy ratio in dB and in terms of the residual energy existing outside the excess Nyquist bandwidth - this being the usual way of expressing the energy of a digital signal. Recalling that $E(\omega_o)$ is the energy below the excess Nyquist frequency and $E(\infty)$ is the total energy, then E(h) the energy outside the specified bandwidth is:

$$E(h) = E(\infty) - E(\omega_o) \qquad (3.2.3)$$

normalizing with respect to $E(\omega_o)$, we obtain:

$$\frac{E(h)}{E(\omega_o)} = \frac{E(\infty)}{E(\omega_o)} - 1 \qquad (3.2.4)$$

expressing this equation in terms of λ (equation 3.1.11) and the final answer in dB, we obtain:

$$\left[\frac{E(h)}{E(\omega_o)}\right]_{dB} = 10 \log_{10} (\lambda^{-1}-1) \qquad (3.2.5)$$

This simple relation enables us to express the energy ratio directly in dB.

In the previous section we considered two types of samples at the transversal filter output:

i) Impulses

ii) Pulses or staircase

The energy ratio of these samples is now considered beginning with impulse type samples.

In the second chapter, it was shown that the TF transfer function $H(\omega)$ has a periodicity $\omega_p = 2\pi/D$ (equation 2.1.15) shown in figure 3.2.1a. Due to this periodicity, it is only necessary to consider the energy in one half of a period i.e. (π/D). Recalling that E_w is the energy associated with the weighting function $w(t)$ (equation 3.1.8) and that for impulses the spectrum is flat (3.1.23), we get:

$$E_w = \frac{1}{2\pi} \int_{-\pi/D}^{\pi/D} |W(\omega)|^2 \, d\omega = \frac{1}{D} \qquad (3.2.6)$$

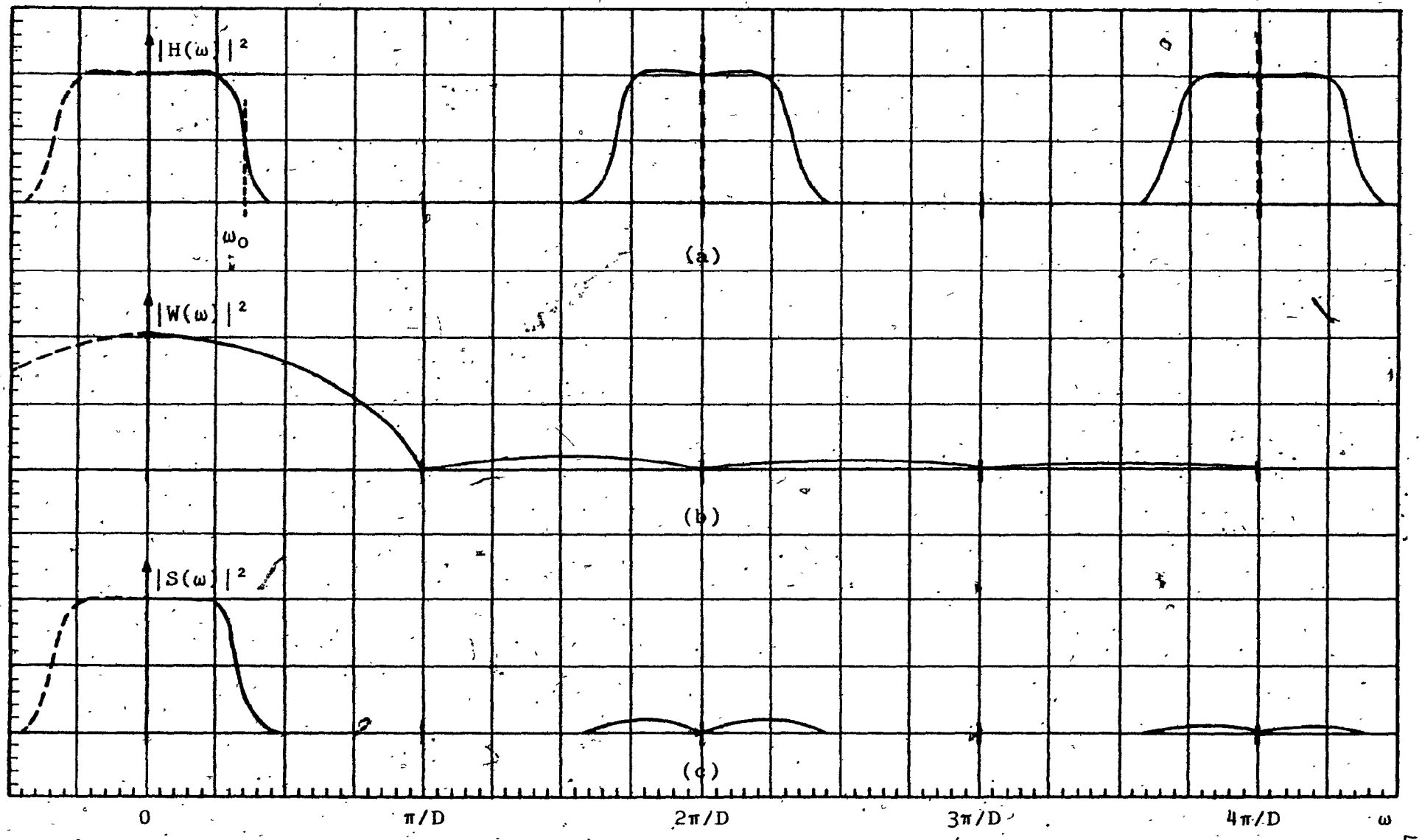

Fig. 3.2.1 - Transversal Filters Transfer Function Periodicity

substituting this result into 3.1.30 the elements of the Q matrix become:

$$q_o = \frac{1+\alpha}{K}$$

$$q_\ell = \frac{1+\alpha}{K} \cdot \text{sinc}\{\pi(1+\alpha)(\ell-1)\} \quad ; \quad \text{for } \ell > 0$$

These equations were used in the program BTF1 (Appendix A1). The excess Nyquist bandwidth (α) was arbitrarily set to 40% and the program was run for different values of K's and L's. The data obtained is given in table 3.2-A and is shown plotted in fig. 3.2.2. At first glance we would conclude that these results are very enthusiastic, but in practice impulse type samples are very difficult to obtain, and cannot be transmitted through limited bandwidth communication channel. We will now consider a more realistic type of waveform, where the samples are represented by pulses of D-sec of duration. In this case due to the magnitude decay of the function $W(\omega)$, figure 3.2.1b, the resulting spectrum $|S(\omega)|^2$ will decrease (figure 3.2.1-c), and the energy can in consequence be computed for the entire spectrum.

Substituting equation 3.1.22 into 3.1.8, we obtain:

$$E_w = \int_{-D/2}^{D/2} \omega(t)^2 \, dt = D \qquad (3.2.4)$$

N_t	L	K	(Max. Eigen.)λ	Energy Ratio dB
9	1	4	.99600049	-23.96
13	1	6	.99661309	-24.69
17	1	8	.99696126	-25.16
21	1	10	.99717530	-25.48
25	1	12	.99731854	-25.70
29	1	14	.99742066	-25.87
33	1	16	.99749698	-26.00
37	1	18	.99755612	-26.11
41	1	20	.99760326	-26.20
17	2	4	.99980451	-37.09
25	2	6	.99982306	-37.52
33	2	8	.99983565	-37.84
41	2	10	.99984395	-38.07
49	2	12	.99984975	-38.23
57	2	14	.99985402	-38.36
65	2	16	.99985729	-38.45
73	2	18	.99985989	-38.53
81	2	20	.99986200	-38.60
25	3	4	.99998882	-49.52
37	3	6	.99998950	-49.79
49	3	8	.99999007	-50.03
61	3	10	.99999047	-50.21
73	3	12	.99999075	-50.34
85	3	14	.99999096	-50.44
97	3	16	.99999112	-50.52

40% Excess Nyquist Frequency

Table 3.2-A - Impulse type Transversal Filter Energy Ratio

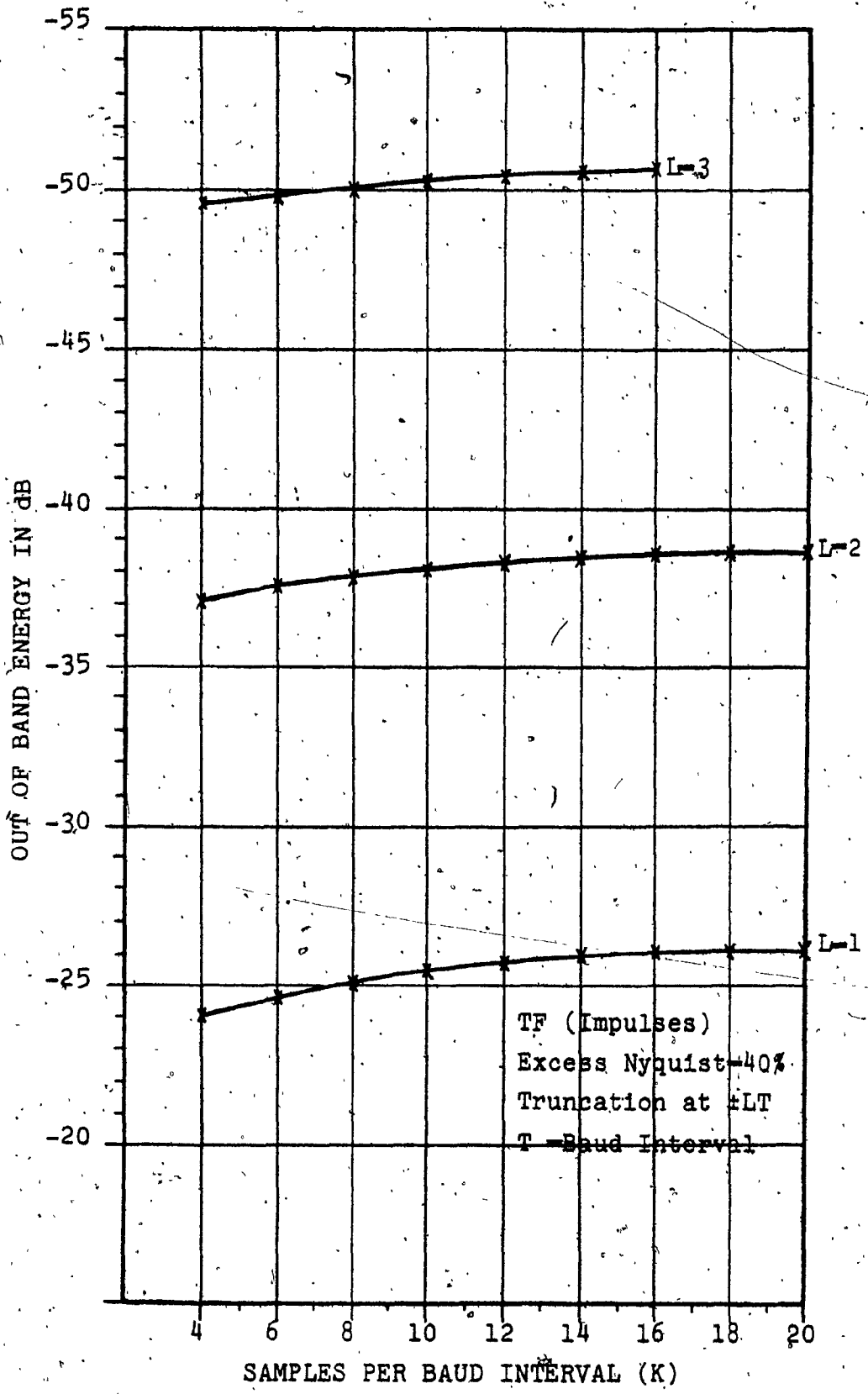

Fig. 3.2.2 - Impulse Type TF Energy Ratio

and the elements of the matrix are:

$$q_\ell = \frac{1}{\pi K}\int_0^{\pi(1+\alpha)} \operatorname{sinc}^2\left(\frac{x}{2K}\right)\cos\{\frac{x}{K}(\ell-1)\}\,dx$$

This equation was employed in the program BTF1 (see appendix) which was again run for different values of K's and L's with the 40% excess Nyquist frequency kept constant. Table 3.2-B and graph of figure 3.2.3 were obtained. From this graph, we may conclude that for the practical Transversal Filter (pulses) most of the energy is concentrated in the main (L=1) and second (L=2) lobes. This behavior is not surprising since most of the area and therefore energy is concentrated in the main and second lobes, as shown in figure 3.1.2. It is worthwhile noting that an increase in the number of samples causes the energy to approach a maximum which can only be exceeded by increasing the number of lobes.

However, for the pulse type transversal filter, the behavior of the energy ratio with respect to the total number of coefficients N_t (Table 3.2-B) can be summarized as:

i) For N_t less or equal to 37 the largest energy ratio is achieved in one lobe (L=1).

ii) For N_t greater than 37 the largest energy ratio is obtained for L=2.

In next section we will see that the eye pattern for a one lobe TF is not symmetrical, indicating a possible

N_t	L	K	(Max. Eigen.)λ	Energy Ratio dB
9	1	4	.98322832	-17.68
13	1	6	.99105873	-20.45
17	1	8	.99387733	-22.10
21	1	10	.99521868	-23.10
25	1	12	.99596820	-23.93
29	1	14	.99643319	-24.46
33	1	16	.99674370	-24.86
37	1	18	.99696266	-25.16
41	1	20	.99712370	-25.40
17	2	4	.98565688	-18.37
25	2	6	.99346951	-21.82
33	2	8	.99624374	-24.24
41	2	10	.99753877	-26.08
49	2	12	.99824639	-27.55
57	2	14	.99867496	-28.77
65	2	16	.99895414	-29.80
73	2	18	.99914615	-30.68
81	2	20	.99928387	-31.45
25	3	4	.98573886	-18.40
37	3	6	.99357098	-21.89
49	3	8	.99635385	-24.37
61	3	10	.99765309	-26.28
73	3	12	.99836280	-27.85
85	3	14	.99879241	-29.18
97	3	16	.99907205	-30.32

40% Excess Nyquist Frequency

Table 3.2-B Pulse type Transversal Filter Energy Ratio

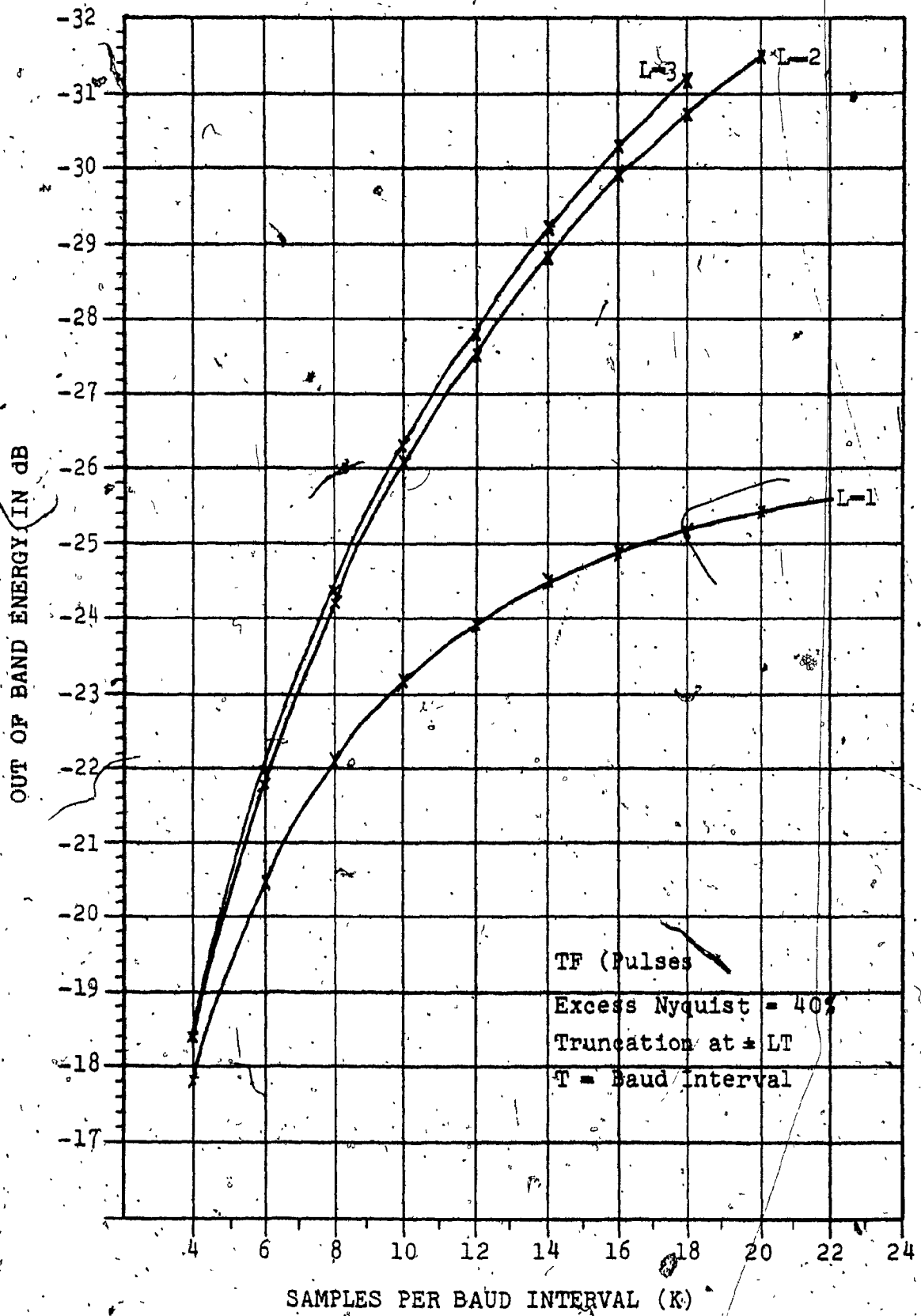

Fig. 3.2.3 - Pulse Type TF Energy Ratio

degradation in probability of error, that fact is confirmed in chapter four. If this degradation is acceptable, the one lobe transversal filter can be used. Otherwise, the two lobe filter is required.

These results will be very usefull in chapter four where the design of a Transversal Filter is considered.

3.3 Binary Transversal Filter Eye Pattern

In the previous sections, Transversal Filters were discussed in general. In this section, after defining the Binary Transversal Filter (BTF), a method will be developed of displaying by simulation, the eye pattern of the digital waveform present at the output of the filter [25, p. 61 to 63]. As a result of this simulation, it will be shown that, if the BTF coefficients employed are those obtained by Mueller's Technique, then the eye diagram is completely open at the center, thus, demonstrating that the Intersymbol Interference inherent to the filter is negligible.

A Transversal Filter in general can accept, with some restrictions, almost any kind of waveform at its input. A special class of transversal filter which can respond satisfactorily to binary waveforms only is called Binary Transversal Filter. Since in data transmission the basic signal is a binary waveform, it is obvious that the Binary Transversal Filter is the most appropriate for our needs. Also, it is important to notice that the practical implemen-

tation of a BTF is substantially less complex than the one required for a general Transversal Filter. For example, a Transversal Filter implemented by means of digital techniques would usually require [2] a sampling device, an A/D (Analog to Digital) and a D/A (Digital to Analog) converters and digital multipliers in addition to what a BTF needs to fully perform its function.

Recalling that the output signal of a Transversal Filter can be obtained using equation 2.1.6, we replace in that equation t' by t-nD (equation 2.1.3 and 2.1.4) and the index "i" with "m" using relation 3.1.17a. We then obtain:

$$y(t) = \sum_{m=1}^{2n+1} c_m \, x(t-(m-1)D) \qquad (3.3.1)$$

Assuming that the input signal x(t) is a pulse sequence p(t), and is of the return to zero form (RZ) defined by:

$$p(t) = 1 \quad \text{for } 0 < t \leq D$$
$$p(t) = 0 \quad \text{elsewhere} \qquad (3.3.2)$$

It is noted that this definition of RZ implies a 100% duration cycle and corresponds to a binary one. If we now suppose that the input signal x(t) exists in the

interval $0 < t < NT$, where N is a very large integer and T is the baud interval, then the following equation can represent a fairly long random sequence of pulses:

$$x(t) = \sum_{i=0}^{N} a_i \, p(t-iT) \qquad (3.3.3)$$

where a_i is a discrete random variable having the following statistics:

$$a_i = \begin{cases} 0 \\ 1 \end{cases} \quad \text{and} \quad \text{prob}(0) = \text{prob}(1) = \frac{1}{2}$$

In practice it is important to keep the probability of zeros and ones almost equal for two major reasons [15]:

i) The transmission of a long sequence of zeros results in a long period without timing information, and

ii) Since in the majority of cases the channel does not pass zero frequencies (dc) then the transmission of a long sequence of ones results in dc wonder.

To achieve almost equal probability of zeros and ones a scrambler and a descrambler are used at the transmitter and receiver ends respectively.

Recalling that in one baud interval of T-sec we have K samples (equation 3.1.2), equation 3.3.3 becomes:

$$x(t) = \sum_{i=0}^{N} a_i \, p(t-iKD) \qquad (3.3.4)$$

Substituting 3.3.4 into 3.3.1 and inverting the order of summations, we obtain:

$$y(t) = \sum_{i=0}^{N} \sum_{m=1}^{2n+1} c_m a_i p(t-(m-1)D-iKD) \qquad (3.3.5)$$

Considering the definition of p(t) (equation 3.3.2) and this last equation, we can easily conclude that the signal y(t) is composed of pulses having identical shape p(t) but different amplitudes. As a result of this statement, the time t does not have to be scanned continuously but only at regularly spaced intervals of ℓD units of time, where ℓ is an integer running for practical purposes from zero to (2n+1)(N+1). If D is set equal to one unit of time, then equation 3.3.5 becomes:

$$y_\ell = \sum_{i=0}^{N} \sum_{m=1}^{2n+1} c_m a_i p(\ell-iK-m+1) \qquad (3.3.6)$$

where $0 \leq \ell \leq (2n+1)(N+1)$.

We have finally arrived at the equation that represents the BTF output signal. In using this equation to display the eye diagram, we will follow essentially the same technique used to observe the eye pattern on an oscilloscope. The horizontal (X) axis of the graph will represent a time period while the vertical (Y) axis, the amplitudes of the waveform. The total length of the (X) axis is divided into 2K slots of

D units of time each adding up to a total of 2T-sec or 2 bauds intervals. For each "ℓ" running from zero to 2K, a line segment is drawn in each time slot D according to the amplitude of the sample y_ℓ. Since the upper limit of "ℓ" is much larger than 2K (end of the X axis) once "ℓ" has reached this limit, the new samples are simply drawn starting again from the origin of the graph. This process is repeated over and over until "ℓ" reaches the limit (2n+1)(N+1).

A computer program called SMTF given in Appendix (A2) was written in order to obtain the values of y_ℓ. These values were then stored on an array. A subroutine called PRBS was developed in order to generate the Pseudo Random Binary Sequence (equation 3.3-3) [16, pp. 323-327]. In our particular case the period of the pseudo random sequence was set to 127 bits before repeating. A special computer subroutine called PLOT converted and noted the data on magnetic tape. The tape is then processed by a minicomputer which is coupled to a plotter and the simulated eye diagram is finally displayed.

The result of the entire process for different types of BTF's is shown by figure 3.3.1 to 3.3.4.

The eye diagrams displayed in these figures are self explanatory, nevertheless, some conclusions may be drawn from them.

First, we notice that the eye diagram is always

maximaly open at its center which proves what was stated in the beginning of this section.

Secondly, comparing figure 3.3.1 (one lobe BTF) to the others, we notice a certain absence of amplitude symmetry, meaning that the average value of the waveform cannot be set equal to zero. This dc offset will bias the waveform and a degradation of the bit error rate (BER) performance is expected. The practical proof of this last statement will be given in the next chapter where the measurement of the BER of a one lobe BTF has shown a degradation at low BER.

Figure 3.3.2 and 3.3.3 are similar; but some difference can be observed at the zero crossing (dashed lines) [25, p. 62] of the eye diagram. For the 40% Excess Nyquist Filter, the peak to peak jitter of the zero crossing is less than the 30% one, which indicates that the time jitter is reduced if the excess Nyquist Bandwidth is relaxed.

Finally, the only difference between figure 3.3.4 and figures 3.3.2 and 3.3.3 is in the number of samples per baud interval. By increasing the number of samples, the eye diagram becomes smoother, and in consequence the energy ratio increases (figure 3.2.3). Due to practical constraints, the number of Transversal Filter coefficients cannot be increased indefenitely. The most important of these are:

i) Coefficients accuracy [18].

As the number of samples per baud interval (T) becomes

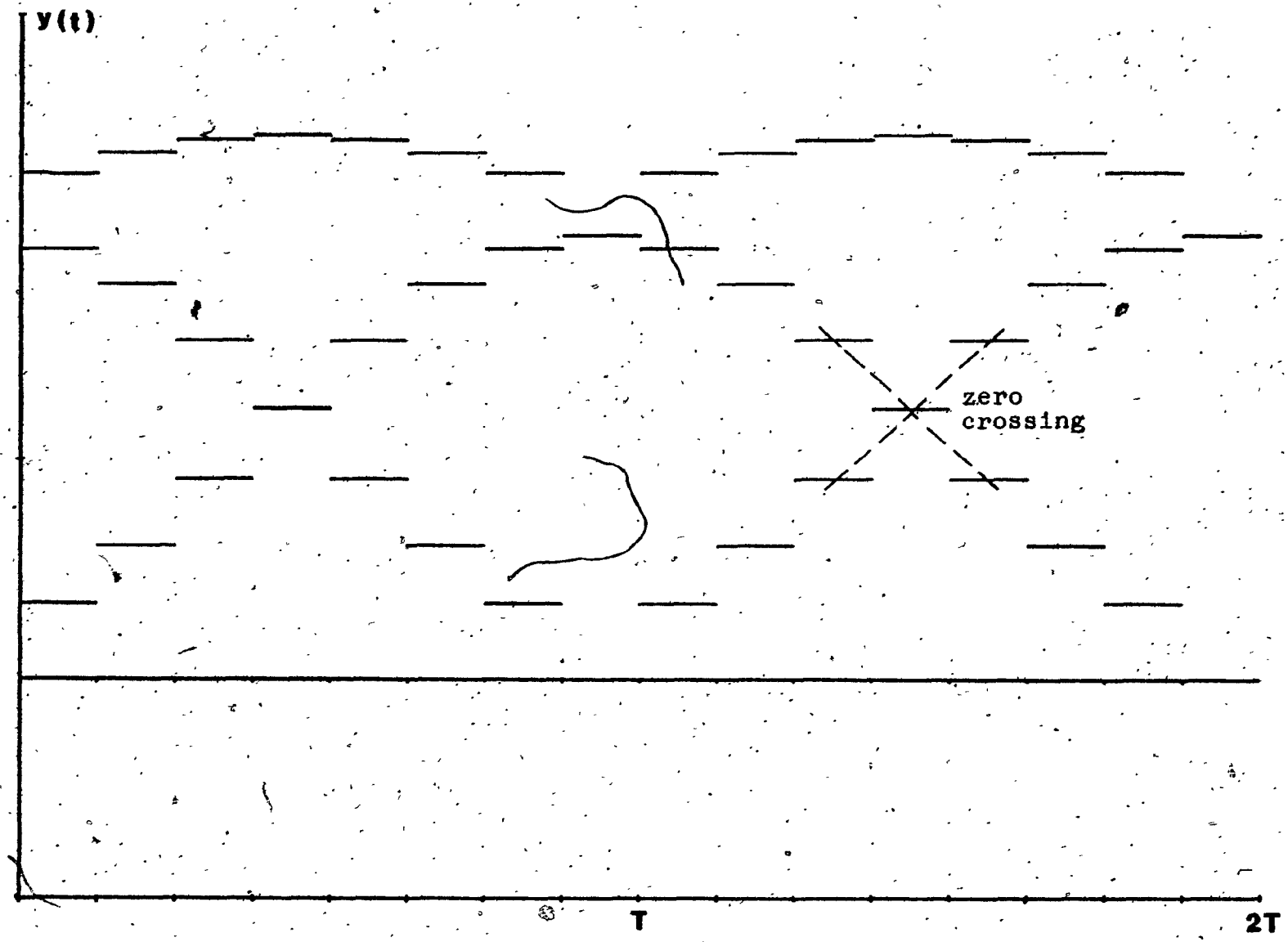

Fig. 3.3.1 - BTF Eye Diagram Simulation (K=8, L=1, α=.4)

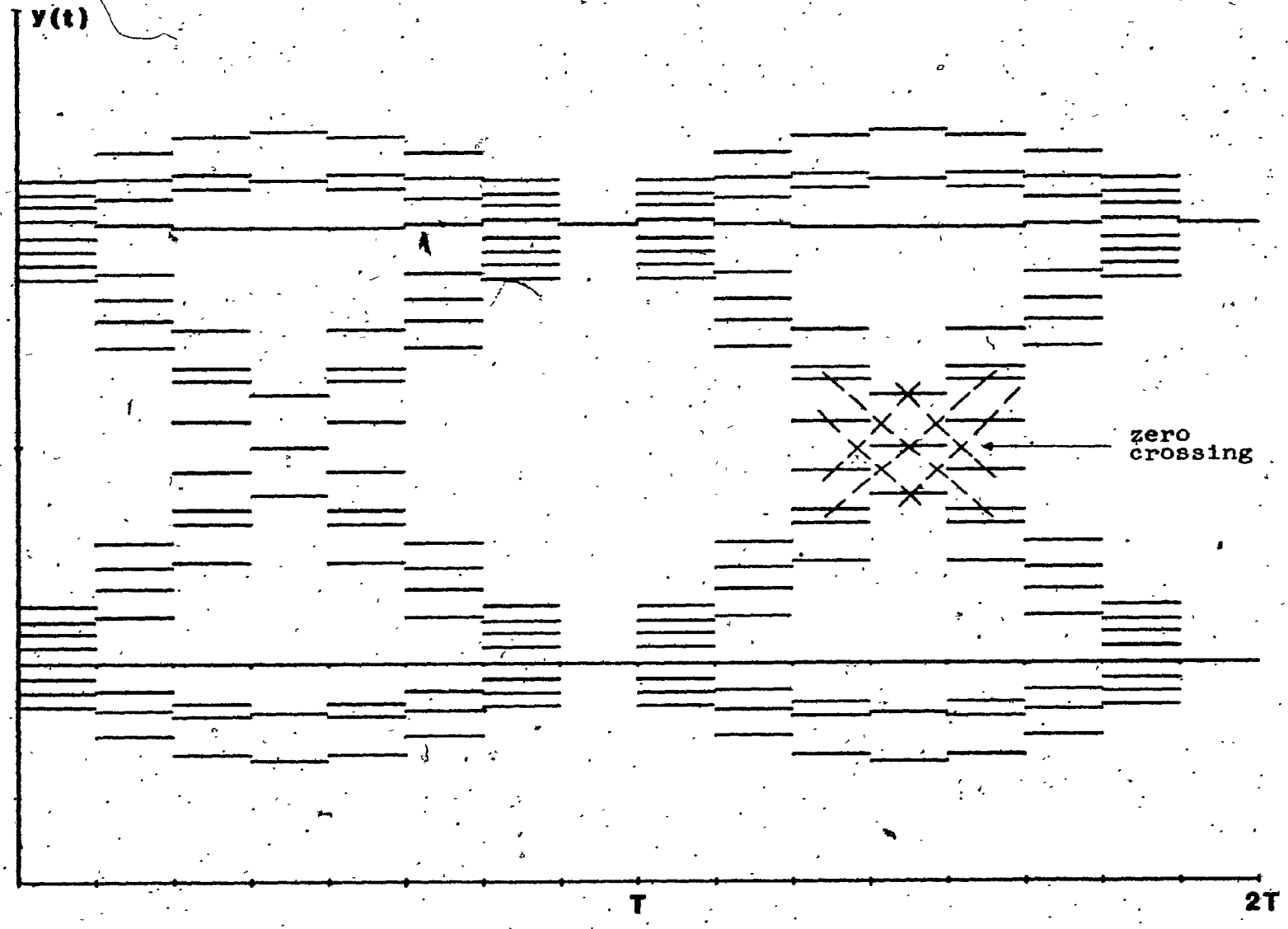

Fig. 3.3.2 - BTF Eye Diagram Simulation (K=8, L=2, α=.4)

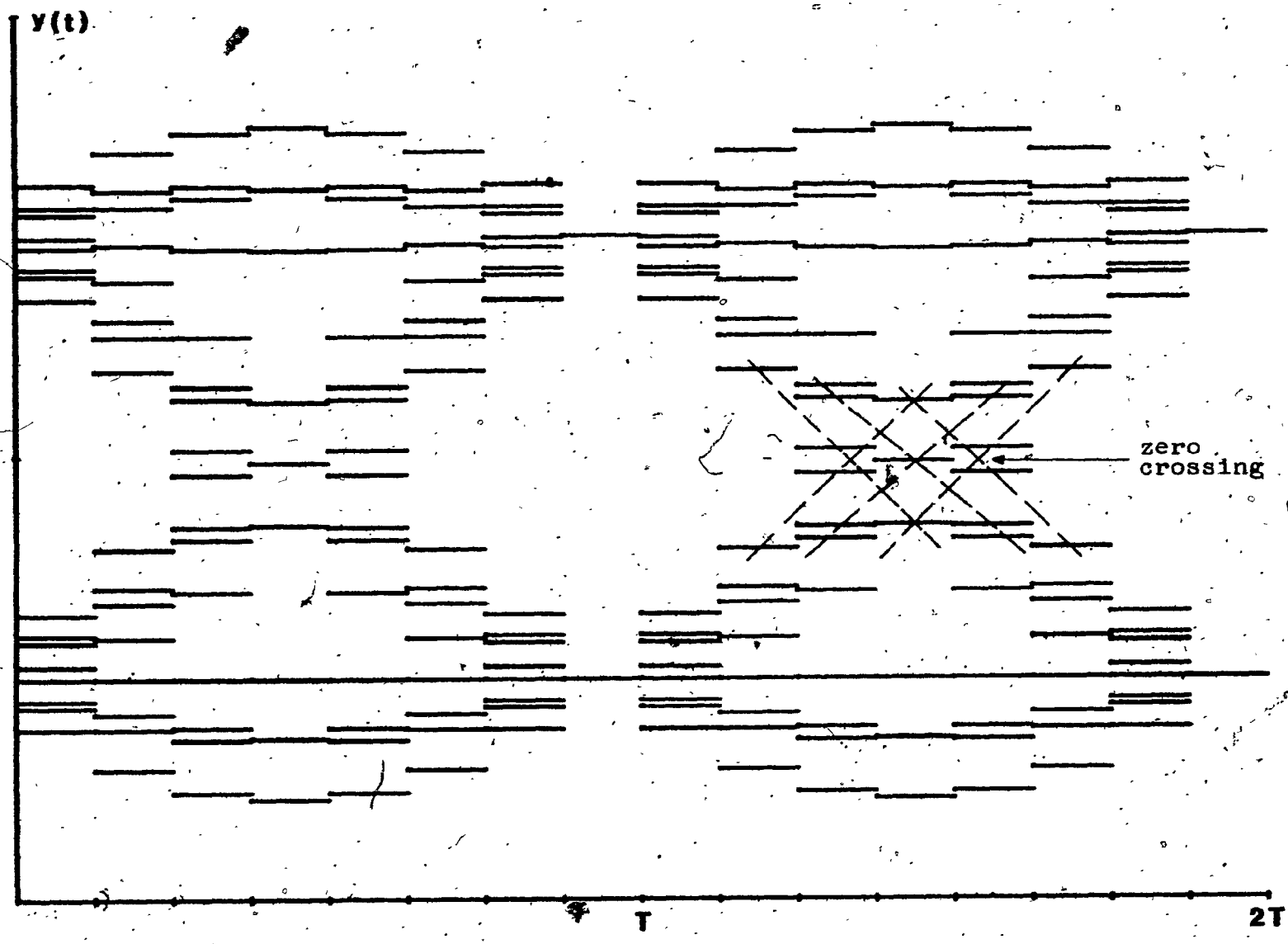

Fig. 3.3.3 - BTF Eye Diagram Simulation (K=8, L=2, α=.3)

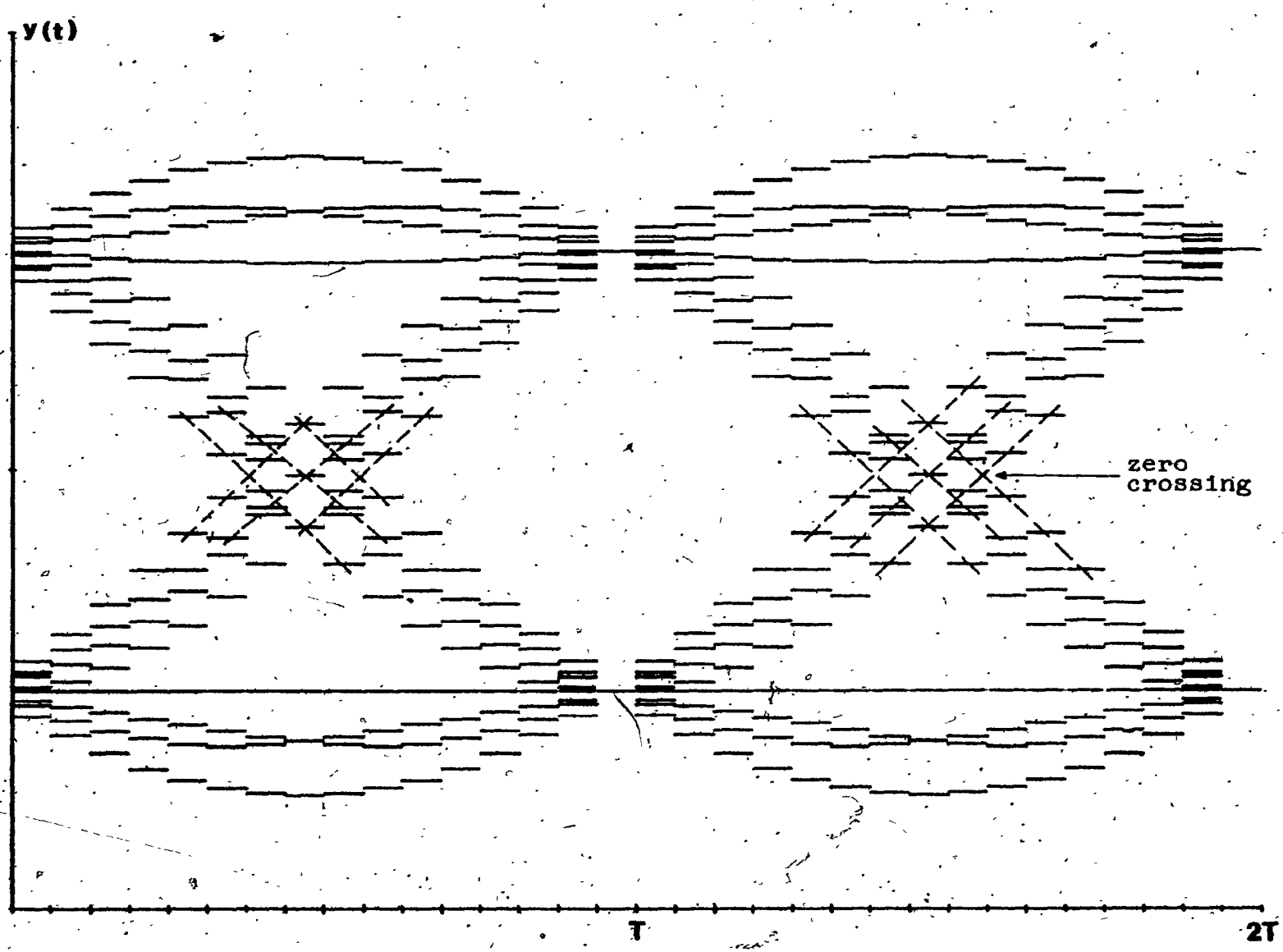

Fig. 3.3.4 - BTF Eye Diagram Simulation (K=16, L=2, α=.4)

very large, the difference in value between adjacent samples becomes very small consequently, the coefficients' accuracy must be high in order to keep the samples in a specified order.

ii) Hardware maximum switching speed.

This restriction is applicable when the Transversal Filter is implemented using digital techniques. Because the time delay "D" is inversely proportional to the number of samples per baud interval "K" (D=T/K), the greater is K, the smaller, D. This forcing the digital circuitry to operate at higher speeds.

A method to get around these restrictions will be discussed in a later section. It consists of cascading an analog low pass filter with the Transversal Filter.

3.4 Sensitivity of the BTF Energy Ratio to Changes in the Coefficients

In section 3.2, we established the energy ratio of a Transversal Filter, assuming the optimum coefficients obtained by Mueller's method. The objective of this section is to evaluate the degradation in the energy ratio performance considering real coefficients, i.e. coefficients which are accurate only within some specified limits.

A first attempt to solve this problem was made utilizing the conventional definition of sensitivity [2, p. 7] but no success was achieved in establishing a relation between energy ratio and coefficients accuracy. The problem was then approached using a statistical method and successful results were obtained. The statistical method essentially involved computing the energy ratio of filter coefficients which have been perturbed at random. It is evident that to obtain meaningful results, the perturbation has to be within a specified range. This process is repeated for a large number of times (e.g. 100) until enough samples of the energy ratio are obtained. The mean and the standard deviation of 50 and 100 samples were computed, and are given in Tables 3.4-A, B, C. Since the results were very similar, we have concluded that one hundred samples were sufficient for statistical purposes.

BTF Characteristics			Optimum Coefficients		± 1% Coefficients Accuracy						
					50 Samples			100 Samples			
					$E(h)/E(\omega_o)$			$E(h)/E(\omega_o)$			
L	K	Excess Nyquist	$\frac{E(\omega_o)}{E(\infty)}$	$\frac{E(h)}{E(\omega_o)}$dB	Mean	Stand. Dev.	dB Mean	Mean	Stand. Dev.	dB Mean	Mean Energy Ratio (dB) Degrad.
1	8	30%	.9918395	-20.85	.0082554	.0000106	-20.83	.0082548	.0000097	-20.83	.02
1	8	41%	.99402229	-22.21	.0060405	.0000109	-22.19	.0060400	.0000099	-22.19	.02
2	8	30%	.99588559	-23.84	.0041588	.0000096	-23.81	.00415877	.0000092	-23.81	.03
2	8	40%	.99624374	-24.24	.0037974	.0000097	-24.21	.0037975	.0000093	-24.21	.03

Table 3.4-A - Expected Value of the BTF Energy Ratio for ±1% Coefficients Accuracy.

BTF Characteristics			Optimum Coefficients		± 5% Coefficients Accuracy						Aver. Energy Ratio (dB) Degrad.
					50 Samples			100 Samples			
					$E(h)/E(\omega_o)$			$E(h)/E(\omega_o)$			
L	K	Excess Nyquist	$\frac{E(\omega_o)}{E(\infty)}$	$\frac{E(h)}{E(\omega_o)}$dB	Mean	Stand. Dev.	dB Mean	Mean	Stand. Dev.	dB Mean	
1	8	30%	.99183905	-20.85	.0089115	.0002663	-20.50	.0089978	.0002434	-20.51	.34
1	8	41%	.99402229	-22.21	.0066849	.0002721	-21.75	.0066719	.0002482	-21.76	.45
2	8	30%	.99488559	-23.84	.0048164	.0002400	-23.17	.0048149	.0002308	-23.17	.67
2	8	40%	.99624374	-24.24	.0044449	.0002428	-23.52	.0044456	.0002337	-23.52	.72

Table 3.4-B – Expected Value of the BTF Energy Ratio for ±5% Coefficients Accuracy

BTF Characteristics			Optimum Coefficients		±10 Coefficients Accuracy						Aver. Energy Ratio (dB) Degrad.
					50 Samples			100 Samples			
					$E(h)/E(\omega_o)$			$E(h)/E(\omega_o)$			
L	K	Excess Nyquist	$\frac{E(\omega_o)}{E(\infty)}$	$\frac{E(h)}{E(\omega_o)}$dB	Mean	Stand. Dev.	dB Mean	Mean	Stand. Dev.	dB Mean	
1	8	30%	.99183905	-20.85	.0109666	.0010691	-19.60	.0109124	.0009792	-19.62	1.25
1	8	41%	.99402229	-22.21	.0087033	.0010917	-20.60	.0086519	.0009975	-20.63	1.58
2	8	30%	.99588559	-23.84	.0068691	.0009624	-21.63	.0068629	.0009274	-21.63	2.21
2	8	40%	.99624374	-24.24	.0064661	.0009735	-21.89	.0064689	.0009392	-21.89	2.35

Table 3.4-C - Expected Value of the BTF Energy Ratio for ±10% Coefficients Accuracy

The out of band to in band energy ratio for a Transversal Filter was given by equation 3.2.4, being:

$$\frac{E(h)}{E(\omega_o)} = \frac{E(\infty)}{E(\omega_o)} - 1 \qquad (3.4.1)$$

where $E(\infty)$ is the total output energy and $E(\omega_o)$ is the energy below the specified excess Nyquist frequency, where $\omega_o = 2\pi \{(1+\alpha) f_N\}$.

To calculate the total energy, we simply substitute equation 3.2.4 into 3.1.9 and replace D by T/K, obtaining:

$$E(\infty) = \hat{c}^T \hat{c}\ T/K \qquad (3.4.2)$$

now, expressing T, the baud interval in terms of the Nyquist frequency f_N, we have:

$$E(\infty) = \hat{c}^T \hat{c}\ (2f_N K)^{-1} \qquad (3.4.3)$$

To evaluate the energy below the specified excess Nyquist frequency, and integral equation similar to (3.1.10) was used:

$$E(\omega_o) = \frac{1}{\pi} \int_0^{\omega_o} |W(\omega)|^2\ |H(\omega)|^2\ d\omega \qquad (3.4.4)$$

The filter transfer function $H(\omega)$ was then replaced

by 3.1.3 and, the weighting function $W(\omega)$ by 3.1.24, allowing the evaluation of the energy using numerical integration [11].

From equation 3.4.4, we can deduce that the in band energy depends not only on $H(\omega)$ but also on $W(\omega)$. Although the sensitivity study here concentrated exclusively on $H(\omega)$, it is important to note that perturbation or imperfections of the weighting function $W(\omega)$ will also degrade the energy ratio performance. Further studies should be conducted to evaluate if these imperfections in $W(\omega)$ are a dominant factor. Some possible examples are: pulse leading and trailing edges, top tilt and/or overshoots.

The coefficients c_i of the Binary Transversal Filter were perturbed using the following relation:

$$\tilde{c}_i = c_i \{1+RANDU \times PER\} \qquad (3.4.5)$$

where $\tilde{c}_i$ are the perturbed coefficients, RANDU is a random variable uniformly distributed between -1 and +1 and PER is the specified coefficients accuracy.

Assuming the coefficients c_i are statiscally independent, it can be shown that equation 3.4.5 accurately models the physical realization of the BTF [18].

In our study, values of 1%, 5%, 10% were given to PER.

The mean value ($\bar{X}$) and the standard derivation (σ) of the energy ratio were computed using the following relations [20]:

$$\bar{X} = \frac{1}{N} \sum_{i=1}^{N} X_i \qquad (3.4.6)$$

and

$$\sigma = \sqrt{\frac{\Sigma X_i^2 - (\Sigma X_i)^2/N}{N-1}} \qquad (3.4.7)$$

where N is the total number of samples and X_i the sample value.

A computer program called SENST given in appendix A3 was implemented in order to evaluate the energy ratio and its statistics. The mean value of the energy ratio was expressed in dB using a relation similar to 3.2.5. In order to check the accuracy of the program SENST in calculating the energy ratio the value of λ or $E(\omega_o)/E(\infty)$ was computed initially using non-perturbed optimum coefficients. The value of λ (see table 3.4-A, B, C) was then compared with the maximum eigenvalue computed using BTF1 (appendix A1) (see table 3.2-A,B) and no discrepancies were found for up to eight significant digits, proving the validity of program SENST.

The out of band to in band energy ratio $[E(h)/E(\omega_o)]$ was then evaluated for different types of filters. Several of

these filters were implemented in practice, and their performance results are given in the next chapter.

From tables 3.4-A, B, C, the first conclusion that can be drawn is that, contrary to what were our expectations before this study, the Binary Transversal Filter's coefficients do not have to be extremely accurate to keep the energy ratio within practical limits. Tables 3.4-A, B, C also show that the standard deviations are fairly narrow indicating uncomplicated filter repeatability.

In order to force the eye diagram of a BTF (sec. 3.3) to be maximaly open at its center, an empirical rule should be followed, requiring that the coefficients' accuracy be at least one half the minimum difference existing between two adjacent coefficients. In this manner, two steps of the eye (see figure 3.3.1 to 3.3.4) can in the worst case be of equal amplitude without ever exceeding each other.

Observing this rule, we arrive at the conclusion that the coefficients accuracy should be kept below the ±2.5% value.

3.5 Binary Transversal Filter Power Spectrum Density

This section describes a method of calculating and plotting the power spectrum density of the Binary Transversal Filter output signal.

Because in digital transmission, the signal feeding the transversal filter is a random binary sequence of pulses, and because that the BTF is a linear device, the power spectrum density can be calculated using any of the two following methods. The first method involves taking the Fourier Transform of the Autocorrelation function for a fairly long sequence of pulses [13]. While the second utilizes a formula given by Bennet and Davey for random binary signals [12, p. 316].

The first method is fairly general and when employed with the proper care is applicable to a wide class of random signals. As it would be expected, the price payed for this generality is a fairly complex computer program, consisting essentially of a discrete Autocorrelation algorithm followed by a Fast Fourier Transform.

In contrast, the second method although restricted to random binary signals, requires a comparatively insignificant amount of effort to implement the computer program. Because its simplicity and adequacy for our need, this second method was adopted. The remainder of this section will describe it in detail.

A formula relating the Power Spectral Density to the Fourier Transform of a binary signal was given by Bennet and Davey [12] and also by Dupraz [14]. The equations being similar we have chosen the one given in the former reference.

$$G(f) = 2f_s\, p(1-p)|Y_1(f)-Y_2(f)|^2 + f_s^2|pY_1(0)+(1-p)Y_2(0)|^2\, \delta(f) + 2f_s^2 \sum_{m=1}^{\infty} |pY_1(mf_s)+(1-p)Y_2(mf_s)|^2\, \delta(f-mf_s) \qquad (3.5.1)$$

where:

$Y_i(f)$ is the Fourier Transform of $y_i(t)$

p is the a priory probability of $y_1(t)$

(1-p) is the a priory probability of $y_2(t)$

f_s is the signaling frequency (T^{-1}) or bit rate

and:

$y_1(t)$ is the signal associated with a binary one

$y_2(t)$ is the signal associated with a binary zero

Assuming that zeros and ones have equal probability of being transmitted i.e. $p=(1-p)=\frac{1}{2}$, that the binary zero is represented by the absence of information ($y_2(t)=0$), and finally, that $f_s=2f_N$ where f_N is again the Nyquist frequency, equation 3.5.1 takes the form:

$$G(f) = f_N|Y_1(f)|^2 + f_N^2[Y_1(0)]^2\, \delta(f) + 2f_N^2 \sum_{m=1}^{\infty} |Y_1(2mf_N)|^2\, \delta(f-2mf_N) \qquad (3.5.2)$$

Because in digital communications it is necessary to avoid the transmission of dc components through the channel, the zero frequency term ($Y_1(0)$) will disappear in 3.5.2. In the majority of practical situations, this can be achieved by inserting a relatively large valued capacitor at the output of the filter. Equation 3.5.2 now becomes:

$$G(f) = f_N|Y_1(f)|^2 + 2f_N^2 \sum_{m=1}^{\infty} |Y_1(2mf_N)|^2 \delta(f-2mf_N) \quad (3.5.3)$$

At this stage, the power spectrum density $G(f)$ can be computed once the function $Y_1(f)$ is specified. Considering a Binary Transversal Filter, excited by a single binary one of D-sec of duration, the Fourier Transform of the signal $y_1(t)$ can be obtained by substituting equations 2.1.8a and 3.1.2 into 3.1.5, and then changing ω by $2\pi f$:

$$Y_1(f) = S(f) = D \operatorname{sinc}(\pi fD)\, e^{-j2\pi fa} \sum_{i=-n}^{n} c_i\, e^{-j2\pi ifD} \quad (3.5.4)$$

Replacing D by $(2Kf_N)^{-1}$, "a" by nD (equation 2.0.4), n by KL (equation 3.1.1d), equation 3.5.4 becomes:

$$Y_1(f) = \frac{1}{2Kf_N} \operatorname{sinc}\left\{\frac{\pi f}{2Kf_N}\right\} e^{-j\pi Lf/f_N} \sum_{i=-n}^{n} c_i\, e^{-j\pi if/f_NK} \quad (3.5.5)$$

Recalling that in our application, the BTF has linear phase, guaranteed by the even symmetry of the coefficients

c_i, i.e. $c_i = c_{-i}$ (equation 3.1.1b), equation 3.5.5 can be further simplified, becoming:

$$Y_1(f) = \frac{1}{2Kf_N} \operatorname{sinc}\left[\frac{\pi f}{2Kf_N}\right] e^{-j\pi Lf/f_N} \{c_0 + 2 \sum_{i=1}^{n} c_i \cos(\pi i f/f_N K)\} \quad (3.5.6)$$

Now substituting this last equation into 3.5.3 and setting $f = xf_N$, we obtain:

$$G(x) = \frac{1}{4K^2 f_N} \operatorname{sinc}^2\left\{\frac{\pi}{2K} x\right\} \left|c_0 + 2 \sum_{i=1}^{n} c_i \cos\left(\frac{\pi x i}{K}\right)\right|^2 + \frac{1}{2K^2} \sum_{m=1}^{\infty} \left\{\operatorname{sinc}^2\left(\frac{\pi m}{K}\right) \left|c_0 + 2 \sum_{i=1}^{n} c_i \cos\left(\frac{2\pi m i}{K}\right)\right|^2\right\} \delta(x-2m) \quad (3.5.7)$$

This equation was programmed on a digital computer (see appendix A4, program SPECT) and the power spectrum density was plotted on a dB scale, using the following known relation:

$$[G(f)] \text{ dB} = 10 \log_{10} \left\{\frac{G(x)}{G(x_o)}\right\} \quad (3.5.8)$$

where x_o corresponds approximately to the low cut off frequency of the filter.

In the actual program SPECT, x_o was set to 10^{-5},

and the Nyquist frequency (f_N) equal to unity. Using a plotting technique similar to the one employed in section 3.3, it was possible to display (see figure 3.5.1 to 3.5.3) the power spectrum dinsity of various types of Binary Transversal Filters.

The results of these simulations are of value in that they can predict the measurements of the fourth chapter, and of particular interest - the discrete spectral lines appearing at multiples of the bit rate.

Since at this stage the power spectrum density is available, we can, using the trapezoidal rule of integration [17], compute the energy in any given bandwidth and hence the energy ratio.

The procedure used in calculating the out of band to in band energy ratio $\{E(h)/E(\omega_0)\}$ is similar to the one described in last section. The differences are detailed as follows:

i) The numerical integration was done using a Trapezoidal algorithm instead of Romberg's, and incremental frequencies steps of .01 f_N were used.

ii) Since the integration could not be computed up to infinity, it was truncated at 40 f_N. It was concluded that this value was sufficient since the difference in energy ratio for 20 f_N or 40 f_N was less than 1 dB (see table 3.5-A).

iii) The coefficients c_i were unperturbed.

Unfortunately, the results obtained by this method (see table 3.5-A) were not as enthusiastic as those of last section. The reason for these discrepancies are still to be clarified. Nevertheless, the importance of this exercise will become apparent in next section where the power spectrum density and the energy ratio of the combination of a BTF and an analog LPF will be evaluated.

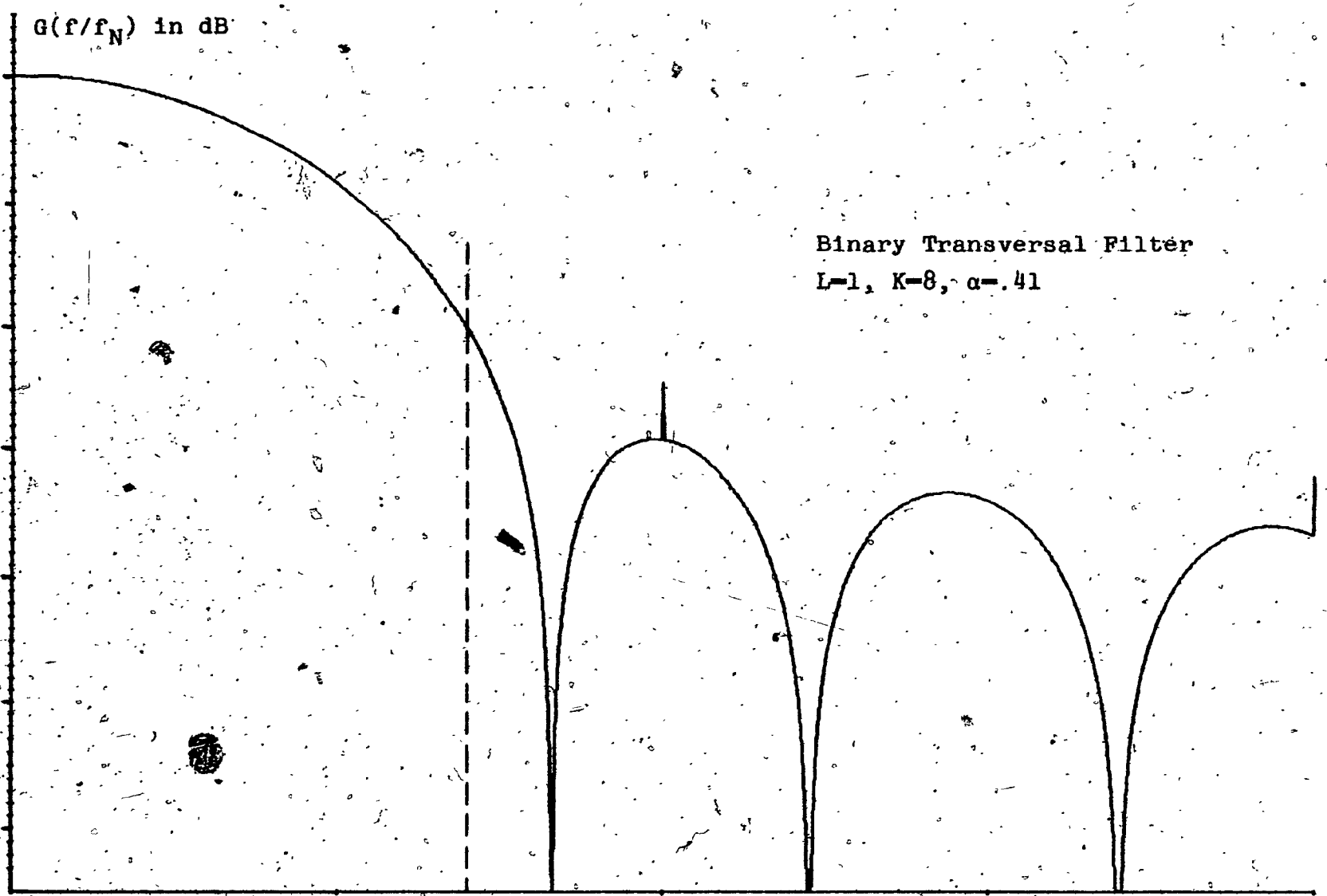

Fig. 3.5.1 - B.T.F. Power Spectrum Density

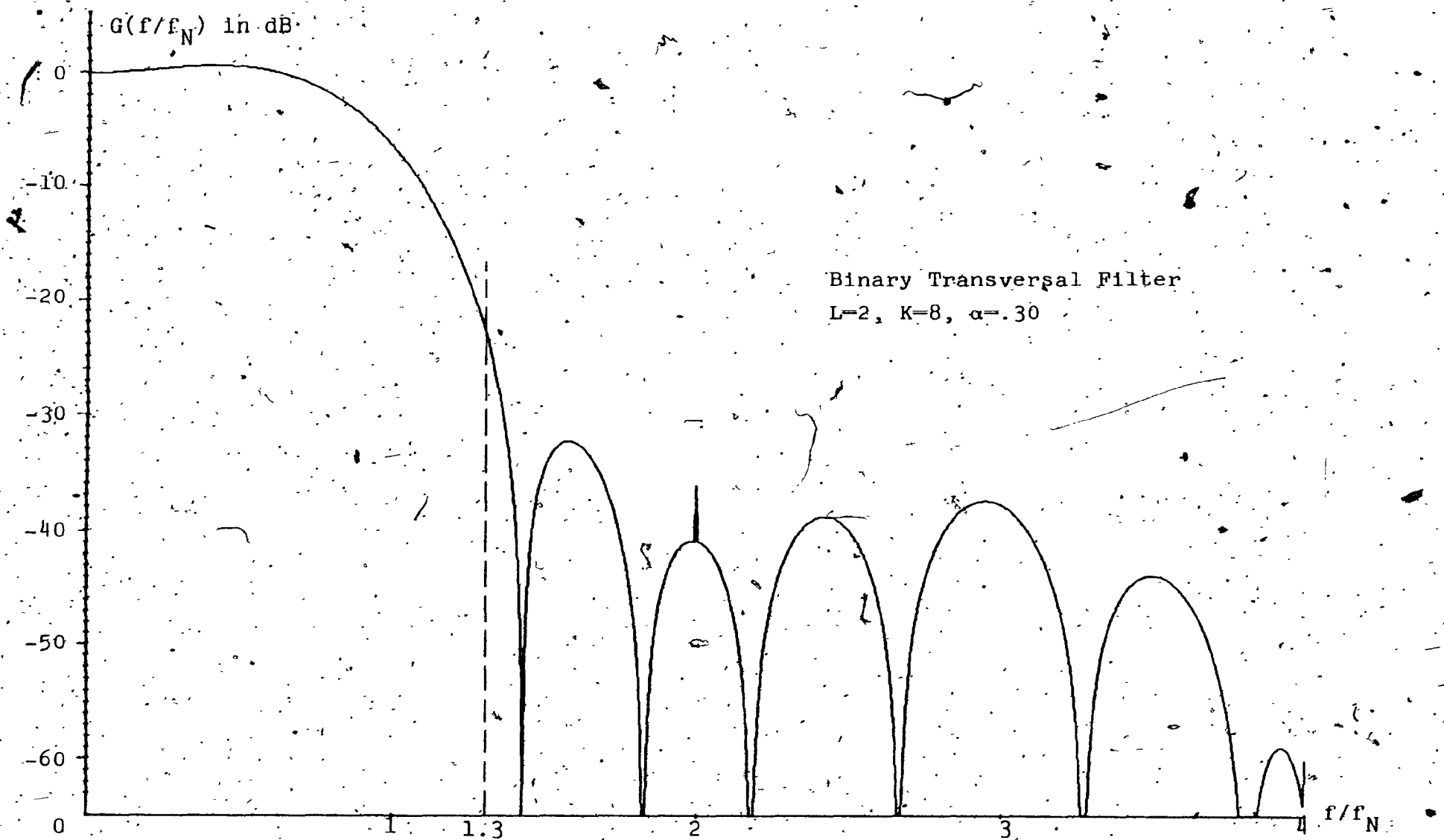

Fig. 3.5.2 - B.T.F. Power Spectrum Density

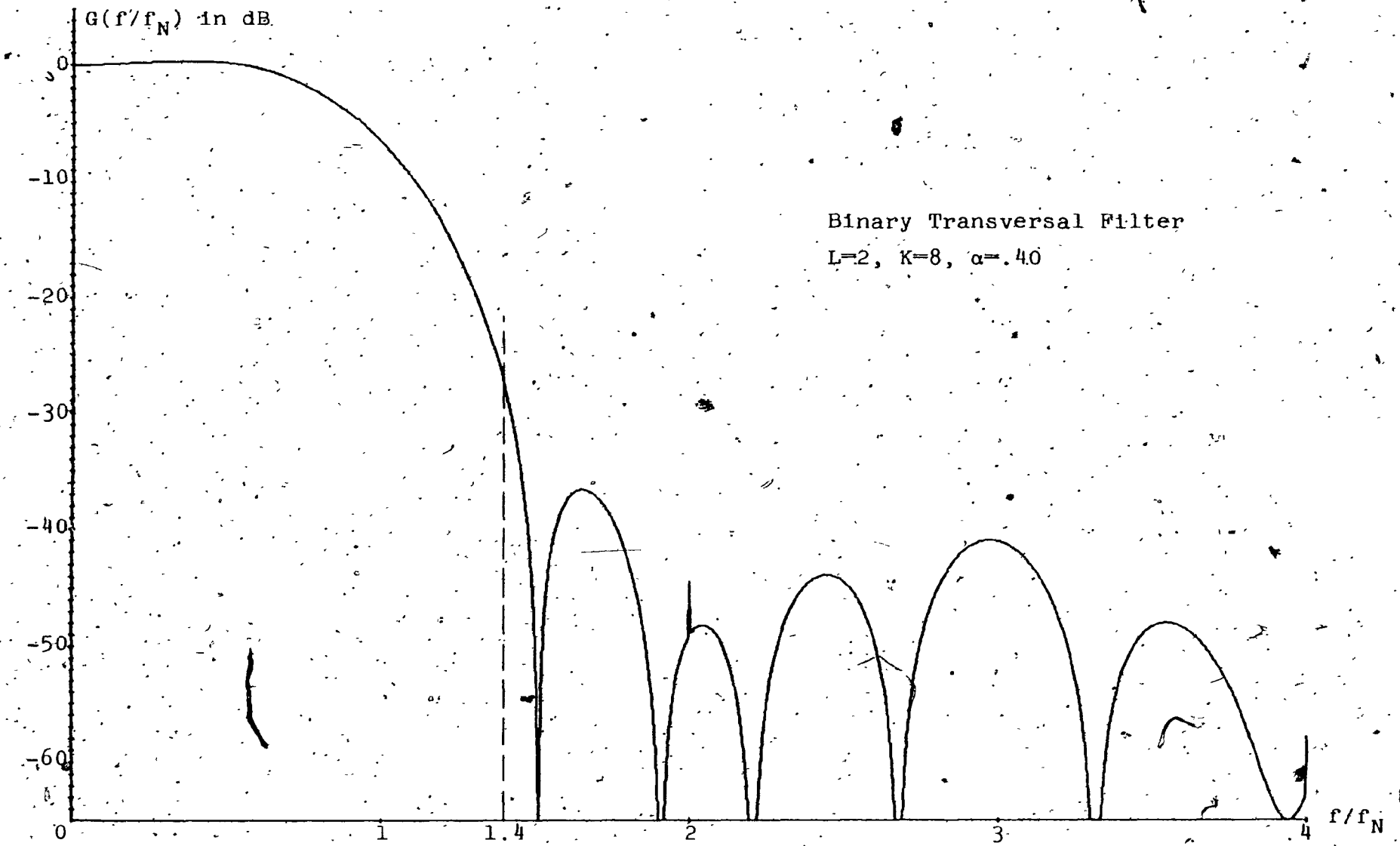

Fig. 3.5.3 — B.T.F. Power Spectrum Density

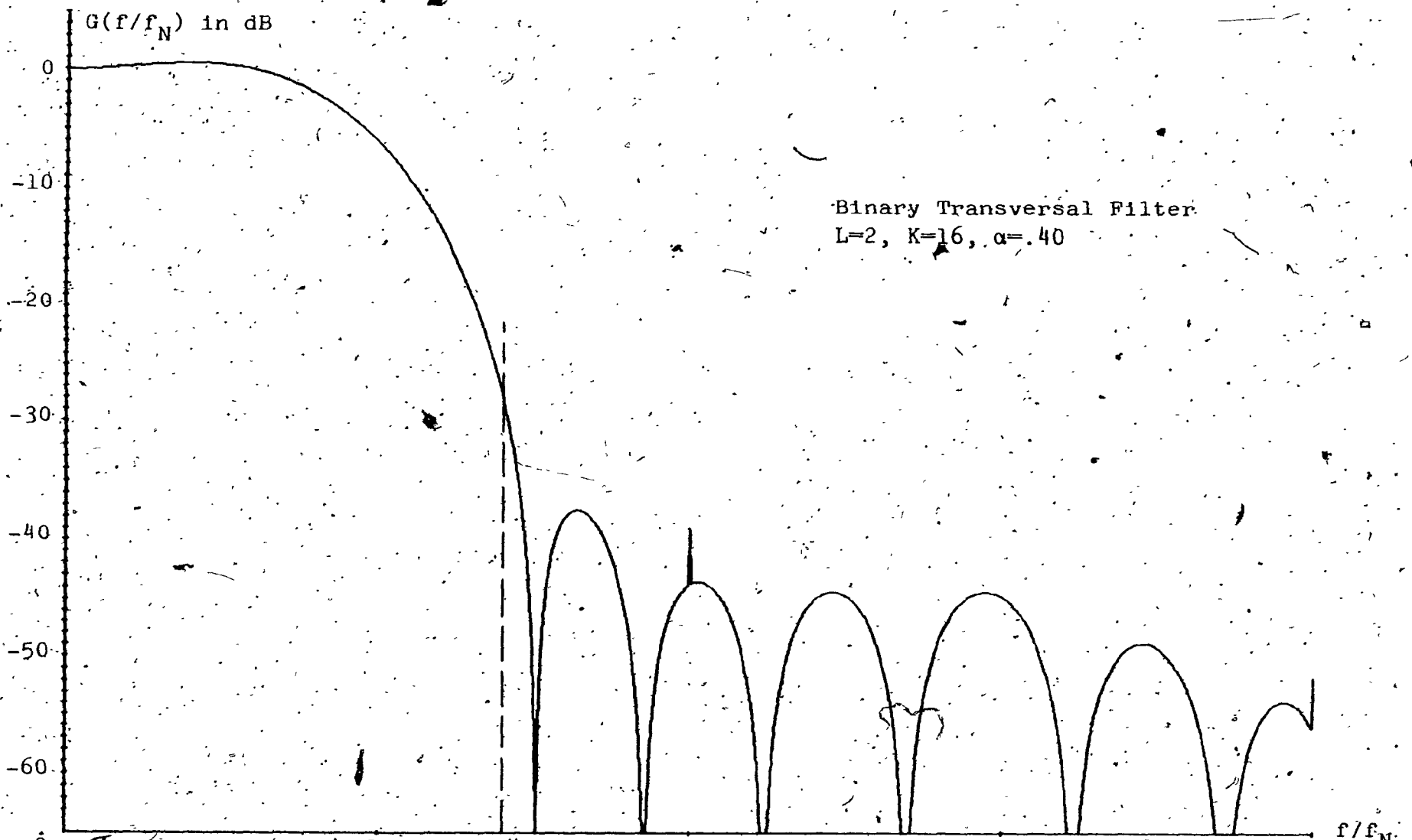

Fig. 3.5.4 - B.T.F. Power Spectrum Density

BTF Characteristics			Optimum (1) Energy Ratio (dB)	Computed (2) Energy* Ratio (dB)	Integral Truncated at	Error (1)-(2) dB
L	K	α				
1	8	.41	-22.21	-18.86	$40f_N$	-3.35
2	8	.3	-23.84	-24.51	$40f_N$	.67
2	8	.4	-24.24	-25.27	$40f_N$	1.03
2	8	.4	-24.24	-26.15	$20f_N$	1.91

* Trapezoidal rule of integration

Table 3.5-A - Energy Ratio Computed from Power Spectrum Density

3.6 Energy Ratio Performance of a Binary Transversal Filter Followed by a Low Pass Filter

The intent of this section is to investigate the effect of combining a Butterworth type second order Low Pass filter with the Binary Transversal Filter, as illustrated in figure 3.6.1.

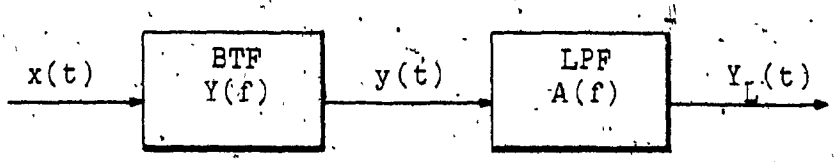

Fig. 3.6.1: Combined Binary Transversal Filter and Low Pass Filter network

In section 3.2, it was shown that to achieve in a 40% excess Nyquist bandwidth, an energy ratio of 28 dB, a BTF having a minimum of 57 coefficients (from table 3.2-: L=2, K=14) was required.

Recalling that one of the major restrictions in increasing the number of samples per baud interval (K) is the hardware switching speed, it is not difficult to conclude that the lower the K value, the simpler is the practical realization of the BTF.

Experimentally, it was found that, for a data bit rate of 32 kbits, and for COS-MOS logic devices, K=8 was the largest value that could be used without a noticeable degradation in the pulse's shape. But for K=8, the maximum energy ratio is in the range of 24 dB. A method of increasing this

energy ratio can be found in a hybrid filter that is the combination of a digital Binary Transversal Filter with an analog Low Pass Filter. The purpose of this arrangement is to attenuate further the higher order component of the BTF spectrum (see figure 3.2.1-c). Depending on the order and on the cut off frequency of the Low Pass Filter, the resulting eye pattern can be made continuous.

In our study, a second order Low Pass filter having a Butterworth response [19] was arbitrarily chosen.* The cut off frequency of the filter required to minimize the intersymbol interference of the hybrid network was determined experimentally to be approximately 2.8 f_N (45 kHz), where f_N is the Nyquist frequency (16 kHz). This cut off frequency (f_c) was then fine tuned until the aperture of the continuous eye diagram becomes maximum.

It is important to notice that a hybrid network will limit the original digital BTF's self-adaptability to different bit rates. Fortunately, in the majority of cases the BTF is designed for a specific bit rate and adaptability is not an important factor. The following paragraphs will detail hybrid BTF techniques.

Assuming that $Y_1(f)$ and $A(f)$ are the frequency responses of the BTF and LPF respectively (see figure 3.6.1) then the overall response $Y_L(f)$ is given by:

$$Y_L(f) = Y_1(f) \cdot A(f) \qquad (3.6.1)$$

* Since linear phase is required, a Bessel or a Butterworth-Thompson filter would yield better results.

and the magnitude squared is:

$$|Y_L(f)|^2 = |Y_I(f)|^2 \cdot |A(f)|^2 \qquad (3.6.2)$$

The first term on the right hand side was given in equation 3.5.6. For a Butterworth second order LPF the magnitude of the frequency response is [27, p. 285]:

$$|A(f)|^2 = \frac{A_o^2}{(f/f_c)^4+1} \qquad (3.6.3)$$

where

A_o = filter gain at zero frequency

f_c = filter cut off frequency (3 dB point)

Setting A_o equal to one and $f_c = \gamma f_N$, where γ was determined experimentally to be 2.80, equation 3.6.3 becomes:

$$|A(f)|^2 = \{1+(f/\gamma f_N)^4\}^{-1} \qquad (3.6.4)$$

Finally, the power spectrum density G(f) of the hybrid filter is obtained by replacing in equation 3.5.3 $|Y_I(f)|^2$ by $|Y_L(f)|^2$ (equation 3.6.2). A function called HLPF based on this development (see Appendix A4) was added to the computer program SPECT in order to calculate the attenuation due to the Low Pass Filter. The out of band to

in band energy ratio was evaluated using the same program (SPECT) as in last section, and the results for different BTF/LPF are given in table 3.6-A.

The power spectrum density of the hybrid filter is not displayed in this section as it is very similar to that shown in figure 3.5.1 to 3.5.4. The reasons for these similarities lie in the fact that a second order Butterworth LPF has a slow monotonically decreasing transfer function, and at $4f/f_N$ only 7 dB of additional attenuation can be observed.

In addition, an improvement of the hybrid filter over that of the BTF alone can be noticed. For example, with the results obtained in last section (Table 3.5-A) the difference in energy ratio (Table 3.6-A) due to truncating the integral at $4\ f_N$ instead of $40\ f_N$ is negligible, proving that most of the energy is concentrated in the specified excess Nyquist bandwidth. It is also interesting to notice that as much as 5 dB improvement in energy ratio exists between the 40% and 30% excess Nyquist hybrid filter (L=2, K=8) while less than .5 dB was observed using the BTF alone.

Before concluding, some mention must be made of the work of F.S. Hill and W.V. Lee [26] who have presented a syntesis method for the hybrid Binary Transversal Filter - Low Pass Filter combination. In their method, the BTF coefficients and the LPF cut off frequency (f_c) were determined using a

computational routine which minimized the so called digital Mean Square Error (MSE*). The most important result of their work is the extremely low number of BTF coefficients required. Using a 4th order Butterworth filter and only a 5 coefficients BTF almost ideal Nyquist pulses were obtained.

It is evident, in view of Hill and Lee's results, that further research should be conducted towards a modified Mueller method which would possibly optimize the BTF coefficients and the Low Pass Filter simultaneously.

* The digital MSE is the variance of the peak distortion [26]

BTF Characteristics			Without LPF		With LPF		Integral Truncated at	Improvement in Energy Ratio (1)-(2)
K	L	α	Optimum Energy Ratio (dB)	Computed (1) Energy * Ratio (dB)	Computed (2) Energy * Ratio (dB)	f_c/f_N		
1	8	.41	-22.21	-18.86	-21.97	2.80	40 f_N	3.11
1	8	.41	--	--	-22.00	2.80	4 f_N	--
2	8	.30	-23.84	-24.51	-32.23	2.80	40 f_N	7.72
2	8	.30	--	--	-32.30	2.80	4 f_N	--
2	8	.40	-24.24	-25.27	-38.05	2.80	40 f_N	12.78
2	8	.40	--	--	-38.22	2.80	4 f_N	--

* Trapezoidal rule of integration

Table 3.6-A - Energy Ratio for a Hybrid BTF-LPF Network

CHAPTER 4

DESIGN AND EVALUATION OF A BTF FOR SATELLITE COMMUNICATIONS

4.1 Design of a Binary Transversal Filter for Satellite Communications

The theory described in the previous chapters will now be applied to an example satellite communications [32, 33]. Attention will be focused in particular on the design of a premodulation filter for the Single Channel per Carrier (SCPC), Pulse Code Modulation (PCM), Multiple Access Demand Assignment Equipment (SPADE) [22].

The SPADE system was conceived to make optimum utilization of Satellite transponders interconnecting earth stations carrying light traffic. In this system, the Frequency Division Multiplexed (FDM) channels are not preassigned i.e., an idle channel can be used by any of the ground stations. A communication link can be established between any two earth stations by the simple demand of the one originating the call. The so called DASS (Demand Assignment Signaling and Switching) control assigns at random one of the available channels. Experts in this field [22] have concluded that SPADE is more efficient in the sense of power and bandwidth per channel than any of the presently used methods.

A maximum of 800 channels, occupying 36 MHz of bandwidth, can be transmitted via a single satellite transponder. The overall characteristics of the SPADE system are:

Channel encoding	PCM
Modulation	4 Phase PSK (coherent)
Bit rate	64 Kb/s
Bandwidth per channel	38 kHz
Channel spacing	45 kHz
Stability requirements	±2 kHz (with AFC)
Bit error rate at threshold	10^{-4} (Eb/N_o 10.5 dB)

The SPADE multichannel frequency allocation spectrum is shown in figure 4.1.1 [22]. Note at the bottom of the spectrum the presence of the Common Signaling Channel (CSC). It is through this channel that the Demand Assignment Signaling and Switching is done. An outgrowth of the SPADE system is the so called SCPC (Single Channel per Carrier) which uses preassignment channels [28]. The SCPC has more stringent specifications than SPADE in order to achieve better performances.

The simplified block diagram of the 4 Phase or QPSK modulator shown in figure 4.1.2 was taken from A.M. Werth [21]. Notice the two low pass filters preceeding the modulator.

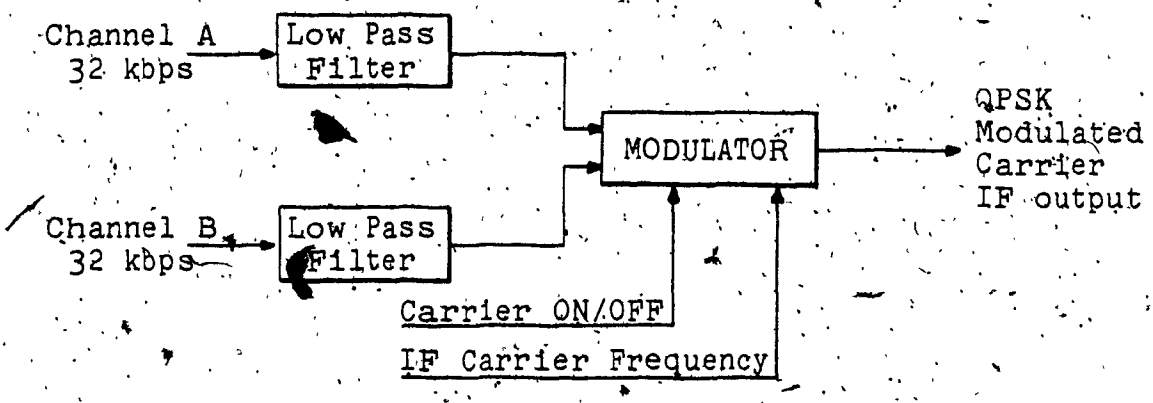

Figure 4.1.2: SPADE QPSK Modulator block diagram.

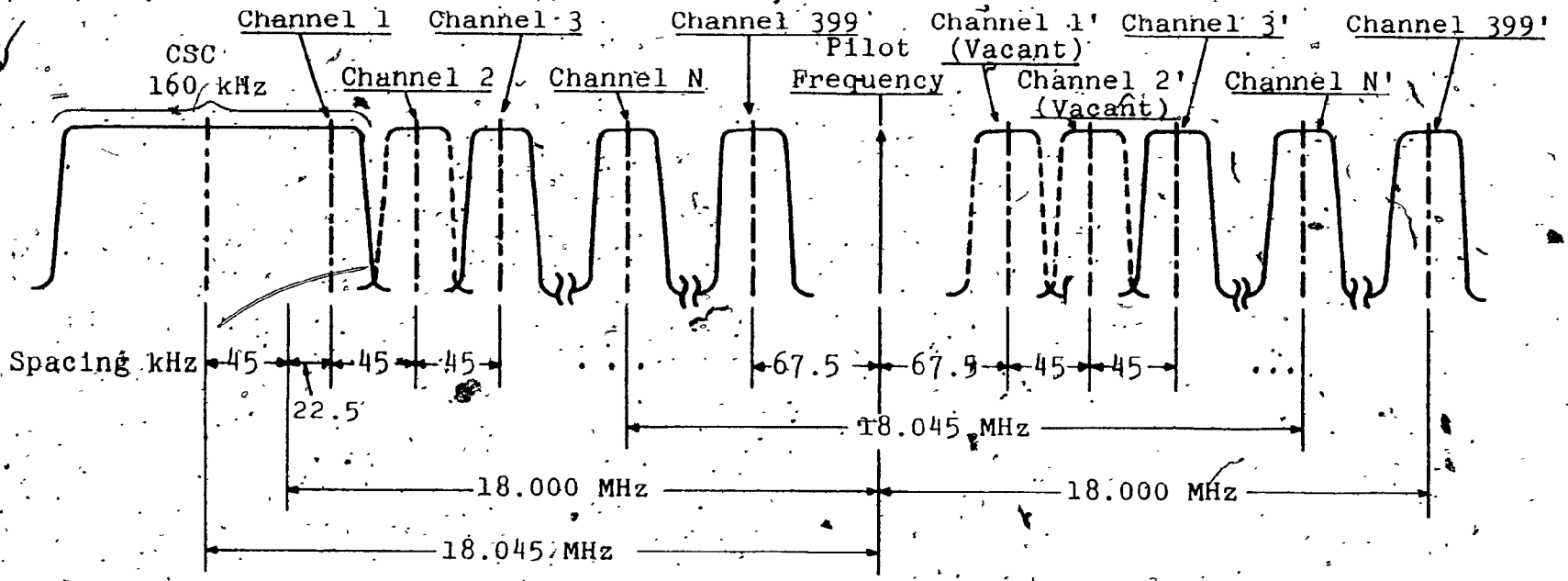

98 MHz	116 MHz	134 MHz	Terminal IF (Typical)
52 MHz	70 MHz	88 MHz	Station IF
			Intelsat IV Transponder 10
6.302 GHz	5.320 GHz	6.338 GHz	Uplink
4.077 GHz	4.095 GHz	4.113 GHz	Downlink

Figure 4.1.1 – SPADE Frequency Allocation Spectrum

The specifications for the two filtered 32 kbps data streams (Chs A and B) are [23]:

a) Out of channel band signal power (i.e., power content at frequencies ≥ 22.5 kHz) after low pass filtering shall be greater than 26 dB down from the in band signal power. (This is equivalent of saying that the out of band to the in band energy ratio shall be less than -26 dB, where all frequencies greater than 22.5 kHz are considered out of band. This corresponds to 1.406 times the Nyquist Frequency (α=40.6%); f_N=16 kHz)

b) Jitter occurring in the form of filtered data zero crossing error due to filtered phase nonlinearity shall be less than or equal to 7% of a bit interval (i.e., 31.25 x .07 = 2.1875 μsec).

As stated at the beginning of this chapter, a hybrid Binary Transversal Filter was designed and tested; this filter fully complied with these specifications.

In the process of developing the final BTF, a first prototype was implemented which did not meet the SPADE specifications. Nevertheless, the circuit diagram and the test results of this filter will be included in the next section as they confirm the theoretical predictions of chapter 3. This filter could be employed in situations where the requirements are less stringent.

4.2 Binary Transversal Filter Circuit Description

In this section, the general principle of operation of a Binary Transversal Filter implemented with digital techniques is given.

As stated in the beginning of this chapter, two BTF's were completely designed and evaluated. The first one designated BTF 1-8, where the first digit following "BTF" represent the number of lobes (L-1) and the second, the number of samples per baud interval (K-8). This filter had a 41% excess Nyquist bandwidth. The second was a hybrid type filter and was called BTF 2-8. Of this last model, three units were assembled and tested, two of them had a 30% excess Nyquist bandwidth and one 40%.

The block diagram of a Binary Transversal Filter is shown in figure 4.2.1. An external clock (dashed lines) generates sharp pulses which are K times faster then the data bit rate (1/T).

This clock is used for two purposes:

i) To shift toward the right the content of the digital shift register (flip, flop) DS_i. At each clock pulse the content of DS_i is transferred to DS_{i+1}.

ii) To drive the "divide by K" module which in turn generates pulses having a width of D-sec (equation 3.1.2).

The next stage is a differentiator and a buffer, which converts the D-sec width pulses into positive impulses.

These bit rate spikes synchronize the external random data generator (dashed lines) whose output is binary and of the Non Return to Zero format. An "and" logic gate combines these NRZ random pulses with the D-sec periodic pulses arriving from the "divide by K" module. This leads to Return to Zero type pulses. If a binary one is present at the output of the random generator and a pulse of width "D-sec" at the output of the divider then a pulse p(t) (see section 3.3) will start propagating through the shift registers. Depending on the sign of the coefficients "c_i", a buffer or a buffer inverter is used at the output of the corresponding flip flop. These buffers are required to avoid the voltage drop due to the loading resistors R_i. At the output of each buffer/inverter a resistor $R_i = a/c_i$ is employed to approximate a current proportional to c_i.

These resistors are the physical realization of multiplicative constants. All resistors are connected to the input of an operational amplifier used in its inverting configuration. An inverted staircase approximation of the Nyquist type pulse is present at this point. Afterwards, an active low pass filter follows which smoothens and inverts again the staircase response of the BTF. The final output of the filter is a continuous wave truncated at L lobes (see equation 3.1.1 d).

Having established the general principle of operation of the BTF a review of the differences between the BTF 1-8 and BTF 2-8 models is now given.

The circuit diagram of BTF 1-8 is given in figure 4.2.2.

This filter was implemented using TTL logic devices and the response was truncated at one lobe (L=1). As a result, the inverters were not required. The buffers also were not necessary due to the relatively low output impedance of the TTL devices compared to the resistors R_i. The values of the resistors R_1 to R_{16}, as well as the following information is given in table 4.2-a:

1st column - BTF coefficients c_i accurate up to 8 digits

2nd column - The exact value of the resistors ($R_i=a/c_i$)

3rd Column - The standard 1% resistor which is the closest to the exact value.

4th column - The error in percent between the last two colums.

Note that the value of the middle coefficient is normalized to unity and the corresponding exact resistor has a standard 1% value, in this manner the nominal percentage error for the middle multiplier is always nul.

As it will be demonstrated in next section, this filter did not comply with the SPADE specifications and for

this reason it has never gone beyond the stage of a prototype. For this same reason no low pass filter was permanently added to it, although some measurements were taken using an external low pass filter.

The circuit diagram for the BTF 2-8 is given in figure 4.2.3.

This filter having a total of 32 coefficients* was implemented using COS-MOS integrated circuits to take advantage of this relatively low power dissipation in comparison with other families. In this case buffer and buffer inverters were required for two reasons: first, due to the relatively high output impedance of the MOS devices and, second, due to the inverted polarity of the second lobe.

The resistance values R_1 to R_{32} for 30% and 40% excess Nyquist bandwidth are given in tables 4.2-B and 4.2-C respectively.

A Butterworth second order low pass filter was

* Note: The actual number of coefficients required is the total less one. This is due to the fact that the first and last coefficients are always zero and appear exactly at the same time instant with respect to the bit interval (see figure 3.1.2).

designed and tuned following the guide lines given in [27]. At the output of this filter a 150 μF capacitor was used to eliminate the dc component present at that point. This capacitor with the associated resistors is the realization of a very low frequency high pass filter discussed in section 3.4. To match the Operational Amplifier output impendance with the 75 ohms requirement a minimum loss resistive device was used. A double sided printed circuit artwork for the BTF 2-8 was prepared and is shown in figure 4.2.4-a and 4.2.4-b.

The final assembled version of the BTF 2-8 is shown in figure 4.2.5. Notice that all input and output signals are accessible through the filter front pannel BNC connectors. Provision was also made to have these signals on the rear plugboard via A, B, C, D pins (figure 4.2.4-b).

Finally, figure 4.2.6 shows the BTF 2-8 components layout. This drawing greatly facilitates the filter assembling procedure.

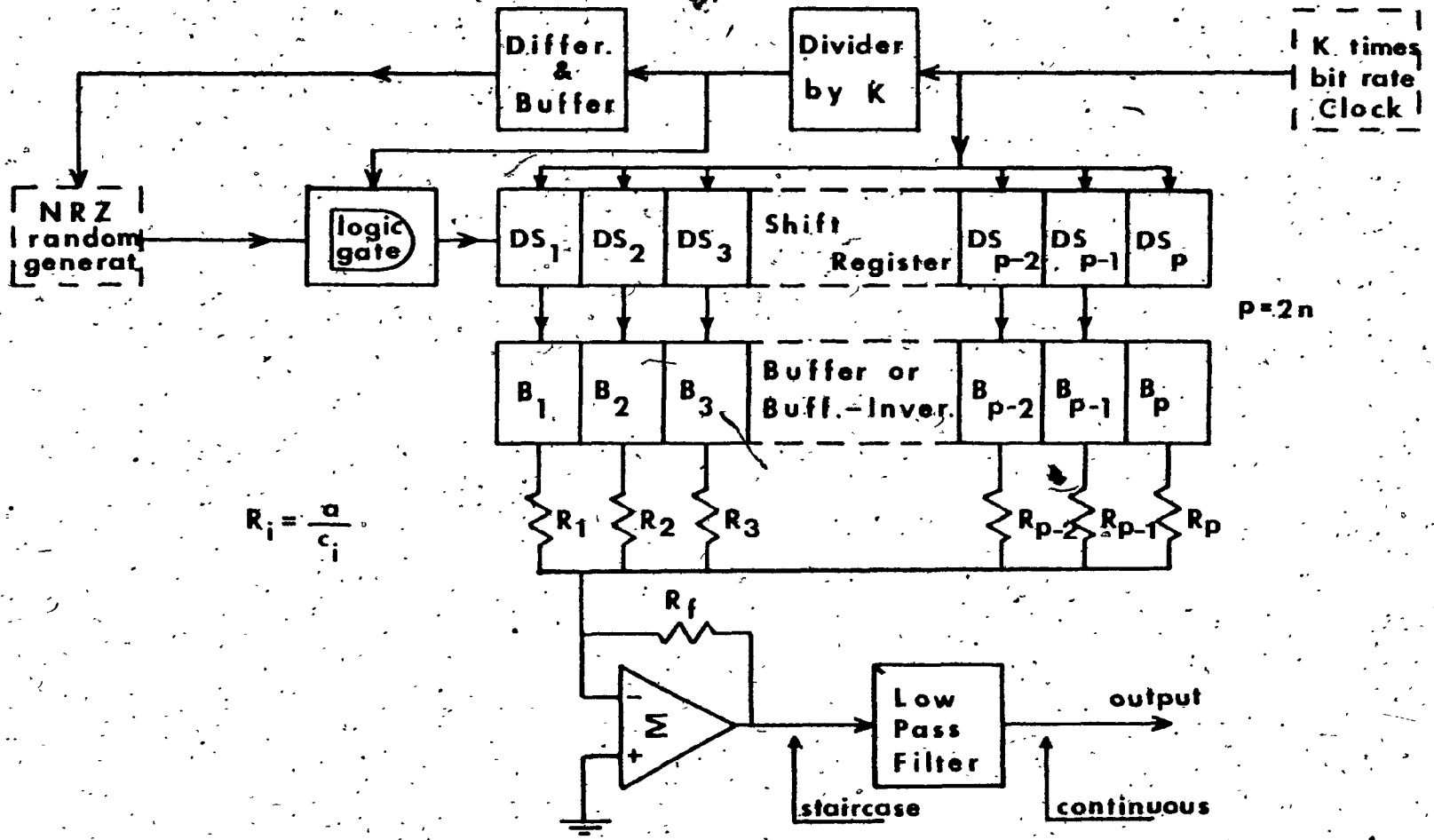

Fig. 4.2.1 - Binary Transversal Filter General Block Diagram

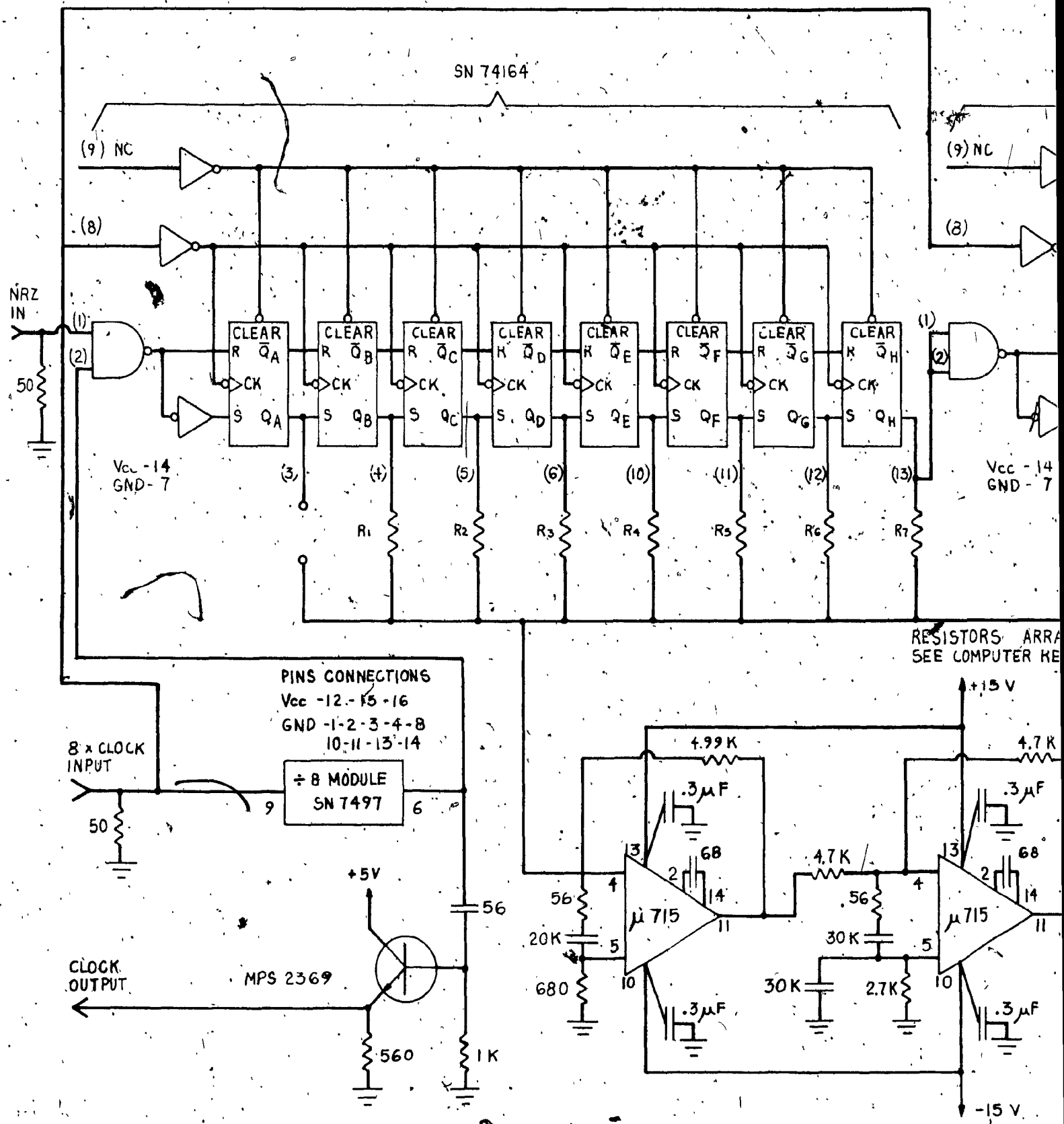
SN 74164
(9) NC
(8)
NRZ IN
(1)
(2)
50
CLEAR
R $\bar{Q}_A$
CK
S Q_A
CLEAR
R $\bar{Q}_B$
CK
S Q_B
CLEAR
R $\bar{Q}_C$
CK
S Q_C
CLEAR
R $\bar{Q}_D$
CK
S Q_D
CLEAR
R $\bar{Q}_E$
CK
S Q_E
CLEAR
R $\bar{Q}_F$
CK
S Q_F
CLEAR
R $\bar{Q}_G$
CK
S Q_G
CLEAR
R $\bar{Q}_H$
CK
S Q_H
Vcc - 14
GND - 7
(3)
(4)
(5)
(6)
(10)
(11)
(12)
(13)
R_1
R_2
R_3
R_4
R_5
R_6
R_7
RESISTORS ARRA
SEE COMPUTER KE
PINS CONNECTIONS
Vcc -12-15-16
GND -1-2-3-4-8
10-11-13-14
8 x CLOCK INPUT
÷ 8 MODULE
SN 7497
9
6
+5V
56
CLOCK OUTPUT
MPS 2369
560
1K
+15 V
4.99K
4.7K
.3μF
68
56
20K
680
μ715
30K
2.7K
-15 V
UNLESS OTHERWISE SPECIFIED
CAPACITORS IN μF
RESISTORS IN OHMS

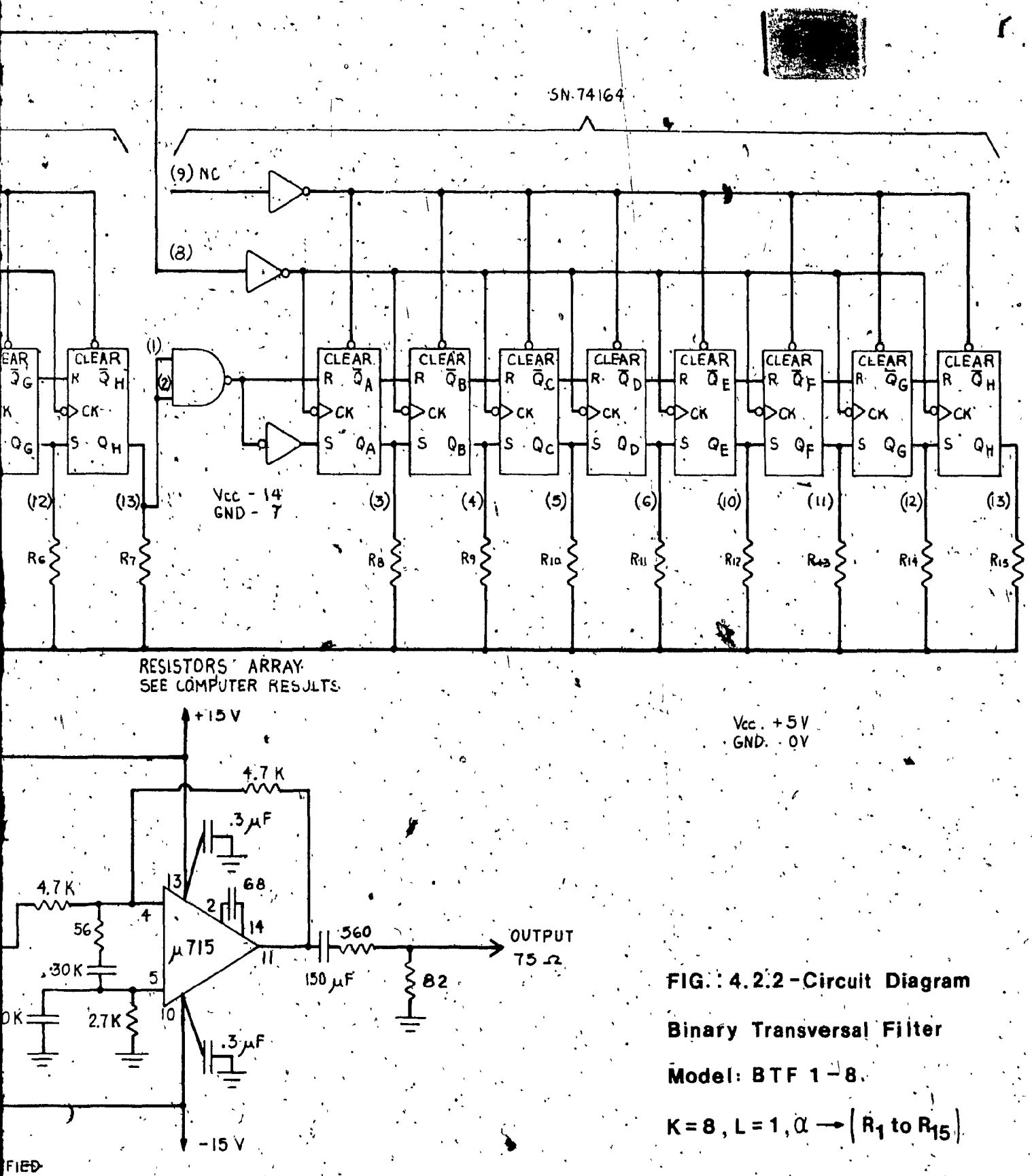

FIG.: 4.2.2 - Circuit Diagram

Binary Transversal Filter

Model: BTF 1 - 8.

K = 8, L = 1, α → $\{R_1$ to $R_{15}\}$

BINARY TRANSVERSAL FILTER
K = 8 L = 1 EXCESS NYQUIST = .41

COEFFICIENTS	RESISTORS	STANDARD 1%	% ERROR
C 1 =0.00000000	R 0 = XXXXXXX	XXXXXXX	XXXXXXX
C 2 = .16796938	R 1 = 29.70779 KOHMS	29.40 KOHMS	-1.04
C 3 = .29789642	R 2 = 16.75079 KOHMS	16.90 KOHMS	.89
C 4 = .45054517	R 3 = 11.07547 KOHMS	11.00 KOHMS	-.68
C 5 = .61172443	R 4 = 8.15727 KOHMS	8.25 KOHMS	1.14
C 6 = .76393489	R 5 = 6.53197 KOHMS	6.49 KOHMS	-.64
C 7 = .88905395	R 6 = 5.61271 KOHMS	5.62 KOHMS	.13
C 8 = .97131464	R 7 = 5.13737 KOHMS	5.11 KOHMS	-.53
C 9 =1.00000000	R 8 = 4.99000 KOHMS	4.99 KOHMS	-.00
C 10 = .97131461	R 9 = 5.13737 KOHMS	5.11 KOHMS	-.53
C 11 = .88905391	R 10 = 5.61271 KOHMS	5.62 KOHMS	.13
C 12 = .76393487	R 11 = 6.53197 KOHMS	6.49 KOHMS	-.64
C 13 = .61172444	R 12 = 8.15727 KOHMS	8.25 KOHMS	1.14
C 14 = .45054521	R 13 = 11.07547 KOHMS	11.00 KOHMS	-.68
C 15 = .29789645	R 14 = 16.75079 KOHMS	16.90 KOHMS	.89
C 16 = .16796933	R 15 = 29.70780 KOHMS	29.40 KOHMS	-1.04
C 17 =0.00000000	R 16 = XXXXXXX	XXXXXXX	XXXXXXX

Table 4.2-A: BTF 1-8 (α=.41) coefficients and resistors values

BINARY TRANSVERSAL FILTER
K = 8 L = 2 EXCESS NYQUIST = .40

COEFFICIENTS	RESISTORS	STANDARD 1%	% ERROR
C 1 =0.00000000	R 0 = XXXXXXX	XXXXXXX	XXXXXXX
C 2 =-.03299356	R 1 = 303.08947 KOHMS	301.00 KOHMS	-.69
C 3 =-.06035330	R 2 = 165.69101 KOHMS	165.00 KOHMS	-.42
C 4 =-.08915840	R 3 = 112.15993 KOHMS	113.00 KOHMS	.75
C 5 =-.11235153	R 4 = 89.00635 KOHMS	88.70 KOHMS	-.34
C 6 =-.12127514	R 5 = 82.45713 KOHMS	82.50 KOHMS	.05
C 7 =-.10701756	R 6 = 93.44261 KOHMS	93.10 KOHMS	-.37
C 8 =-.06208577	R 7 = 161.06751 KOHMS	162.00 KOHMS	.58
C 9 =0.00000000	R 8 = XXXXXXX	XXXXXXX	XXXXXXX
C 10 = .13280122	R 9 = 75.30051 KOHMS	75.00 KOHMS	-.40
C 11 = .27725692	R 10 = 36.06763 KOHMS	35.70 KOHMS	-1.02
C 12 = .44073954	R 11 = 22.68914 KOHMS	22.60 KOHMS	-.39
C 13 = .60859588	R 12 = 16.43126 KOHMS	16.50 KOHMS	.42
C 14 = .76386724	R 13 = 13.09128 KOHMS	13.00 KOHMS	-.70
C 15 = .88964507	R 14 = 11.24044 KOHMS	11.30 KOHMS	.53
C 16 = .97156468	R 15 = 10.29268 KOHMS	10.20 KOHMS	-.90
C 17 =1.00000000	R 16 = 10.00000 KOHMS	10.00 KOHMS	0.00
C 18 = .97156468	R 17 = 10.29268 KOHMS	10.20 KOHMS	-.90
C 19 = .88964507	R 18 = 11.24044 KOHMS	11.30 KOHMS	.53
C 20 = .76386724	R 19 = 13.09128 KOHMS	13.00 KOHMS	-.70
C 21 = .60859588	R 20 = 16.43126 KOHMS	16.50 KOHMS	.42
C 22 = .44073954	R 21 = 22.68914 KOHMS	22.60 KOHMS	-.39
C 23 = .27725692	R 22 = 36.06763 KOHMS	35.70 KOHMS	-1.02
C 24 = .13280122	R 23 = 75.30051 KOHMS	75.00 KOHMS	-.40
C 25 =0.00000000	R 24 = XXXXXXX	XXXXXXX	XXXXXXX
C 26 =-.06208577	R 25 = 161.06751 KOHMS	162.00 KOHMS	.58
C 27 =-.10701756	R 26 = 93.44261 KOHMS	93.10 KOHMS	-.37
C 28 =-.12127514	R 27 = 82.45713 KOHMS	82.50 KOHMS	.05
C 29 =-.11235153	R 28 = 89.00635 KOHMS	88.70 KOHMS	-.34
C 30 =-.08915840	R 29 = 112.15993 KOHMS	113.00 KOHMS	.75
C 31 =-.06035330	R 30 = 165.69101 KOHMS	165.00 KOHMS	-.42
C 32 =-.03299356	R 31 = 303.08947 KOHMS	301.00 KOHMS	-.69
C 33 =0.00000000	R 32 = XXXXXXX	XXXXXXX	XXXXXXX

Table 4.2-B: BTF 2-8 (α=.40) coefficients and resistors values

BINARY TRANSVERSAL FILTER.
K = 8 L = 2 EXCESS NYQUIST = .30

COEFFICIENTS	RESISTORS	STANDARD 1%	% ERROR
C 1 =0.00000000	R 0 = XXXXXXX	XXXXXXX	XXXXXXX
C 2 =-.05088995	R 1 = 196.50246 KOHMS	196.00 KOHMS	-.26
C 3 =-.08429580	R 2 = 118.62988 KOHMS	118.00 KOHMS	-.53
C 4 =-.11622969	R 3 = 86.03654 KOHMS	86.60 KOHMS	.65
C 5 =-.13878888	R 4 = 72.05188 KOHMS	71.50 KOHMS	-.77
C 6 =-.14326229	R 5 = 69.80204 KOHMS	69.80 KOHMS	-.00
C 7 =-.12150981	R 6 = 82.29788 KOHMS	82.50 KOHMS	.25
C 8 =-.06746663	R 7 = 148.22142 KOHMS	147.00 KOHMS	-.82
C 9 =0.00000000	R 8 = XXXXXXX	XXXXXXX	XXXXXXX
C 10 = .14356928	R 9 = 69.65278 KOHMS	69.80 KOHMS	.21
C 11 = .29221407	R 10 = 34.22149 KOHMS	34.00 KOHMS	-.65
C 12 = .45646856	R 11 = 21.90731 KOHMS	22.10 KOHMS	.88
C 13 = .62208039	R 12 = 16.07509 KOHMS	16.20 KOHMS	.78
C 14 = .77319600	R 13 = 12.93333 KOHMS	13.00 KOHMS	.52
C 15 = .89441023	R 14 = 11.18055 KOHMS	11.30 KOHMS	1.07
C 16 = .97285588	R 15 = 10.27901 KOHMS	10.20 KOHMS	-.77
C 17 =1.00000000	R 16 = 10.00000 KOHMS	10.00 KOHMS	0.00
C 18 = .97285592	R 17 = 10.27901 KOHMS	10.20 KOHMS	-.77
C 19 = .89441021	R 18 = 11.18055 KOHMS	11.30 KOHMS	1.07
C 20 = .77319599	R 19 = 12.93333 KOHMS	13.00 KOHMS	.52
C 21 = .62208044	R 20 = 16.07509 KOHMS	16.20 KOHMS	.78
C 22 = .45646860	R 21 = 21.90731 KOHMS	22.10 KOHMS	.88
C 23 = .29221403	R 22 = 34.22149 KOHMS	34.00 KOHMS	-.65
C 24 = .14356925	R 23 = 69.65280 KOHMS	69.80 KOHMS	.21
C 25 =0.00000000	R 24 = XXXXXXX	XXXXXXX	XXXXXXX
C 26 =-.06746659	R 25 = 148.22150 KOHMS	147.00 KOHMS	-.82
C 27 =-.12150981	R 26 = 82.29788 KOHMS	82.50 KOHMS	.25
C 28 =-.14326229	R 27 = 69.80204 KOHMS	69.80 KOHMS	-.00
C 29 =-.13878888	R 28 = 72.05188 KOHMS	71.50 KOHMS	-.77
C 30 =-.11622977	R 29 = 86.03648 KOHMS	86.60 KOHMS	.65
C 31 =-.08429573	R 30 = 118.62998 KOHMS	118.00 KOHMS	-.53
C 32 =-.05088997	R 31 = 196.50236 KOHMS	196.00 KOHMS	-.26
C 33 =0.00000000	R 32 = XXXXXXX	XXXXXXX	XXXXXXX

Table 4.2-C: BTF 2-8 (α=.30) coefficients and resistors values

Hybrid binary transversal filter

MODEL: BTF 2-8

K = 8, L = 2, $\alpha \rightarrow (R_1$ to $R_{32})$

32K BITS

UNLESS OTHERWISE SPECIFIED
CAPACITORS IN PF
RESISTORS IN OHMS
Vcc = +5 VOLTS

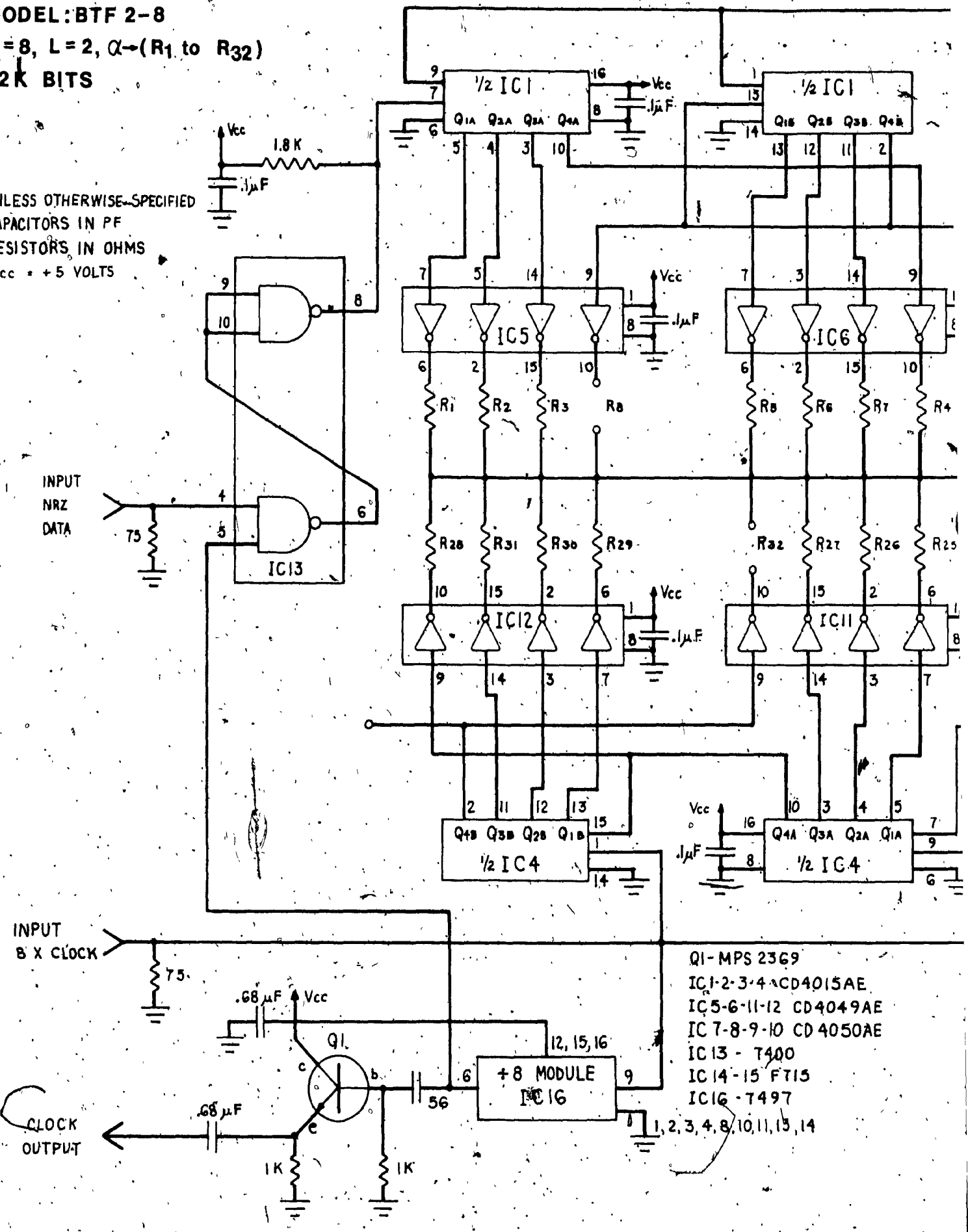

Q1 - MPS 2369
IC 1-2-3-4 CD4015AE
IC 5-6-11-12 CD4049AE
IC 7-8-9-10 CD4050AE
IC 13 - T400
IC 14-15 FT15
IC 16 - T497

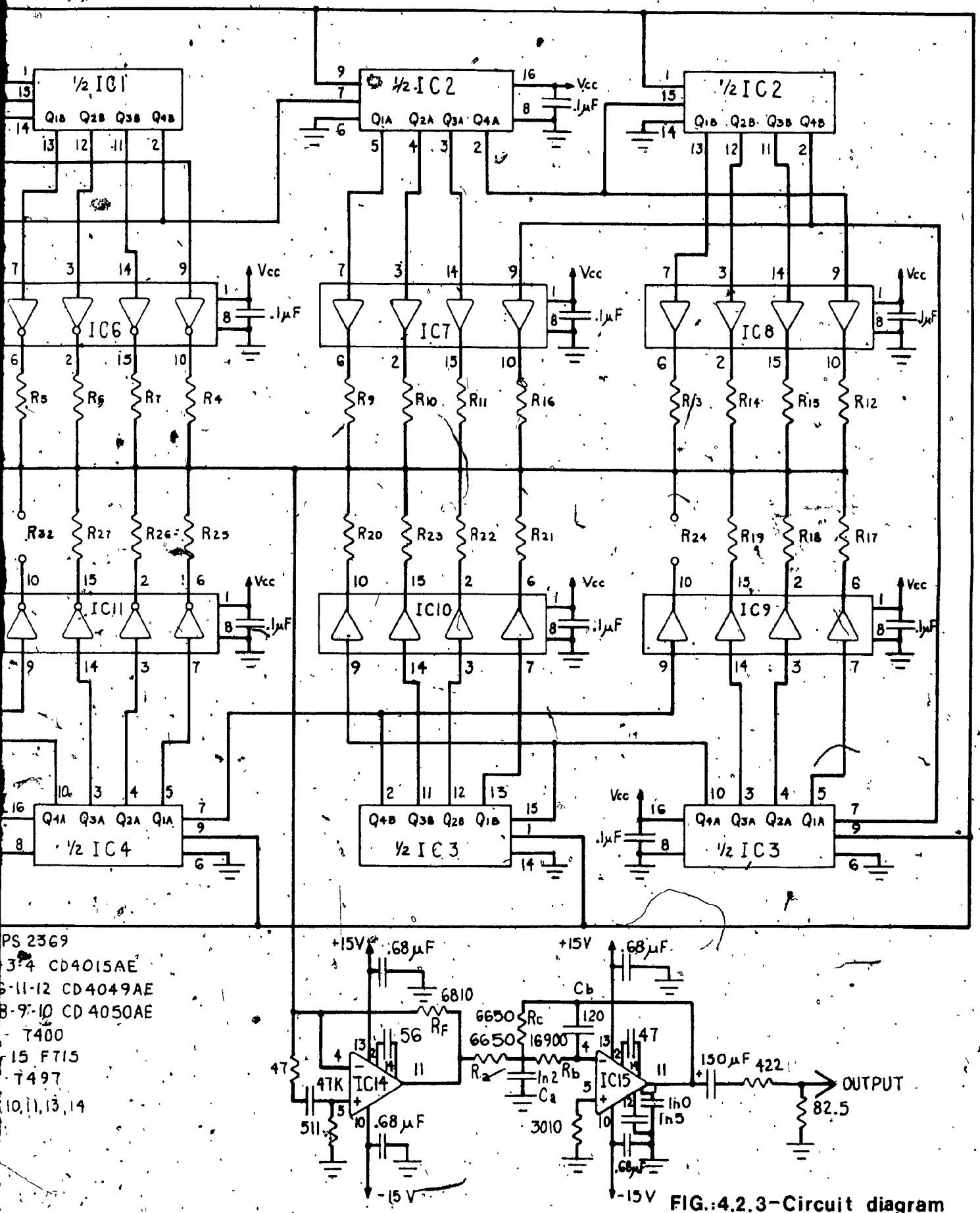

PS 2369
3-4 CD4015AE
6-11-12 CD4049AE
8-9-10 CD4050AE
- T400
15 FT15
T497
10,11,13,14

FIG.:4.2.3–Circuit diagram

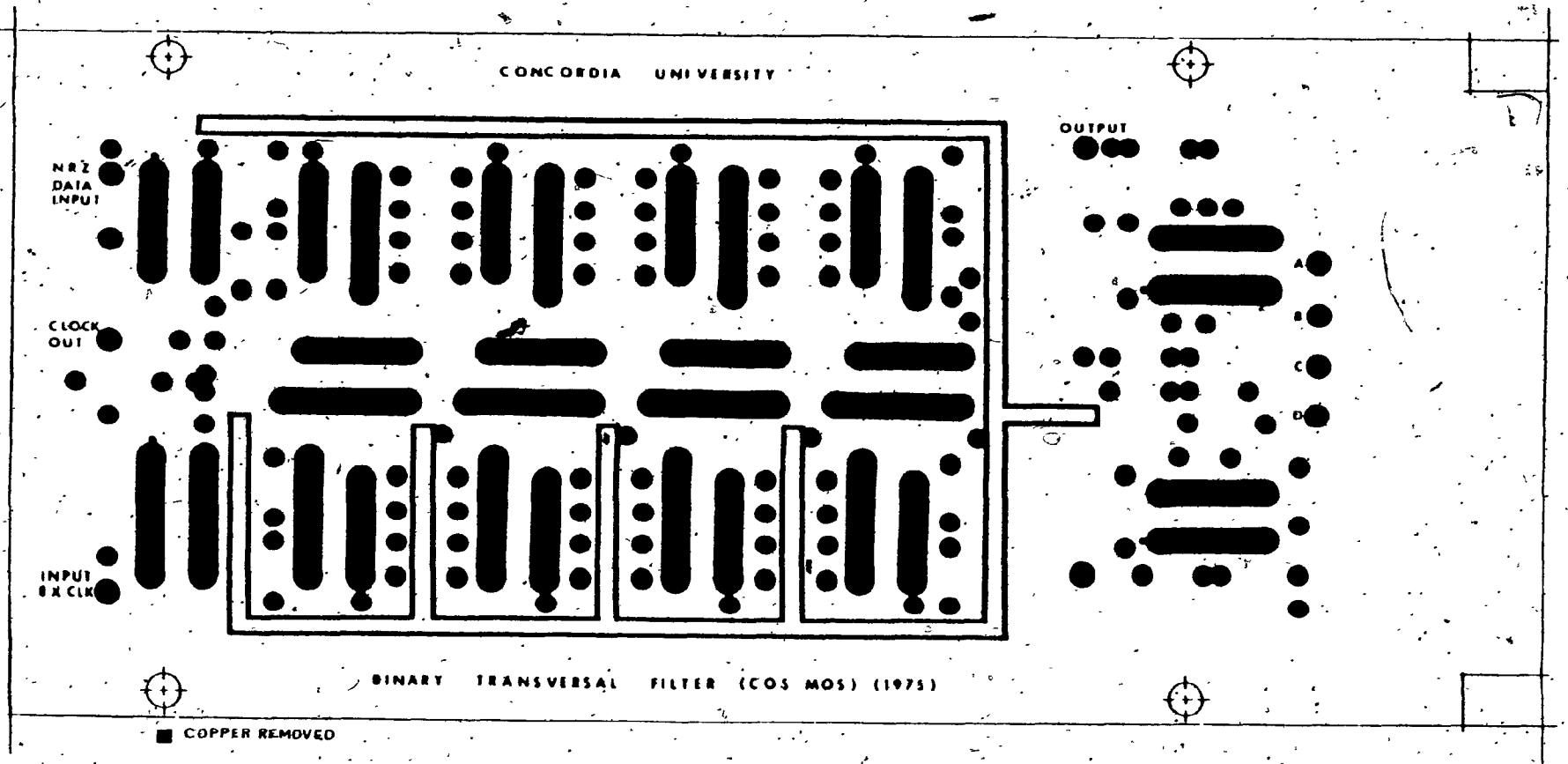

Figure 4.2.4-a: BTF 2-8 - Printed Circuit Artwork Components side

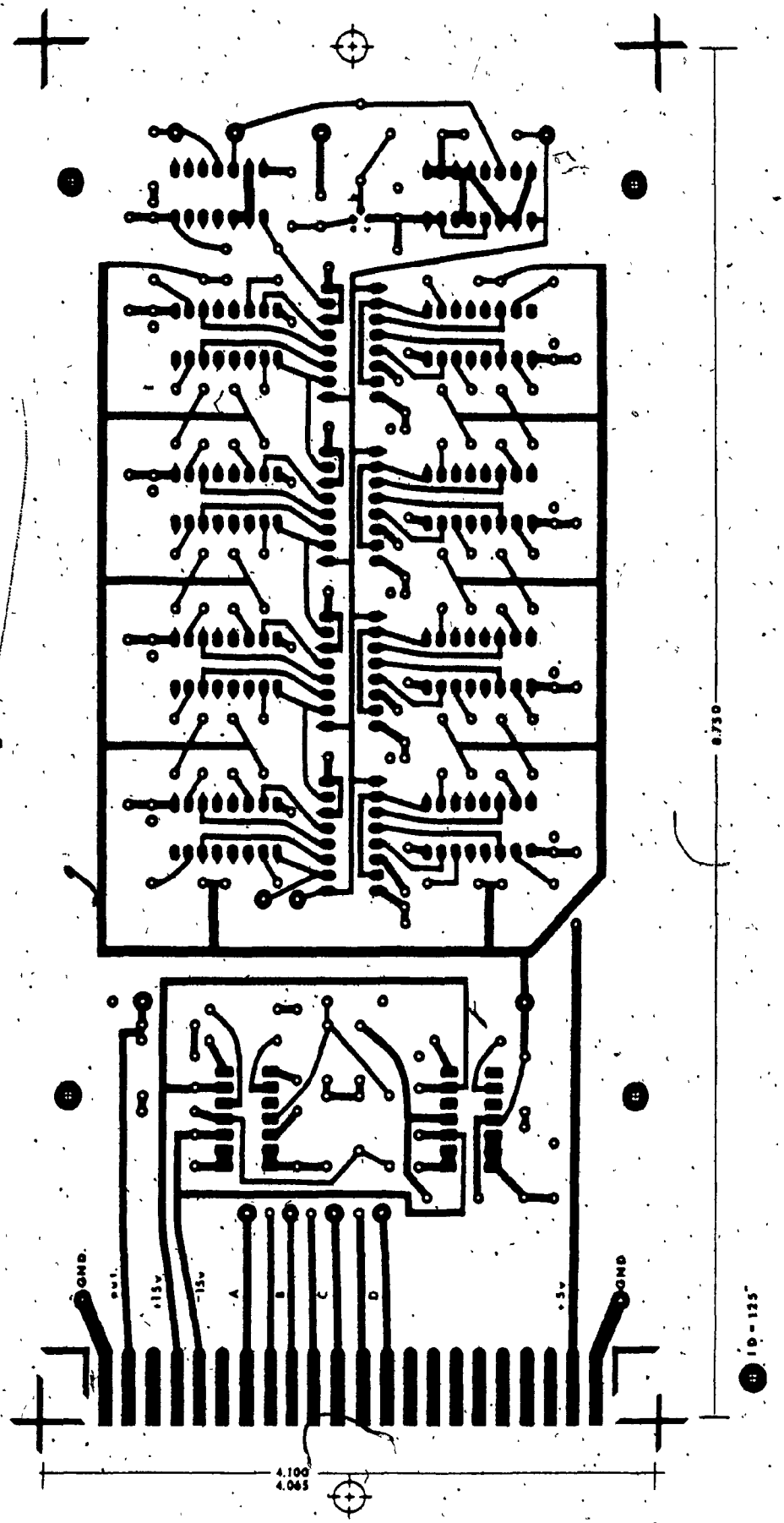

Figure 4.2.4-b: BTF 2-8 - Printed Circuit Artwork Soldering Side

FIG. 4.2.5 – Hybrid binary transversal filter BTF2-8

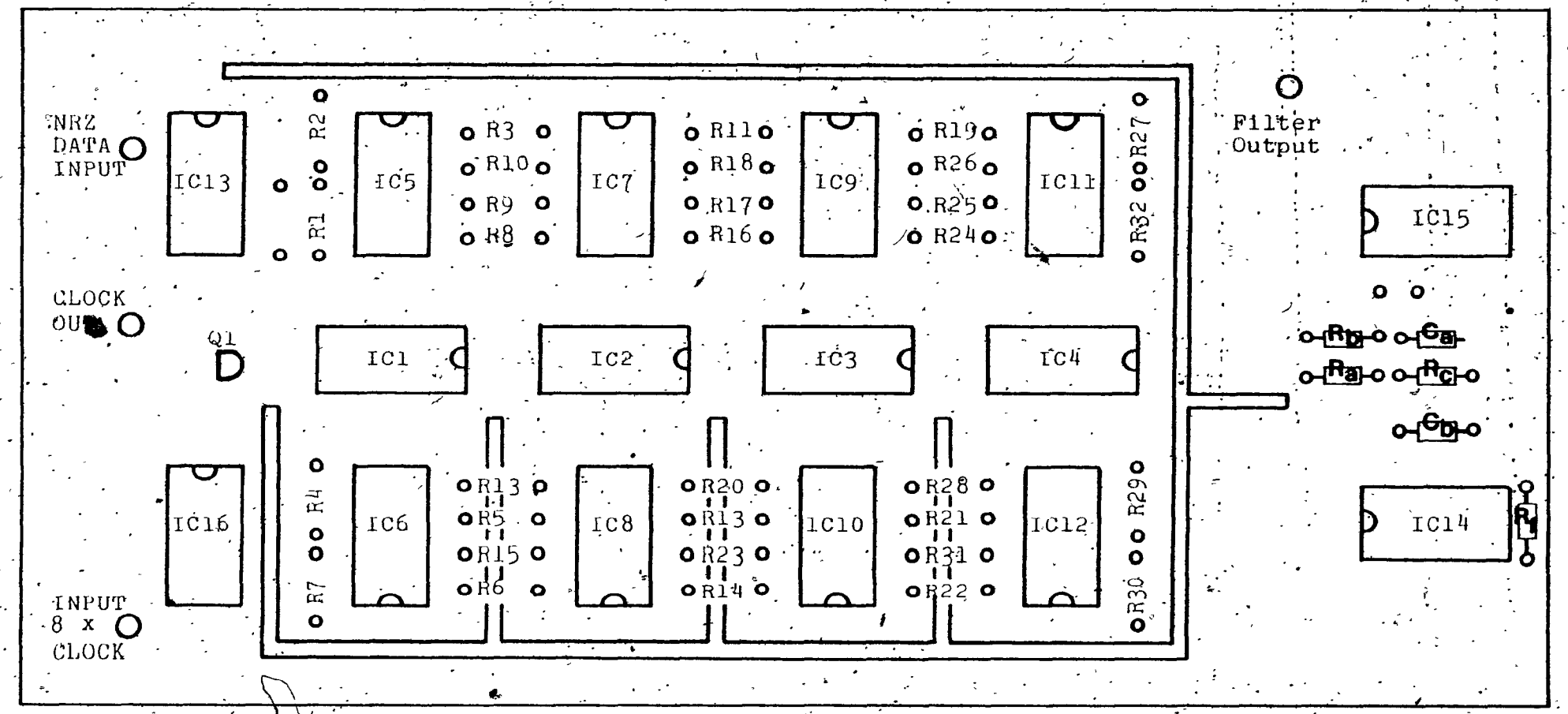

Figure 4.2.6: Binary Transversal Filter (BTF 2-8) Components Layout

4.3 Measurement techniques and Test Results

This section describes the different set-ups and techniques utilized in measuring the Binary Transversal Filter performances. These measurement results are given.

Figure 4.3.1 shows the test bench equipped for low frequency digital communications performance evaluations.

Excluding the jitter measurement, the following tests were selected in order to characterize the filter performances:

i) Eye Pattern

ii) Power Spectrum Density

iii) In to out of band energy ratio

iv) Probability of error measurement

The zero crossing jitter performance could not be evaluated due to the following reasons:

a) The test equipment available was not suitable to evaluate jitter performance.

b) The SCPC specification did not state if the jitter occurring at zero crossing was a peak to peak or an RMS type jitter. Peak to Peak jitter can be measured directly from the eye pattern, and in this case the BTF 2-8 filter does not meet the requirements. In a recent paper written by M. Asahara et. al. [29] the eye pattern of the QPSK modem for the SCPC system is shown. A very close similarity exists between the BTF 2-8 eye diagram (figure 4.3.4-b)

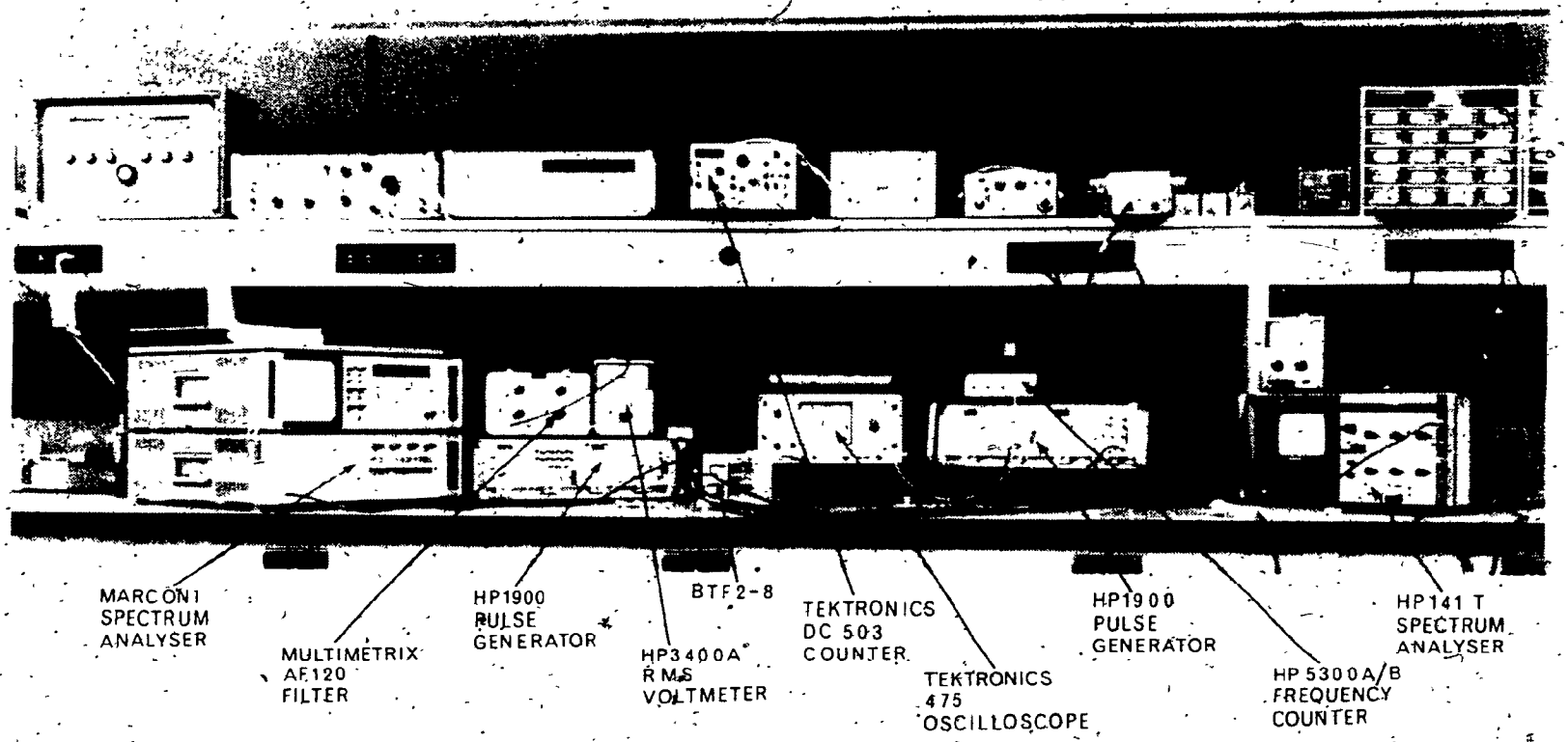

FIG. 4.3.1 – Binary transversal filter test set – up

and the one given in [29]. Since the M. Asahara modem fully complied with the SCPC requirements, we can conclude that the zero crossing jitter performance of the BTF 2-8 is also met.

c) In chapters 2 and 3 it was shown that a Binary Transversal Filter has linear phase, thus the jitter due to filter phase non linearities, theoretically is nul.

The block diagram of the test set-up utilized in evaluating the parameters (i) to (iii) is shown in figure 4.3.2.

All tests were performed feeding the Binary Transversal Filter with the longest pseudo random binary sequence (2^{20}-1) available at the output of the HP 1930A. The data was of the NRZ format.

The eye diagram can be monitored on a continuous basis, and is shown in figures 4.3.3 to 4.3.5. These patterns are very similar to the ones obtained by simulation in section 3.3. The smoothing effect of the low pass filter following the BTF can be clearly noticed in figure 4.3.3-b, 4.3.4-b and 4.3.5. The eye diagrams for the hybrid BTF2-8, having 30% and 40% excess Nyquist bandwidth are very similar. Recalling what was predicted in section 3.3 some difference should be noticed at the zero crossing, effectively 5.4 μsec of peak to peak jitter were measured for the 40% excess Nyquist

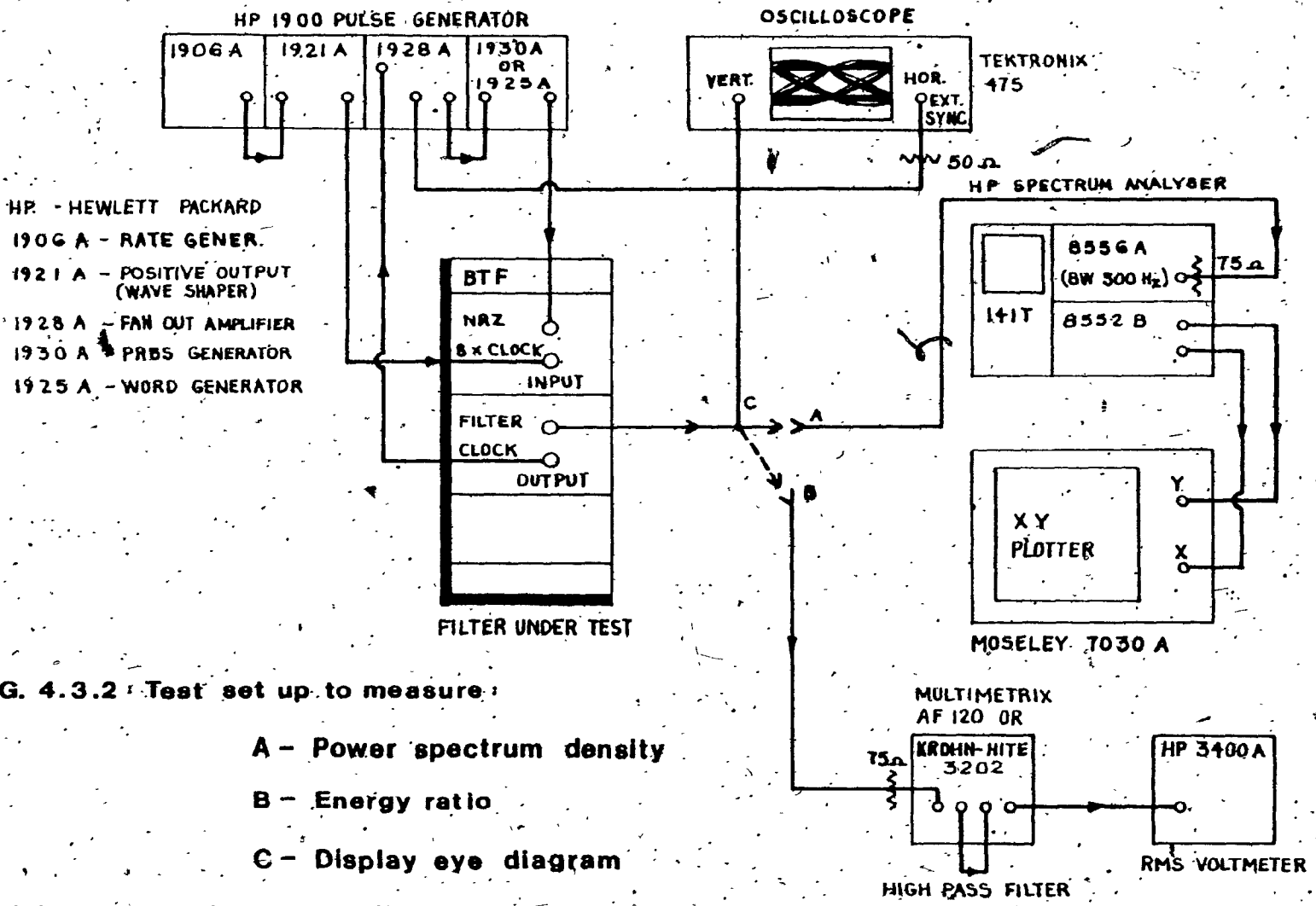

FIG. 4.3.2 : Test set up to measure :

A – Power spectrum density

B – Energy ratio

C – Display eye diagram

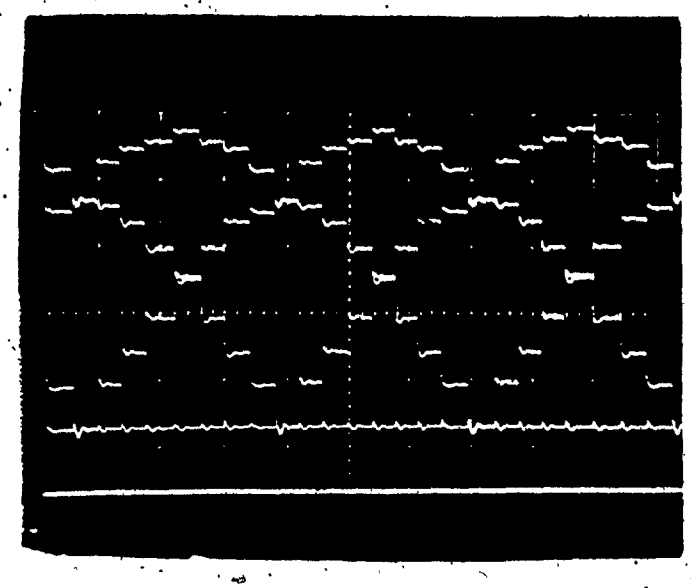

Bit Rate
62.5 kbps

4.3.3-a - BTF 1-8 Eye Diagram

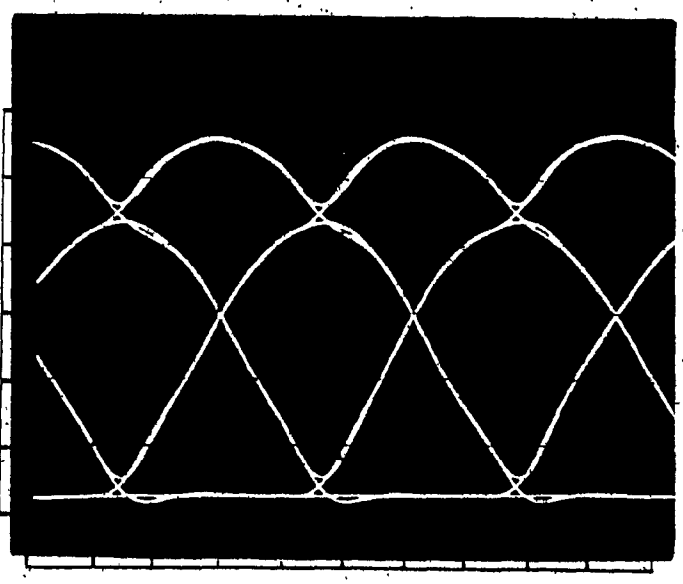

Bit Rate
62.5 kbps

4.3.3-b - Eye diagram of BTF 1-8 followed by 4th order Butterworth LPF (f_c=120 kHz)

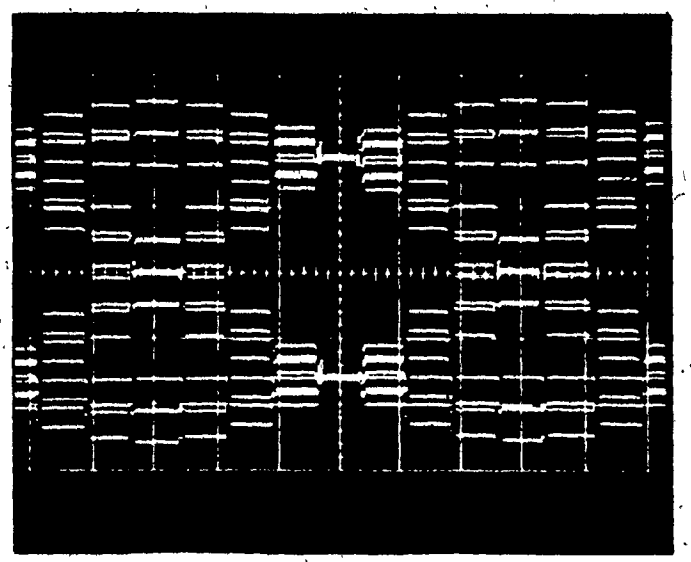

Fig. 4.3.4-a - BTF 2-8 eye diagram (α=.30)

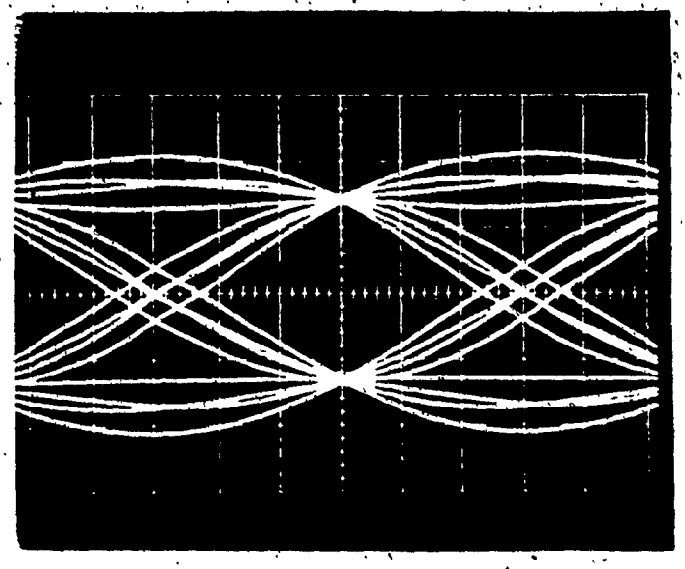

Fig. 4.3.4-b - Hybrid BTF 2-8 eye diagram (α=.30)

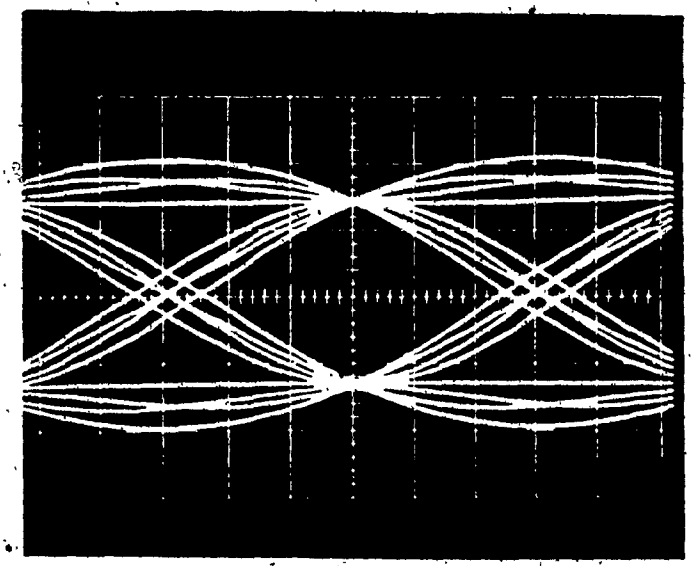

1 volt/Division

Bit Rate
32 kbps

5 μsec/Division

Fig. 4.3.5 - Hybrid BTF 2-8 eye diagram (α=.40)

against 6.7 μsec for the 30% filter (baud interval 31.25 μsec).

The Power Spectrum Density of the different Binary Transversal Filters was also evaluated and is shown in figure 4.3.6 to figure 4.3.9. In the absence of a camera an XY plotter was used to record the Power Spectrum Density. The calibration lines shown in the graphs were obtained in the following manner: After plotting the BTF Spectral density the signal from the Spectrum Analyser tracking generator was fed back into the analyser's input via a calibrated attenuator. For each attenuation setting a calibration line was obtained. Using this technique the errors due to the Spectrum analyser non linearity are compansated for. The measured spectral densities are very similar to the ones predicted in section 3.5. The major discrepancies observed are in the amplitudes of the discrete spectral lines appearing at multiples of the bit rate. Further studies should be conducted in order to find the reasons for these differences. The discrete spectral lines were 10 to 15 dB above the computed value.

Two BTF 2-8 having 30% excess Nyquist were assembled and tested. However from the Power Spectrum density results given in figure 4.3.8-a and figure 4.3.9, we notice that the major differences are below -40 dB and are hence negligible.

The next parameter to be measured is the out of band to the in band energy ratio. The set up used for this measurement is also shown in figure 4.3.2, the technique consists of

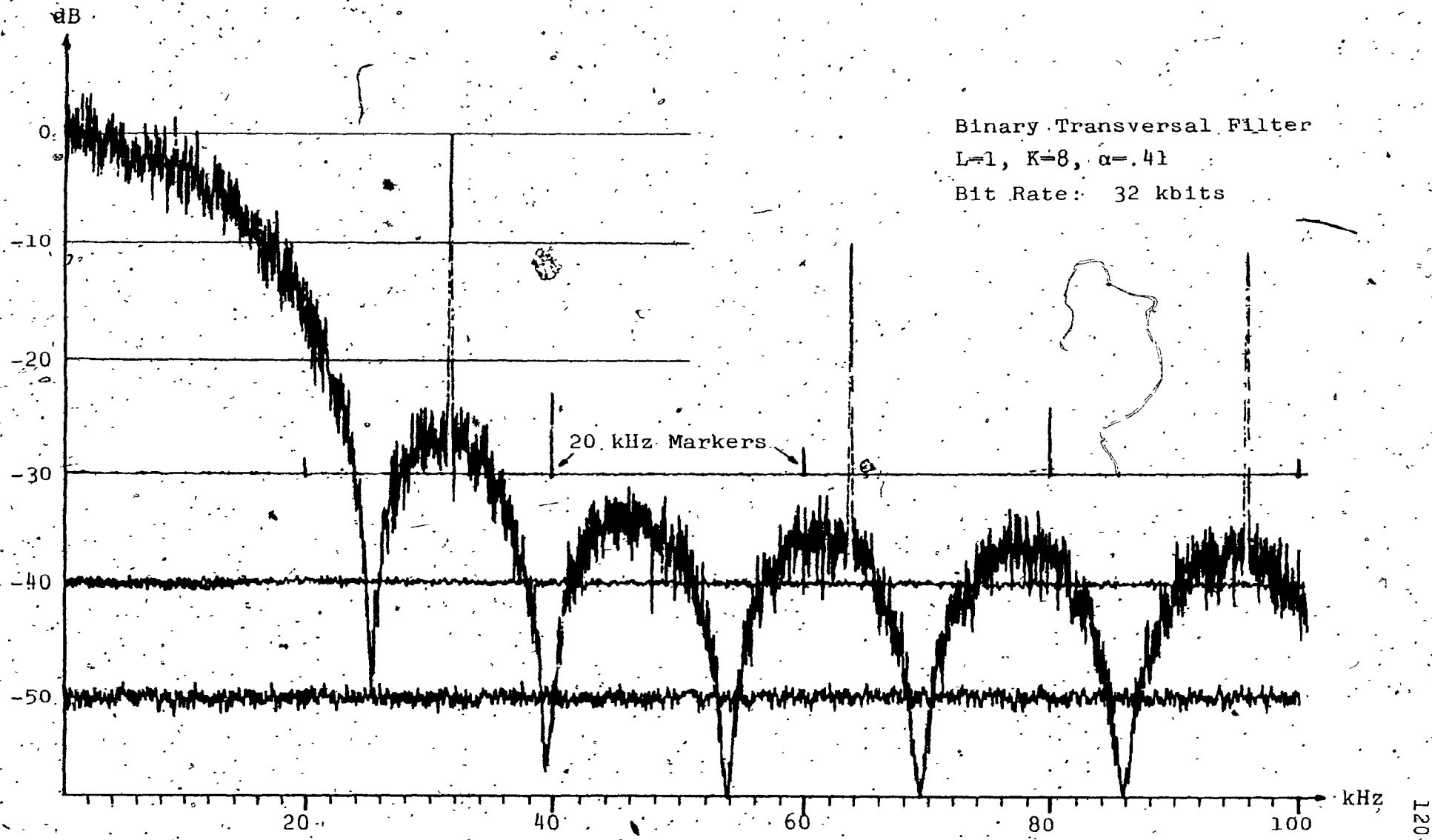

Figure 4.3.6: Measured Power Spectrum Density BTF 1-8 (α=.41)

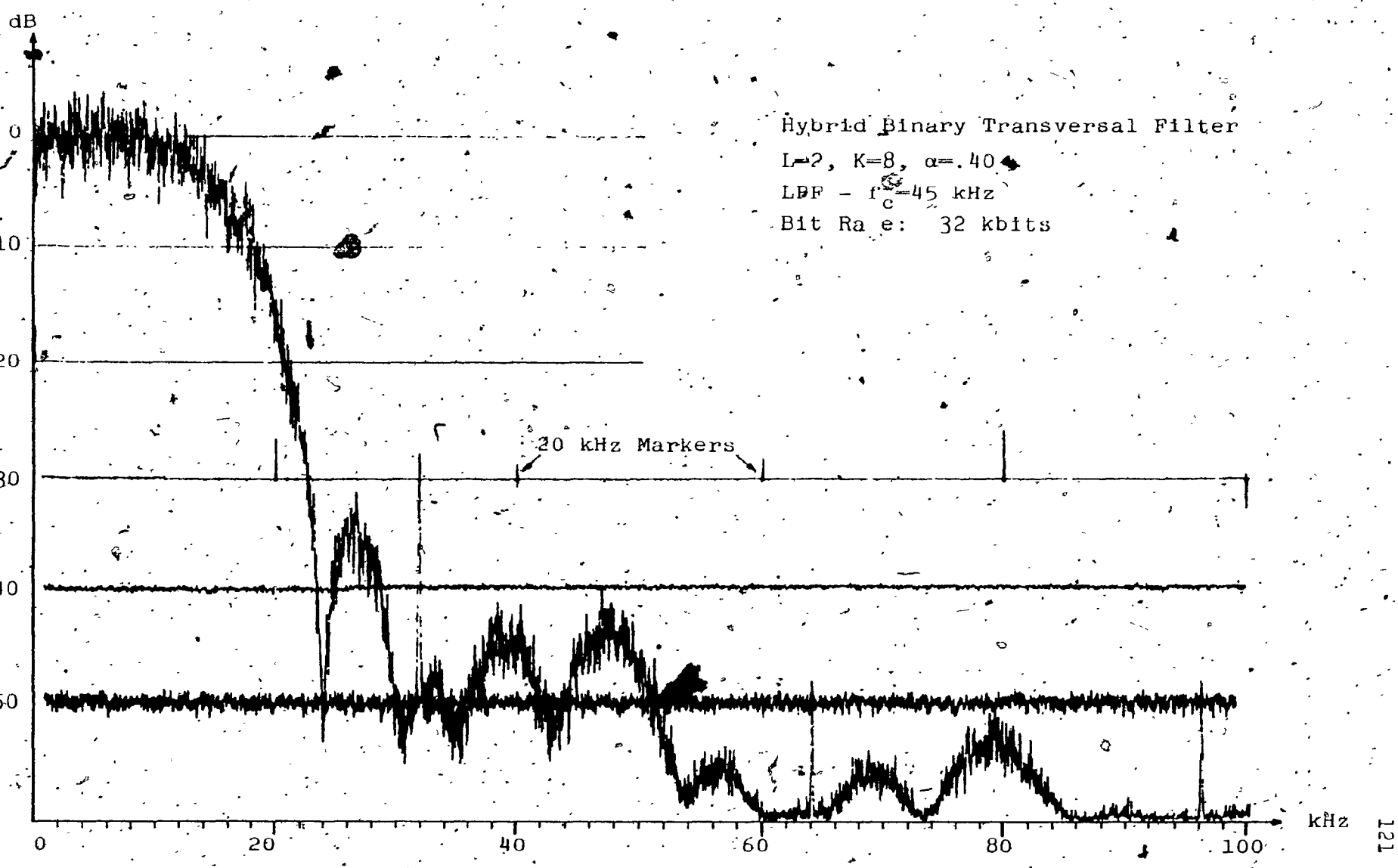

Figure 4.3.7-a: Measured Power Spectrum Density of BTF 2-8 (α=.4)

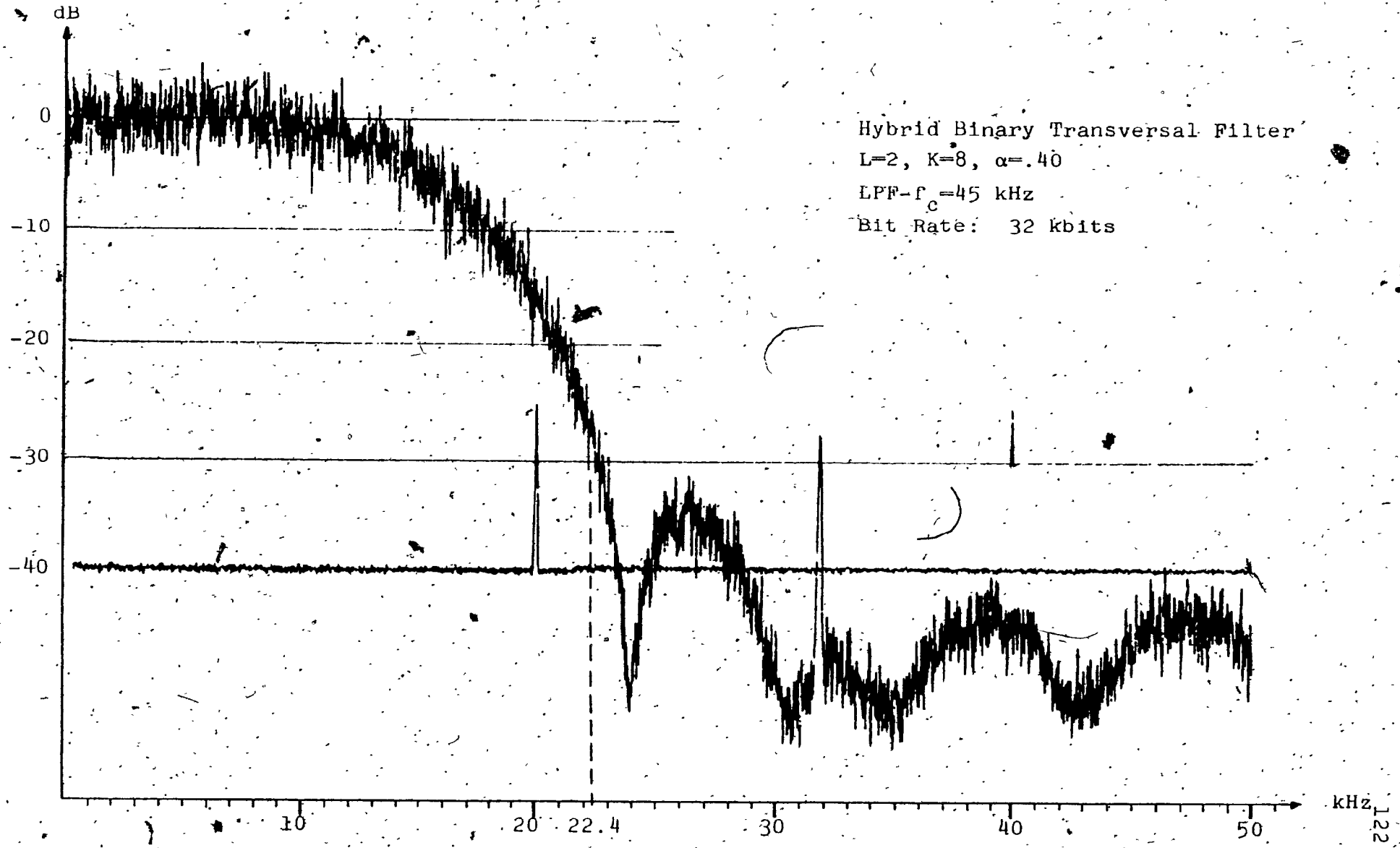

Figure 4.3.7-b: Measured Power Spectrum Density (Frequency scale expanded)

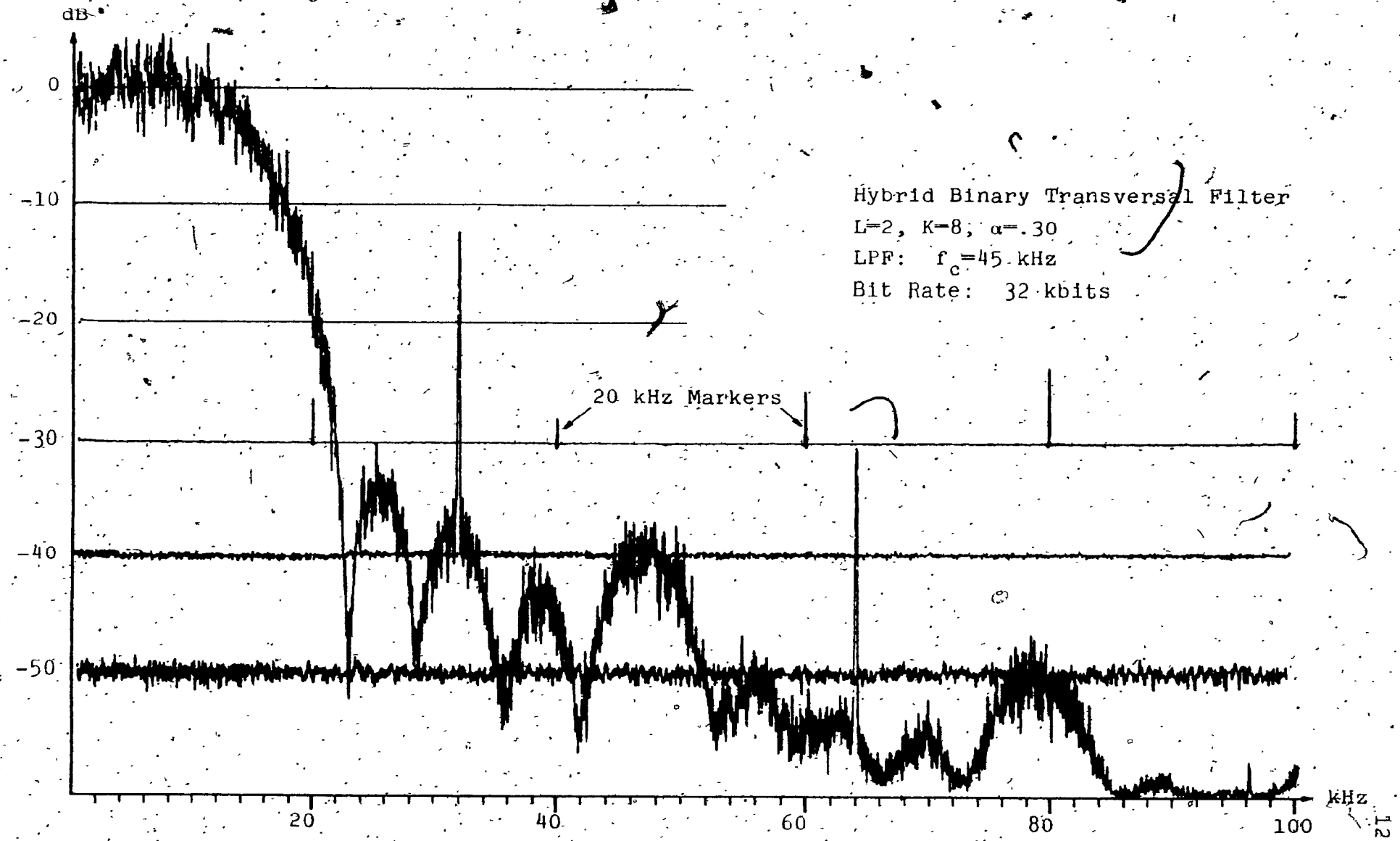

Figure 4.3.8-a: Measured Power Spectrum Density BTF 2-8 (α=.30), Unit No 1

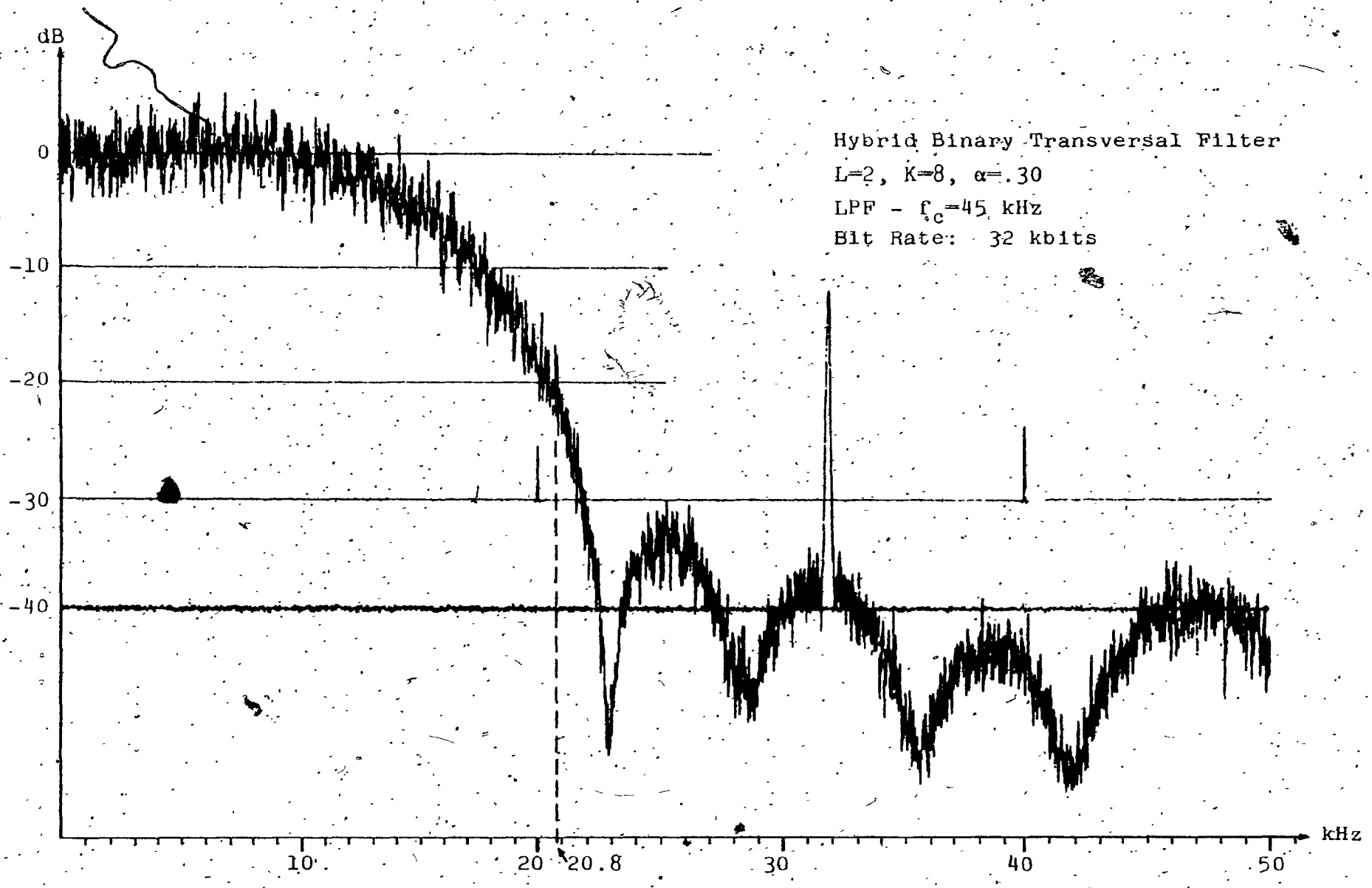

Figure 4.3.8-b: Measured Power Spectrum Density (Frequency scale expanded)

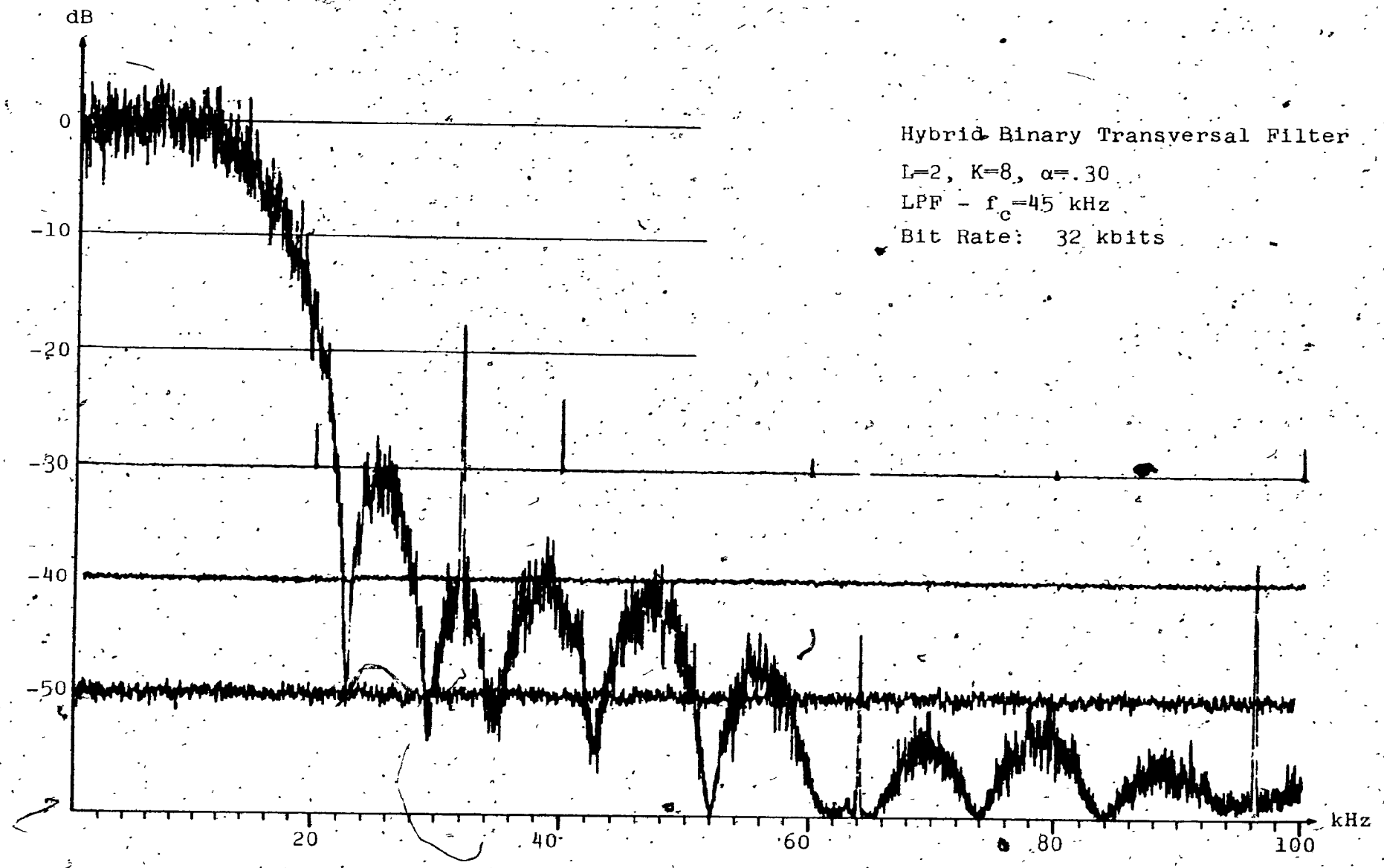

Figure 4.3.9: Measured Power Spectrum Density BTF 2-8 (α=.30), unit No 2

two steps. In the first, the total BTF output energy is measured by tunning the High Pass Filter (HPF) to its lowest cut off frequency (20 Hz). In order to assure that the amount of energy lost in these 20 Hz of bandwidth was not of consequence, a test was done with the HPF bypassed and no difference in the total energy was observed.

The second step consisted of measuring the out of band energy by tunning the HPF cut off frequency to the excess Nyquist frequency (equation 3.1.27). Since the total energy is very close to the in band energy then the energy ratio is simply the ratio of these last two measurements.

The high Pass Filter available was an eighth order Butterworth (48 dB/octave) having 0 dB gain. Its measured high pass frequency characteristic is shown in figure 4.3.10. Comparing the Binary Transversal Filter spectral density roll off with the HPF response it becomes evident that a higher order filter having a steeper response would have given more accurate energy ratio measurements.

The energy ratio results obtained using this technique for different Binary Transversal Filters is given in table 4.3-A.

From this table not much can be concluded, except the fact that the measured energy ratio is relatively close to the computed values considering the characteristics of the High Pass Filter.

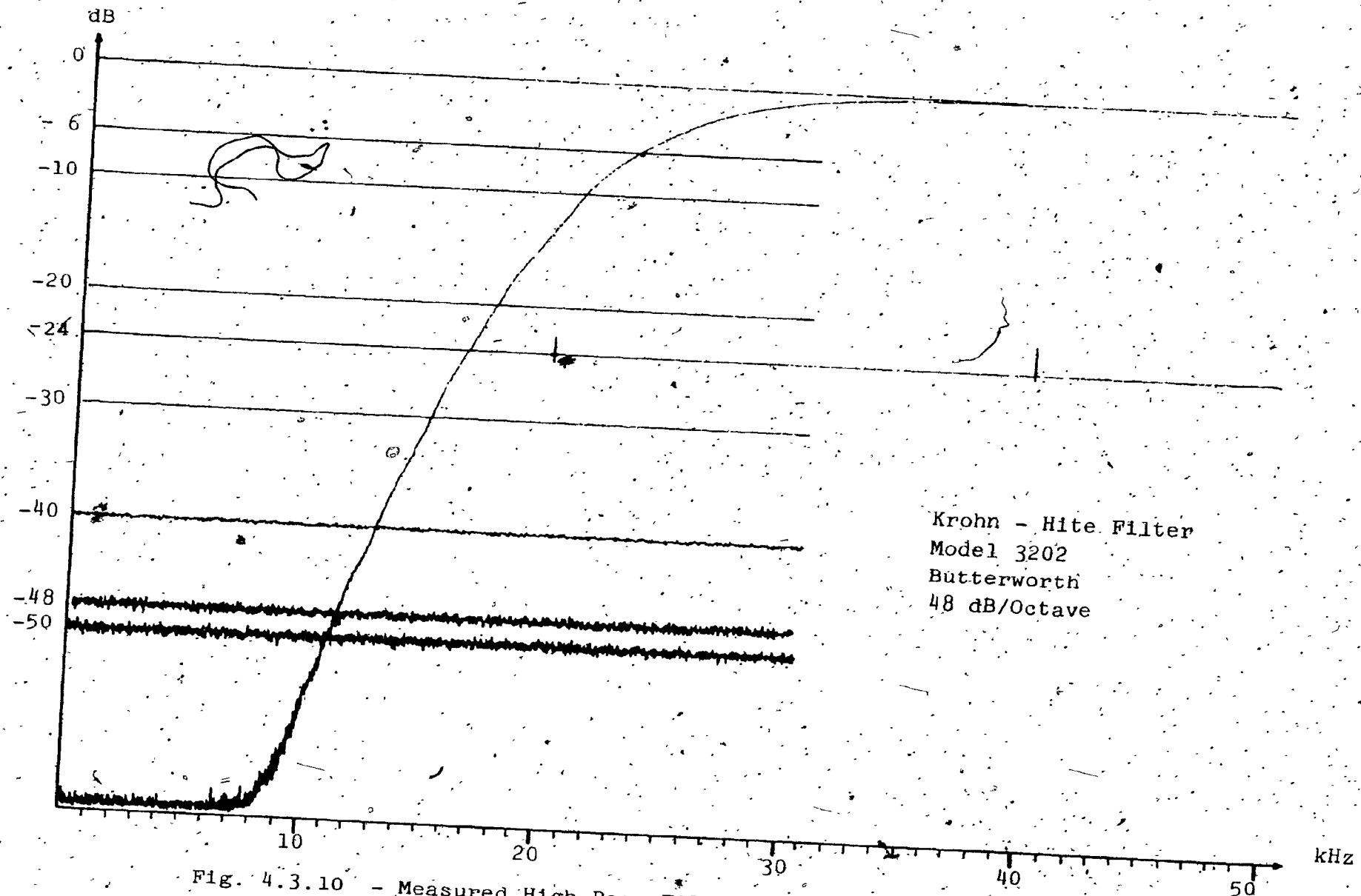

Fig. 4.3.10 - Measured High Pass Filter's frequency response

BTF Characteristics			Measured Energy Ratio in dB	Computed Energy Ratio in dB	HPF (†) Cut off Freq. in kHz	Comments
L	K	α				
1	8	.41	-19	-22.21	22.5	BTF alone
			-21.8	--	22.5	e/w LPF*
2	8	.30	-23.1	23.84	20.8	BTF alone
			-23.3	--	22.5	BTF alone
			-28	-32.30	20.8	e/w LPF**
			-32	--	22.5	e/w LPF**
2	8	.40	-29.7	--	20.8	e/w LPF**
			-35.8	-38.22	22.5	e/w LPF**

† Bit rate: 32 kbits; 22.5 kHz → α=.41; 20.8 kHz → α=.3.

* 4th order Butterworth LPF, fc = 65 kHz.

** 2nd order Butterworth LPF, fc = 45 kHz.

Table 4.3-A - BTF Energy Ratio performance

The probability of error performance of the Binary Transversal Filter was evaluated using conventional measuring techniques [30] and the block diagram of the test set up is shown in figure 4.3.11. An amplifier having 20 dB of gain was inserted in the noise path in order to provide adequate noise power in a noise bandwidth of less than 100 kHz. Preceeding the amplifier a low pass RC filter is inserted limiting the white noise bandwidth to approximately 700 kHz. This filter, indirectly, limiting the amplitude of the noise peaks preventing the amplifier from going into saturation, and deforming the Gaussian Probability Density Function [31]. A 50 to 75 ohms adaptor matches the amplifier output impendance with the variable attenuator. A linear adder (resistive type T network) combined the BTF output signal with the Gaussian noise. This is equivalent to an infinite bandwidth noisy channel. An RC low pass filter (LPF-A) preceeding the data regenerator limiting the noise and the signal bandwidths in order to approximate an almost optimum receiver. The rest of the set-up is conventional.

To obtain the best P(e) (Probability of error) performance the regenerator has to sample the received signal at its maximum eye opening. This is achieved by adjusting the clock via the variable delay generator (HP - 1909A).

The probability of error was evaluated as a function of the measured Signal to Noise ratio, i.e. P(e)=f(S/N), at

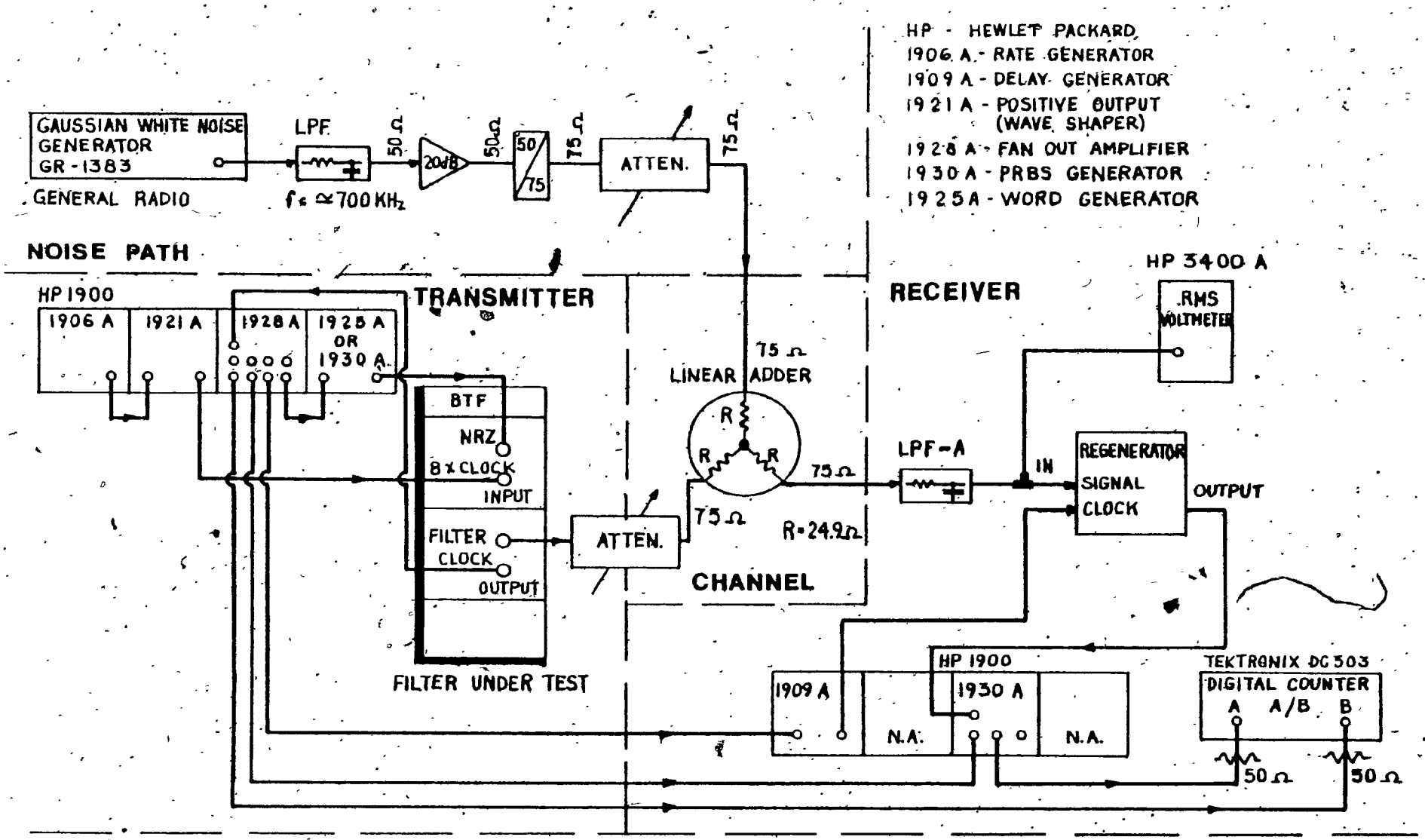

FIG. 4.3.11 – Test set up to measure the probability of error

the regenerator's input. It was then restated in terms of the Energy per bit (Eb) over the Noise density (No) using the following relation [30]:

$$\frac{Eb}{No} = \frac{S}{N} \cdot \frac{BM}{br} \qquad (4.3.1)$$

where BM is the measured noise bandwidth and br is the bit rate.

If fc is the RC low pass filter (LPF-A) cut off frequency, then the equivalent noise bandwidth, or measured noise bandwidth, is [31]:

$$BM = fc \cdot \pi/2 \qquad (4.3.2)$$

Substituting this relation into 4.3.1 and expressing Eb/No in dB, we obtain:

$$\left[\frac{Eb}{No}\right]_{dB} = 10 \log_{10}\left[\frac{S}{N}\right] + 10 \log_{10}\left[\frac{fc}{br}\,\frac{\pi}{2}\right] \qquad (4.3.3)$$

For a bit rate of 32 kbps a first evaluation of the P(e) was done using the LPF-A having a measured fc of 29.2 kHz (BM=45.9 kHz). The results are given in figure 4.3.12. From this graph, we notice that:

1) The P(e) curve for the BTF 2-8, having 30% or 40% excess Nyquist bandwidth, is approximately .6 dB

away from the regenerator performance.

ii) The P(e) curve of the BTF 1-8 (α=.41) diverges from the other curves at low probability of error. This effect is most probably due to the lack of symmetry in the BTF 1-8 eye pattern (see figure 4.3.3-a and 3.3.1).

A second P(e) measurement was taken changing the cut off frequency of LPF-A to 61.2 kHz (BM=96.13 kHz) and the results are shonw in figure 4.3.13. In this case, the regenator P(e) performance was worse than was the case for the BTF 2-8 filters. This is due to the fact that, for equal eye openings at the regenerator input, the BTF 2-8 signal has less energy than the square NRZ pulses.

To conclude we can summaryze as follows:

i) The degradation in the P(e) performance for both BTF 2-8 depends essentially on the equivalent noise bandwidth (BM) of the receiving filter.

ii) The P(e) performance curve for the BTF 1-8 diverges from the others at low error rates.

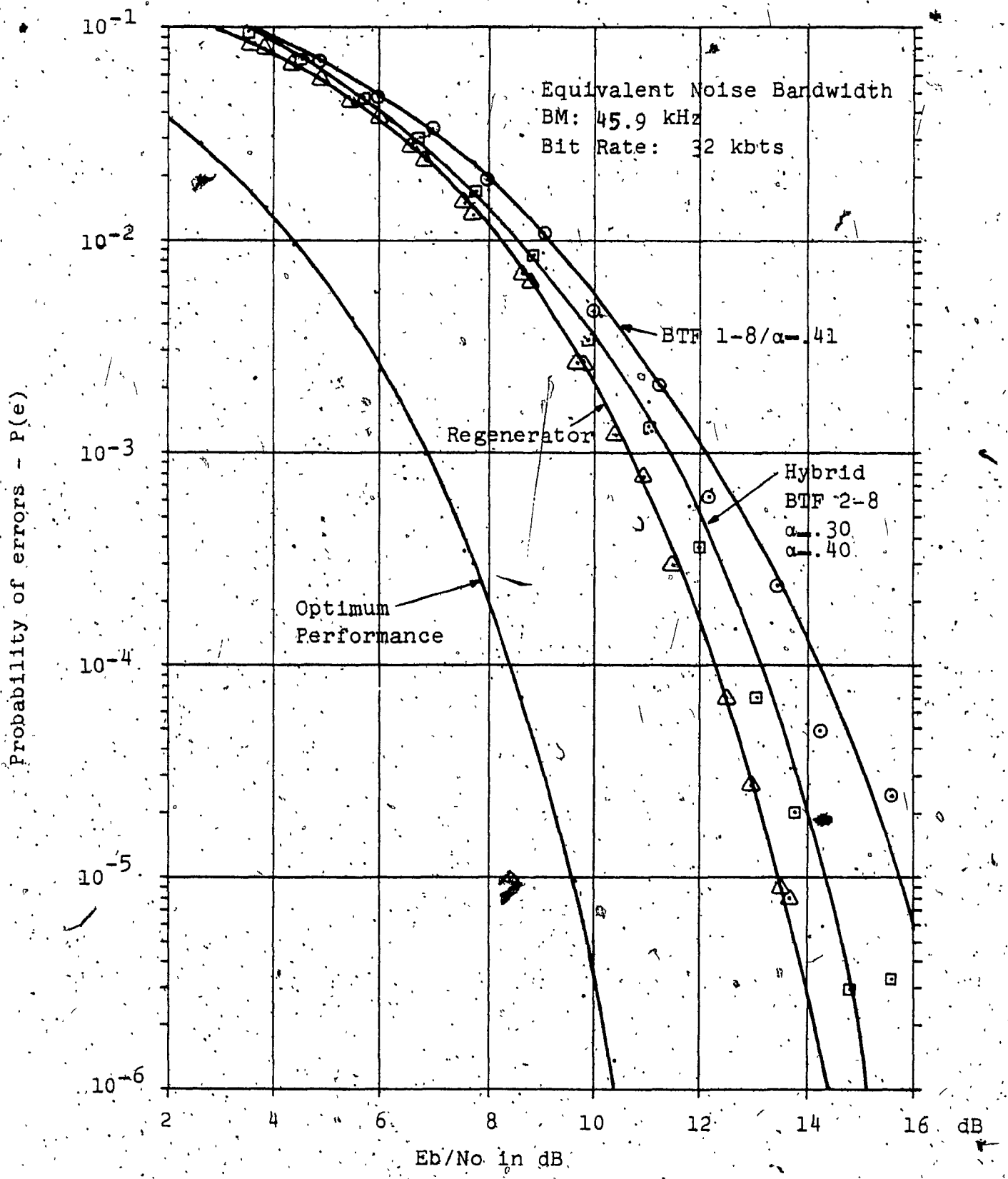

Fig. 4.3.12 - BTF Probability of error Results (BM: 45.9 kHz)

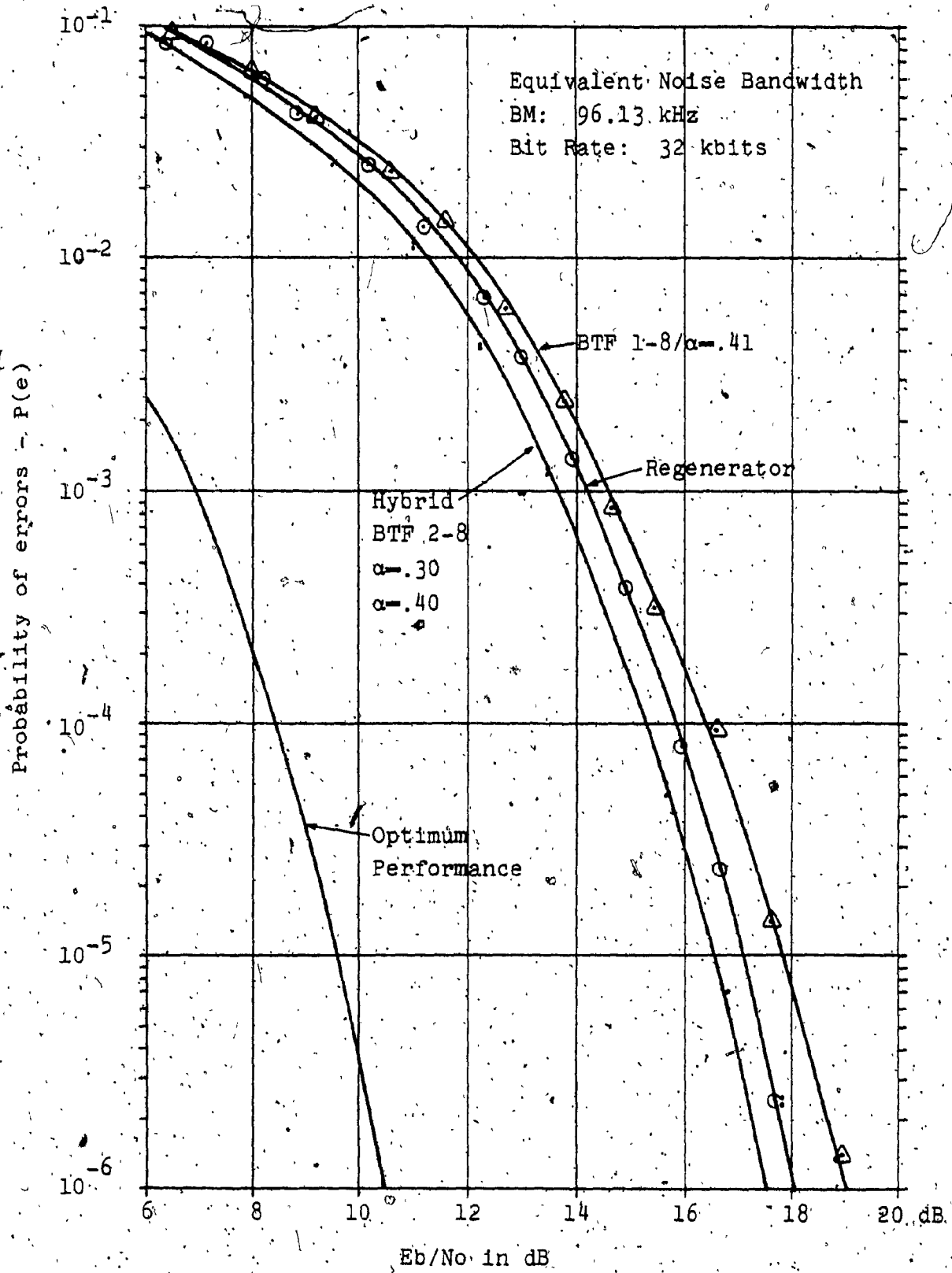

Fig. 4.3.13 - BTF Probability of error results (BM: 96.13 kHz)

CHAPTER 5

CONCLUSION

5.1 Conclusion

Modern narrow-band data communication systems require the generation of precisely shaped pulses having simultaneously small excess Nyquist bandwidth and negligible intersymbol interference. However, as we have seen, analog pulse shaping networks approaching these characteristics (equivalent Nyquist) are rather difficult to design, require group delay equalizers to compensate for filter phase non-linearities, and operate at a single data rate only.

An alternative solution, which has been gaining attention in the past few years, is found in a class of Transversal Filters (TF's) called Binary Transversal Filters (BTF's). As previously described, these filters consist essentially of a number of delay elements, a network of multiplying coefficients, and a summing device. No group delay equalizers are required since the BTF is one of the few filters having a linear phase characteristic when the multiplying coefficients have even symmetry. The BTF is self adaptable to different data rates, however, it has a major disadvantage: it is applicable to binary pulse only.

A survey of some of the presently available TF's synthesis techniques indicated that Mueller's BTF synthesis method is the most appropriate for data transmission. The BTF coefficients obtained by this method are optimum since they maximize the in to out of band energy ratio while minimizing the intersymbol interference.

Using Mueller's coefficients we have seen that the energy ratio performance of a staircase type TF, is a function of the total number of the filter coefficients. These, in turn, depend on the number of samples per baud interval and also on the number of lobes in the filter's impulse response. A two lobe TF was found to be the most economical in term of delaying elements and multipliers as the energy ratio improvement with three lobes was insignificant.

A simulation of the BTF's eye diagram has confirmed the absence of intersymbol interference in the BTF. It also demonstrated that the one lobe BTF has an asymmetric amplitude response which introduces a degradation in the probability of error performance, and that the peak to peak jitter at zero crossing decreases when the excess Nyquist frequency is relaxed.

A sensitivity study conducted on the BTF's energy ratio indicated that this parameter was not sensitive to changes in BTF's coefficients. However, as a practical rule it was established that the coefficients' tolerance should be at least half of the minimum difference existing between any two adjacent coefficients.

The maximum number of filter coefficients was found to be limited mainly by the hardware's maximum switching speed and the coefficients' accuracy.

The BTF's power spectrum density simulation for a filter excited by random sequences of pulses has predicted the existence of discrete spectral lines at regular bit rate intervals. Following this, another simulation was able to show that by appending a simple second order analog low pass filter to the BTF the energy ratio performance could be increased by almost 12 dB depending on the BTF's type.

To confirm these simulations, several filters were physically implemented. A one lobe BTF, realized using TTL logic devices and having 8 samples per baud interval, has confirmed the expected poor energy ratio performance and, also, the degradation of the probability of error at large Eb/No ratios. However, very encouraging results were obtained with a tow lobe BTF, similar to the previous one, but implemented by COS/MOS devices. This filter (BTF 2-8) was designed for use as a premodulation filter in the SCPC-QPSK modem, and it fully complied with the SCPC system specifications.

As a result of the studies conducted here, it is evident that many areas of study remain open in BTF research. It is, however, encouraging that the already demonstrated economic and performance advantages of these filters pointed out an expanded role of the BTF in digital communications technology.

APPENDIX A

Computer Program Instructions

All programs are written in FORTRAN IV Language

A1 - Program BTF1

Input data Card

Field Columns	Punched Value	Format	Description
1- 5	0	I5	Impulse type samples
	1		Pulse type samples
6-10	K	I5	# of samples per baud interval
11-15	L	I5	BTF impulse response truncated at ±L
16-25	α	F10.0	Excess Nyquist bandwidth
26-30	Blank	I5	Programs printout on paper only
	any		BTF coefficients punched on cards

Output

i) The normal output is on paper printout

ii) The coefficients can be obtained on punched cards (See input data card, field columns 26-30)

Field Columns	Description	Format
1- 5	BTF Coefficient number (1 to N_t)	I5
10-20	BTF Coefficient values	E20.14
30-35	# of samples per baud interval (K)	I5
36-40	# of lobes (L)	I5
41-50	Excess Nyquist bandwidth (α)	F10.0

COMPUTER PROGRAM INSTRUCTIONS (Continued)

A2 - Program SMTF

A3 - Program SENST

A4 - Program SPECT

Input data Cards

For the programs SMTF, SENST, SPECT, the input data cards is the deck of punched cards containing the coefficients values obtained from the program BTF1.

Output

The normal printout is on paper.

Programs SMTF and SPECT using the plotting subroutine request the use of magnetic tape.

```
      PROGRAM BTF1 (INPUT,OUTPUT,PUNCH,TAPE1=PUNCH)
C        THIS PROGRAM COMPUTES THE OPTIMUM COEFFICIENTS
C        OF A BINARY TRANSVERSAL FILTER
C        REF. - K. H. MUELLER
C        A NEW APROACH TO OPTIMUM PULSE SHAPING
C        IN SAMPLED SYSTEMS USING TIME DOMAIN FILTERING.
C        BSTJ, VOL.52,NO. 5,PP.723-729, MAY/JUNE 1973
      DIMENSION KA(100)
      COMMON R(100),XMU,XI,A(5050),V(100)
      DOUBLE DPI,XU,XL
      DPI=3.14159265358979323846264D0
      PI=3.141592653589
C        READ INPUT DATA
      READ 10,IAD,MU,M,BETA,IPL
   10 FORMAT(3(I5),F10.0,I5)
      IF(IAD.EQ.0) LET=9HIMPULSES
      IF(IAD.EQ.1) LET=9HSTAIRCASE
      XBET=BETA*100.
      PRINT 20,LET,MU,M,XBET
   20 FORMAT(1H1,10X,'BINARY TRANSVERSAL FILTER'//
     *10X,A9,' OUTPUT'/10X,I2,' SAMPLES PER BAUD INTERVAL (T)'
     */,10X,'TRUNCATION AT +- 'I2,' T'/
     *10X,F7.2,'  EXCESS NYQUIST BANDWIDTH')
      MP=1+2*MU*M
C        GENERATE AUXILIARY VECTOR TO
C        SATISFY INTERSYMBOL INTERFERENCE
      M1=M+1
      M2=M*2
      DO 100 K=1,M2
      MI=MU*(K-1)
      DO 100 I=1,MU
      L=MI+I
      KA(L)=L
      IF(I.EQ.1.AND.K.NE.M1) KA(L)=0
  100 CONTINUE
C        GENERATE  VECTOR R (FIRST ROW OF 'A' MATRIX
      XMU=FLOAT(MU)
      XL=0.0
      XU=DPI*(1.+BETA)
      XPI=PI*(1.+BETA)/XMU
      IOR=8
      DO 200 I=1,MP
      XI=I-1
C        PULSE TYPE SAMPLES DURATION T/K
      IF(IAD.EQ.0) GOTO 220
      CALL ROM(XL,XU,IOR,Y)
      R(I)=Y/PI/XMU
      GOTO 200
C        IMPULSE TYPE SAMPLES
  220 IF(I.EQ.1) GOTO150
      ALFA=XPI*XI
      R(I)=R(1)*SIN(ALFA)/ALFA
      GOTO 200
  150 R(I)=(1.+BETA)/XMU
  200 CONTINUE
C        GENERATE MATRIX 'A' IN MODE 1 STORAGE
      DO 310 I=1,MP
```

```
      IF(KA(I).EQ.0) GOTO 310
      DO 300 J=1,I
      IF(KA(J).EQ.0) GOTO300
      KP=KP+1
      A(KP)=R(1+I-J)
  300 CONTINUE
  310 CONTINUE
      ERR=1.E-10
      MQ=MP-2*M
C        COMPUTE MAX EIGENVALUE AND EIGENVECTOR
      CALL EIGEN(MQ,ERR)
      EDB=10.*ALOG10((1./A(1))-1.)
      PRINT 410,A(1),EDB
  410 FORMAT(1H0,10X,*MAX EIGENVALUE =*,E14.8,/,
     *11X,*ENERGY RATIO =*,F7.2,* DB*,/)
C        REINSERT ZERO COEFFICIENTS IN VECTOR *R*
      KR=0
      DO 500 I=1,MP
      IF(KA(I).EQ.0) GOTO 510
      KR=KR+1
      R(I)=V(KR)
      GOTO 500
  510 R(I)=0.0
  500 CONTINUE
C        NORMALIZE COEFFICIENTS R(I)=R(I)/R(MAX)
      MM=MU*M+1
      RC=R(MM)
      PRINT 540
  540 FORMAT(1H ,10X,*NORMALIZED FILTER COEFFICIENTS*,10X,
     **NORMALIZED RESISTORS ARRAY*//)
      DO 550 I=1,MP
C        COMPUTE RESISTORS ARRAY
      R(I)=R(I)/RC
      RE=R(I)
      IF(RE.EQ.0.0)RE=1.E-30
      RES=1./RE
      PRINT 560,I,R(I),I,RES
  560 FORMAT(1H ,10X,*A*,I3,*=*,1X,1PE15.7,19X,*R*,I3,1X,
     **=*,1X,1PE12.4)
  550 CONTINUE
      IF(IPL.EQ.0) GOTO 610
      DO 570 I=1,MP
C        PUNCH  COEFFICIENTS VALUE ON CARDS
  570 PUNCH 600,I,R(I),MU,M,BETA
  600 FORMAT(I5,5X,E20.14,10X,I5,I5,F10.6)
  610 CONTINUE
      STOP
      END
```

```
      SUBROUTINE ROM(XL,XU,IOR,Y)
C        THIS SUBROUTINE EVALUATES AN INTEGRAL
C         USING ROMBERG ALGORITHM
C        REF.- BAUER, ALGORITHM 60
C          CACM, VOL. 4, ISSUE 6,1961, PP 255
      DOUBLE A(20),FCT,U,XU,XL,DX,XM,F
      DX=XU-XL
      A(1)=(FCT(XL)+FCT(XU))/2.
      N=1
      DO20 IH=1,IOR
      U=0.0
      XM=DX/2./N
      N2=2*N-1
      DO10 J=1,N2,2
   10 U=U+FCT(XL+J*XM)
      A(IH+1)=(U/N+A(IH))/2.
      F=1.
      DO 30 J=1,IH
      K=IH-J+1
      F=4.*F
   30 A(K)=A(K+1)+(A(K+1)-A(K))/(F-1.)
   20 N=N*2
      Y=SNGL(A(1)*DX)
      RETURN
      END
```

```
      DOUBLE FUNCTION FCT(X)
C        THIS FUNCTION  IS THE INTEGRAND
C        OF SUBROUTINE ROM
      COMMON R(100),XMU,XI
      DOUBLE XW,XS,X
      XW=X/2./XMU
      IF(X.EQ.0.0) XS=1.
      IF(X.NE.0.0) XS=(DSIN(XW)/XW)**2
      FCT=XS*DCOS(2.*XW*XI)
      RETURN
      END
```

```
      SUBROUTINE EIGEN(N,ERR)
C        THIS SUBROUTINE COMPUTES THE MAXIMUM
C        EIGENVALUE AND CORRESPONDING EIGEN-
C        VECTOR OF A SYMMETRIC MATRIX
C        REF.- L. FOX AND D. F. MAYERS
C        COMPUTING METHODS FOR SCIENTISTS AND ENG.
C        PP112-11, (CLAREDON PRESS - OXFORD - 1968)
      DIMENSION R(100),A(5050),X(100),C(100)
      COMMON R,XMU,XI,A,X
      EIG=0.0
      NT=0
      NC=(N+1)/2
      DO 5 I=1,N
      C(I)=0.0
    5 IF(I.EQ.NC) C(I)=1.0
   60 EIP=EIG
      KJ=1
      DO 10 I=1,N
      X(I)=0.0
      KJ=KJ+I-1
      KI=KJ
      DO 10 J=1,N
      IF(J.LE.I) KI=KJ+J-1
      IF(J.GT.I) KI=KI+J-1
   10 X(I)=X(I)+C(J)*A(KI)
      XP=0.0
      DO 50 I=1,N
   50 XP=XP+X(I)*C(I)
      EIG=XP
      XN=0.0
      DO 20 K=1,N
   20 XN=XN+X(K)**2
      XN=SQRT(XN)
      DO 30 K=1,N
   30 X(K)=X(K)/XN
      DO 15 I=1,N
   15 C(I)=X(I)
      NT=NT+1
      XRE=ABS(EIG-EIP)
      IF(EIP.EQ.0.0) GOTO 60
      IF(NT.GT.200) GOTO 100
      IF(XRE.GT.ERR) GOTO 60
  100 CONTINUE
      A(1)=EIG
      RETURN
      END
```

```
      PROGRAM SMTF (INPUT,OUTPUT,TAPE10)
C        THIS PROGRAM GENERATES THE EYE DIAGRAM OF
C        A BINARY TRANSVERSAL FILTER OUTPUT SIGNAL.
C        THE BTF INPUT SIGNAL IS A PSEUDO RANDOM
C        BINARY SEQUENCE.
C        MU= NUM. OF SAMPLES PER BAUD INTERVAL (K)
C        M= NUM. OF LOBES (L)
C        BETA= EXCESS NYQUIST BANDWIDTH.
C        C(I)= BTF COEFFICIENTS.
      DIMENSION X(100),C(100),A(20),IX(50),Y(50,50)
C        READ B.T.F. CHARACTERISTICS.
    2 READ 10,MU,M,BETA
   10 FORMAT(40X,I5,I5,F10.6)
      IF(MU.EQ.0) GOTO 1000
C        CLEAR AUXILIARY VECTORS X,A,IX.
      DO 250 ICL=1,100
  250 X(ICL)=0.0
      DO 255 ICL=1,20
  255 A(ICL)=0.0
      DO 260 ICL=1,50
      IX(ICL)=0
C        CLEAR MATRIX Y
      DO 260 ICJ=1,50
  260 Y(ICL,ICJ)=0.0
      NT=2*MU*M
C        READ BTF COEFFICIENTS.
      DO 20 I=1,NT
   20 READ 25,C(I)
   25 FORMAT(10X,E20.6)
      XBET=BETA*100.
C        PRINT BTF CHARACTERISTICS.
      PRINT 35,MU,M,XBET
   35 FORMAT(1H1,5X,'BINARY TRANSVERSAL FILTER EYE DIAGRAM'/
     *6X,I2,' SAMPLES PER BAUD INTERVAL (T)'/
     *6X,'TRUNCATION AT +-'I2' T'/
     *6X,F7.2' EXCESS NYQUIST BANDWIDTH')
      NS=0
C        INITIALIZE PLOTTING SUBROUTINE.
      NP=0
      MUP=MU*2
      LX=8
      LY=6
      XL=FLOAT(2*MU)
      XT=1.
      YL=2.
      XLO=0.
      YLO=-.5
      XCR=0.
      YCR=-.5
      YT=4.
      CALL AXISXYX(10,LX,LY,XT,XL,YL,XLO,YLO,XCR,YCR,YT)
C        CALL PSEUDO RANDOM BINARY SUBROUTINE
    1 CALL PRBS(APR,NS)
      X(1)=APR
      NS=NS+1
C        COMPUTE FILTER OUTPUT.
      DO 50 K=1,MU
```

```
      CO=0.0
      DO 60 J=1,NT
   60 CO=CO+X(J)*C(J)
C        STORE OUTPUT VALUES IN VECTOR A
      A(K)=CO
C        SHIFT ONE STEP TO THE RIGHT THE
C        CONTENT OF VECTOR X
      N1=NT-1
      DO 70 L=1,N1
      KN=NT-L+1
   70 X(KN)=X(KN-1)
C        SET TO ZERO FIRST ELEMENT OF VECTOR X.
      X(1)=0.0
   50 CONTINUE
C        STORE FILTERS OUTPUT VALUE INTO Y MATRIX.
      DO 80 K=1,MU
      NP=NP+1
      NL=IX(NP)
      IF(NL.EQ.0) GOTO 85
      DO 110 I=1,NL
      DIF=ABS(Y(I,NP)-A(K))
      IF(DIF.LE.1.E-5) GOTO 90
  110 CONTINUE
   85 IX(NP)=IX(NP)+1
      Y(IX(NP),NP)=A(K)
   90 IF(NP.EQ.MUP) NP=0
   80 CONTINUE
      IF(NS.LT.124) GOTO1
C        REARRANGE VECTORS OF Y MATRIX
C        IN DECREASING ORDER.
      DO 120 K=1,MUP
      IK=IX(K)
      DO 115 KM=1,IK
      IF(KM.EQ.IK) GOTO 112
      KP=KM+1
      YMIN=Y(KM,K)
      DO 115 I=KP,IK
      IF(YMIN.LE.Y(I,K)) GOTO 105
      YMIN=Y(I,K)
      Y(I,K)=Y(KM,K)
      Y(KM,K)=YMIN
  105 CONTINUE
  115 CONTINUE
  112 CONTINUE
  120 PRINT 200,(Y(I,K),I=1,IK)
  200 FORMAT(1H ,3X,10(1X,F10.7))
C        TRANSFER VALUES FROM Y MATRIX ONTO
C        MAGNETIC TAPE VIA PLOTTING SUBROUTINE.
      DO 150 K=1,MUP
      IK=IX(K)
      DO 150 I=1,IK
      XA=FLOAT(K-1)
      YA=Y(I,K)
      CALL PLOTXYX(XA,YA,0,0)
      XA=FLOAT(K)
      CALL PLOTXYX(XA,YA,1,0)
  150 CONTINUE
```

```
C        CLOSE PLOTTING SUBROUTINE
      CALL ENDPLT(XCR,YCR)
      GOTO 2
1000  CONTINUE
      END
```

```
      SUBROUTINE PRBS(AF,NS)
C        THIS SUBROUTINE  GENERATES AT RANDOM
C        A ZERO OR A ONE EVERY TIME IS CALLED BY
C        THE MAIN PROGRAM. THE BINARY SEQUENCE
C        REPEATS ITSELF AFTER (2**N)-1 CALLS.
      DIMENSION I(20)
C        THE LENGHT OF THE PRBS IS 2**N-1
C        N= NUM. OF SHIFT REGISTERS, MAX. 20.
C        K1= FIRST TAP.
C        K2= SECOND TAP.
C        NS= 0 AT FIRST CALL.
      N=7
      K1=6
      K2=7
      N1=N+1
      ID=0
      IF(I(K1).NE.I(K2)) ID=1
      IF(NS.EQ.0) ID=1
      DO 5 K=1,N1
      KN=N+1-K
    5 I(KN)=I(KN-1)
      I(1)=ID
      AF=FLOAT(I(1))
      RETURN
      END
```

```
      PROGRAM SENST(INPUT,OUTPUT)
C        THIS PROGRAM COMPUTES THE OUT OF BAND TO THE
C        IN BAND ENERGY RATIO OF A BINARY TRANSVERSAL
C        FILTER, COEFFICIENTS OF WHICH HAVE BEEN RANDOMLY
C        PERTURBED WITHIN A SPECIFIED RANGE.
      DIMENSION B(100)
      COMMON XMU,NT,C(100)
C        READ B.T.F. CHARACTERISTICS.
      READ 10,B(1),MU,M,BETA
   10 FORMAT(10X,E20.6,10X,I5,I5,F10.6)
      N=MU*M
      NT=2*N+1
C        READ B.T.F. OPTIMUM COEFFICIENTS.
      DO 20 I=2,NT
   20 READ 30,B(I)
   30 FORMAT(10X,E20.6)
      PRINT 40,MU,M,BETA
   40 FORMAT(1H1,5X,' B.T.F. SENSITIVITY STUDY',/,
     *6X,'K =',I3,4X,'L = 'I2,4X,'EXCESS NYQUIST = ',F6.2,//)
      PI=3.141592653589
      DUM=2.**24-3.
C        INITIALIZE RANDOM FUNCTION.
      CALL RANSET(DUM)
      XMU=FLOAT(MU)
      XL=0.0
      XU=1.+BETA
      XERT=XER=XDB=0.0
      DERT=DER=DDB=0.0
      DO 100 LP=1,101
      XLP=FLOAT(LP-1)
      YLP=XLP-1.
C        SPECIFY COEFFIGIENTS ACCURACY.
      PER=0.05
      IF(LP.EQ.1) PER=0.0
      DO 70 I=1,NT
C        GENERATE RANDOM NUMBERS UNIFORMLY
C        DISTRIBUTED BETWEEN -1 AND +1.
      XRL=RANF(DUM)-.5
C        PERTURB OPTIMUM COEFFICIENNTS WITHIN
C        SPECIFIED RANGE.
   70 C(I)=B(I)*(1.+2.*PER*XRL)
      EC=0.0
C        COMPUTE TOTAL ENERGY.
      DO 80 I=1,NT
   80 EC=EC+C(I)**2
      WT=EC/2./XMU
      WT2=WT/2.
C        COMPUTE ENERGY BELOW SPECIFIED EXCESS
C        NYQUIST FREQUENCY (BETA).
      IOR=8
      CALL ROM(XL,XU,IOR,WEX)
      ERT=WEX/WT2
C        COMPUTE ENERGY RATIO IN DB.
      ER=(WT2/WEX)-1.
      ERDB=10.*ALOG10(ER)
      PRINT 50,ERT,ER,ERDB
   50 FORMAT(1H ,5X,'OUT TO IN BAND ENERGY RATIO'/
```

```
     *6X,E14.8,5X,E14.8,5X,F7.2,' DB'/)
      IF(LP.EQ.1) GOTO 90
C        CALCULATE MEAN VALUES OF 50 AND 100 SAMPLES.
      XERT=XERT+ERT
      XER=XER+ER
      DERT=DERT+ERT**2
      DER=DER+ER**2
      IF(LP.EQ.51.OR.LP.EQ.101) GOTO 95
      GOTO 90
   95 CONTINUE
      AERT=XERT/XLP
      AER=XER/XLP
      ADB=10.*ALOG10(AER)
      PRINT 150,XLP,AERT,AER,ADB
  150 FORMAT(1H ,5X,' MEAN VALUES - NO. OF SAMPLES =',F4.0,/
     *6X,E14.8,5X,E14.8,5X,F7.2,' DB'/)
C        CALCULATE STANDARD DEVIATION OF
C        50 AND 100 SAMPLES.
      SERT=SQRT((DERT-(XERT**2)/XLP)/YLP)
      SER=SQRT((DER-(XER**2)/XLP)/YLP)
      PRINT 160,SERT,SER
  160 FORMAT(1H ,5X,' STANDARD DEVIATION '/
     *6X,E14.8,5X,E14.8,/)
   90 CONTINUE
  100 CONTINUE
      PRINT 60,PER
   60 FORMAT(1H ,5X,E14.8)
      STOP
      END
```

```
      SUBROUTINE ROM(XL,XU,IOR,Y)
C                  THIS SUBROUTINE EVALUATES AN INTEGRAL
C                  USING ROMBERG ALGORITHM
      DIMENSION A(20)
      DX=XU-XL
      A(1)=(FCT(XL)+FCT(XU))/2.
      N=1
      DO20 IH=1,IOR
      U=0.0
      XM=DX/2./N
      N2=2*N-1
      DO10 J=1,N2,2
   10 U=U+FCT(XL+J*XM)
      A(IH+1)=(U/N+A(IH))/2.
      F=1.
      DO 30 J=1,IH
      K=IH-J+1
      F=4.*F
   30 A(K)=A(K+1)+(A(K+1)-A(K))/(F-1.)
   20 N=N*2
      Y=A(1)*DX
      RETURN
      END
```

```
      FUNCTION FCT(F)
C        THIS FUNCTION EVALUATES THE  MAGNITUDE
C        OF THE FREQUENCY RESPONSE OF A BTF
      COMMON XMU,NT,C(100)
      PI=3.141592653589
      XF=PI*F/XMU
      IF(F.EQ.0.0) AF=0.5/XMU
      IF(F.NE.0.0) AF=SIN(XF/2.)/PI/F
      RPW=0.0
      APW=0.0
      DO 10 I=1,NT
      IM=I-1
      OW=IM*XF
      BSI=C(I)*SIN(OW)
      BCO=C(I)*COS(OW)
      RPW=RPW+BCO
      APW=APW+BSI
   10 CONTINUE
      RPW=RPW*AF
      APW=APW*AF
      FCT=RPW**2+APW**2
      RETURN
      END
```

```
      PROGRAM SPECT(INPUT,OUTPUT,TAPE10)
C        THIS PROGRAM COMPUTES THE POWER SPECTRUM
C        DENSITY OF THE BINARY TRANSVERSAL FILTER
C        OUTPUT SIGNAL, A PRBS NRZ SIGNAL HAVING
C        EQUAL PROBABILITY OF ZEROS AND ONES IS
C        ASSUMED AT THE INPUT.
C        IS BASED ON THE FORMULA GIVEN ON PAGE 319
C        OF DATA TRANSMISSION BY BENNET AND DAVEY.
      COMMON XMU,NT,C(100)
C        READ B.T.F. CHARACTERISTICS.
    1 READ 100,C(1),MU,M,BETA
  100 FORMAT(10X,E20.6,10X,I5,I5,F10.6)
      IF(MU.EQ.0) GOTO 1000
      NT=2*MU*M+1
C        READ B.T.F. COEFFICIENTS.
      DO 10 I=2,NT
   10 READ 200,C(I)
  200 FORMAT(10X,E20.6)
      PRINT 150,MU,M,BETA
  150 FORMAT(1H1,5X,*BINARY TRANSVERSAL FILTER POWER SPECTRUM DENSITY*/,
     *6X,* K = *,I2,4X,*L =*I2,4X,*EXCESS NYQUIST = *,F5.2/)
      XMU=FLOAT(MU)
C        DF IS THE FREQUENCY INCREMENT.
      FBIT=32000.
C        FMAX IS THE HIGHEST FREQUENCY.
      FMAX=4.
      DF=FMAX/1000.
      NF=1001.
C        INITIALIZE PLOTTING SUBROUTINE
      LX=10
      LY=7
      XL=FMAX
      XT=1.0
      YL=70.0
      XLO=0.0
      YLO=-65.
      XCR=0.0
      YCR=-65.
      YT=5.0
      CALL AXISXY(10,LX,LY,XT,XL,YL,XLO,YLO,XCR,YCR,YT)
      CALL PLOTXY(0.,0.,0,0)
C        FEX IS THE EXCESS NYQUIST FREQUENCY.
      FEX=1.+BETA
      WT=0.0
C                    NF*DF=HIGHEST FREQUENCY
      WE=0.0
      WM=EX=0.0
      DO 20 J=1,NF
      IPP=0
      J1=J-1
      IF((J1/10)*10.EQ.J1) IPP=1
      F=(J-1)*DF
      KF=IFIX(F*1000.)
      IF(F.EQ.0.0) F=1.E-5
      RF=FBIT*.5*F
      DG=0.0
C        CALCULATE THE POWER SPECTRUM DENSITY.
```

```
      W=HLPF(F)*(SBTF(F)**2)
      IF(J.EQ.1) WO=W
      DBW=10.*ALOG10(W/WO)
C        COMPUTE THE ENERGY USING TRAPEZOIDAL
C        RULE OF INTEGRATION.
      IF(J.GT.1) WE=(W+W1)*DF/2.
      WT=WT+WE
      WD=0.0
      IDEL=7H
C        COMPUTE DISCRETE SPECTRAL COMPONENTS.
      IF(KF.EQ.0.OR.((KF/2000)*2000).NE.KF) GOTO 30
      IDEL=7HDELTA F
      DG=2.*W
      WD=W+DG
      W=WD
      DBWD=10.*ALOG10(WD/WO)
      DBW=DBWD
   30 CONTINUE
      WT=WT+WD
      IF(IPP.EQ.1) PRINT 300,F,RF,W,DBW,IDEL
  300 FORMAT(1H ,2X,F6.3,5H F/FN,3X,F10.2,* HZ*,5X,*SW =*,
     *E14.6,7H V*V/HZ,5X,*SW =*,F7.2,* DB*,5X,A7)
      IF(DBW.LT.-65.) DBW=-65.
C        CALL PLOTTING SUBROUTINE.
      CALL PLOTXY(F,DBW,1,0)
C        STORE THE ENERGY VALUE FOR FREQUENCIES
C        BELOW EXCESS NYQUIST.
      IF(F.LE.FEX)WB=WT
      IF(F.GT.FEX) EX=EX+1.
      IF(F.GT.FEX) WM=WM+W
      W1=W
   20 CONTINUE
      PRINT 600,WB,WT
  600 FORMAT(1H0,10X,E14.8,5X,E14.8)
C        CLOSE PLOTTING SUBROUTINE
      CALL PLOTXY(0.,0.,0,0)
      CALL ENDPLT(XCR,YCR)
C        CALCULATE THE ENERGY RATIO IN DB
      DEW=10.*ALOG10(1.-WB/WT)
      DBM=10.*ALOG10(WM/EX/WO)
      PRINT 550,DEW,FEX,F,DBM
  550 FORMAT(1H0,10X,*ENERGY RATIO =*,F6.2,* DB*,
     *5X,F5.2,*  NYQUIST FREQ. FN*,/,
     *11X,*INTEGRAL COMPUTED UP TO*,F6.2,*  FN*/
     *5X,*AVERAGE STOPBAND ATTENUATION*,F6.2,* DB*)
      GOTO 1
 1000 CONTINUE
      STOP
      END
```

```
      FUNCTION SBTF(F)
C                     THIS FUNCTION COMPUTES THE FOURIER TRANSF.
C                     OF THE BTF IMPULSE RESPONSE
      COMMON XMU,NT,C(100)
      PI=3.141592653589
      XF=PI*F/XMU
      IF(F.EQ.0.0) AF=0.5/XMU
      IF(F.NE.0.0) AF=SIN(XF/2.)/PI/F
      NM=(NT+1)/2
      AN=C(NM)
      NM1=NM-1
      DO 10 J=1,NM1
   10 AN=AN+2.*C(NM+J)*COS(J*XF)
      SBTF=AN*AF
      RETURN
      END
```

```
      FUNCTION HLPF(F)
C                     THIS FUNCTION COMPUTES THE FREQ.
C                     RESPONSE H(JF)*H(-JF) OF A 2ND.
C                     ORDER LOW PASS FILTER
C                     REF- TOBEY, GRAEME, HUELSMAN
C                         OPERATIONAL AMPLIFIERS, 285,320-21
C                     H0=FILTER GAIN
C                     ALFA=1/Q
C                     GAMA= FILTER CUT OFF FREQ. / NYQUIST FREQ.
      H0=1.
      ALFA=SQRT(2.)
      GAMA=2.8
      FB=F/GAMA
      DLPF=FB**4+(ALFA**2-2.)*(FB**2)+1.
      HLPF=H0**2/DLPF
      RETURN
      END
```

APPENDIX B

Hybrid Binary Transversal Filter (BTF 2-8) Specifications

1.0 DESCRIPTION

The Binary Transversal Filter model BTF 2-8 is an optimum low pass filter especially designed for binary pulse shaping. It consists of a 32 weighting coefficients Transversal Filter followed by a second order Butterworth low pass filter.

2.0 INPUT SIGNAL

Pulse type:	Synchronous NRZ
Bit rate:	32 kbps
Pulse amplitude:	4.0 ±.5 Volts
Impedance:	75 Ohms

3.0 INPUT CLOCK

Pulse amplitude:	4.7 ±.2 Volts
Pulse width:	150 ±15 n sec
Repetition rate:	256 kHz
Impedance:	75 Ohms

4.0 OUTPUT CLOCK

Impulse amplitude:	2 V peak
Impulse width at .2 V:	70 n sec
at 1.8 V:	10 n sec
Repetition Rate:	Input clock/8
Impedance:	50 or 75 Ohms

5.0 OUTPUT SIGNAL

Signal amplitude (75 Ohms load):	140 m Volts p/p
	90 m Volts p/p at max: eye opening
Signal Level (75 Ohms Load):	-6.3 dBm
Impedance:	75 Ohms
Energy Ratio:	>30 dB for freq. above 22.5 kHz

6.0 POWER SUPPLY REQUIREMENTS

A:	+ 5 ±.1 Volts dc
B:	+15 ±.3 Volts dc
C:	-15 ±.3 Volts dc

REFERENCES

1. LEUTHOLD, P.E.
   A NEW CONCEPT FOR THE REALIZATION OF DATA MODEMS WITH INTEGRATED DIGITAL FILTERS AND MODULATORS.
   Phillips Res. Repts 27, pp. 223-243, 1972.

2. HUELSMAN, L.P.
   ACTIVE FILTERS: LUMPED, DISTRIBUTED, INTEGRATED, DIGITAL, AND PARAMETRIC.
   McGraw-Hill Book Co., 1970, USA.

3. SCOTT, R.E.
   LINEAR CIRCUITS.
   Addison - Wesley Publishing Co. Inc., 1960.

4. VOELCKER, H.B.
   GENERATION OF DIGITAL SIGNALING WAVEFORMS.
   IEEE Trans. on Comm. Tech., Vol. COM-16, No 1, pp. 81, 93.

5. CARREFOUR, A. Vincent, BOERI, F., DUBUS, F. & ESTEBAN, D.
   SYNTHESIS OF A TRANSVERSAL DIGITAL FILTER DEFINED IN THE COMPLEX PLANE.
   Ann. Telecommun. (France), 28(7-8), pp. 297-303, July - August 1973.

6. KALLMANN, H.E.
   TRANSVERSAL FILTERS.
   Proceeding of the I.R.E., pp. 302, 310, July 1940.

7. HUMPHERYS, De Verl S.
   THE ANALYSIS, DESIGN AND SYNTHESIS OF ELECTRICAL FILTERS.
   Prentice Hall Inc. - Englewood Cliffs, N.J., 1970.

8. MUELLER, K.H.
A NEW APPROACH TO OPTIMUM PULSE SHAPING IN SAMPLED SYSTEMS USING TIME-DOMAIN FILTERING.
Bell Syst. Tech. J., Vol. 52, No 5, pp. 723-729, May - June 1973.

9. RABINER, L.R. & RADER, C.M.
DIGITAL SIGNAL PROCESSING.
IEEE Press, New York, 1972.

10. HAFNER, E.R. & LEUTHOLD, P.E.
TRANSVERSAL FILTERS WITH CONTINUOUSLY TAPPED DELAY LINES (CTT FILTERS).
Proceeding IEEE, Vol. 57, No 12, pp. 2114-2122, December 1969.

11. BAUER, F.L.
ALGORITHM 60 ROMBERG INTEGRATION.
Comm. of the ACM, Vol. 4, issue 6 (1961), p. 255.

12. BENNET, W.R. & DAVEY, J.R.
DATA TRANSMISSION.
McGraw-Hill Book Co., 1965.

13. RICHARDS, P.J.
COMPUTING RELIABLE POWER SPECTRA.
IEEE Spectrum, Vol. 4, pp. 83-90, January 1967.

14. DUPRAZ, J.
LES LARGEURS SPECTRALES DES LIAISONS DE TELEMESURE PCM.
L'Onde Electrique, December 1967.

15. KOBAYASHI, H.

A SURVEY OF CODING SCHEMES FOR TRANSMISSION OR RECORDING OF DIGITAL DATA.

IEEE Trans. on Comm. Tech., Vol. COM-19, No 6, pp. 1087-1100, December 1971.

16. SOUCEK, Branko

MINICOMPUTERS IN DATA PROCESSING AND SIMULATION.

Wiley Interscience - A Division of John Wiley & Sons, Inc., 1972, N.Y.

17. FALL, G.A.

INTRODUCTION TO SCIENTIFIC COMPUTING.

Appleton - Century - Crofts -Mereoith Corporation - NY.

18. PUCKETTE, C.H., BUTLER, W.J. & SMITH, D.A.

BUCKET - BRIDAGE TRANSVERSAL FILTERS.

IEEE Trans. on Comm., Vol. COM-22, No 7, July 1974.

19. DANIELS, R.W.

APPROXIMATION METHODS FOR ELECTRONIC FILTER DESIGN.

McGraw-Hill Book Co. - N.Y., 1974.

20. MENDENHALL, W. & SCHEAFFER, R.L.

MATHEMATICAL STATISTICS WITH APPLICATIONS.

Duxbury Press - Mass., 1973.

21. WERTH, A.M.

SPADE: A PCM FDMA DEMAND ASSIGNMENT SYSTEM FOR SATELLITE COMMUNICATION.

ICC 1970 (IEEE, International Conference on Communications) San Francisco.

22. PUENTE, J.G. & WERTH, A.M.
DEMAND ASSIGNED SERVICE FOR THE INTELSAT GLOBAL NETWORK.
IEEE Spectrum - Vol. 8, No 1, pp. 59-69, Jan. 1971.

23. "SPADE SYSTEM SPECIFICATION"
ICSC Document 39-30E.
Interim Communications Satellite Committee, June 5, 1969.

24. SPAULDING, D.A.
SYNTHESIS OF PULSE - SHAPING NETWORKS IN THE TIME DOMAIN.
Bell Syst. Tech. J., Vol. 48, pp. 2425-2444, Sept. 1969.

25. LUCKY, SALTZ & WELDON
PRINCIPLE OF DATA COMMUNICATIONS.
McGraw-Hill Book Co. - 1968.

26. HILL, F.S. Jr. & LEE W.V.
PAM PULSE GENERATION USING BINARY TRANSVERSAL FILTERS
IEEE Trans. on Comm. Tech., Vol. COM-22, No 7, July 1974
pp. 904, 913.

27. GRAEME, J.G., TOBEY, G.E. & HUELSMANN, L.P.
OPERATIONAL AMPLIFIERS DESIGN AND APPLICATIONS.
McGraw-Hill Book Co., N.Y., 1971.

28. McCLURE, R.B.
STATUS AND PROGRESS OF THE INTELSAT SCPC SYSTEM.
ICC-75, IEEE International Conference on Communications,
San Francisco.

29. ASAHARA, M., TOYONAGA, N, SASAKI, S. & MIYO, T.
A 4 PHASE PSK MODEM FOR AN SCPC SATELLITE COMMUNICATION SYSTEM.
International Conference on Communications, ICC-75, San Francisco, Vol. 1, June 16-18, 1975.

30. FEHER, K.
COURSE EE621 CLASS NOTES
PRINCIPLE OF DIGITAL COMMUNICATIONS.
Concordia University - E. Eng. Dept. - Montreal 1975.

31. TAUB, H. & SHILLING, D.L.
PRINCIPLE OF COMMUNICATION SYSTEMS.
McGraw - Hill Book Co., NY, 1971

32. FEHER, K & DE CRISTOFARO, R.
TRANSVERSAL FILTER DESIGN AND APPLICATION IN SATELLITE COMMUNICATIONS.
Proc. of 1975 Midwest Symposium on Circuits & Systems, Montreal 1975.

33. FEHER, K & DE CRISTOFARO, R.
TRANSVERSAL FILTER DESIGN AND APPLICATION IN SATELLITE COMMUNICATIONS.
IEEE Transactions on Communications, Accepted for publication in 1976.

34. DATA TRANSMISSION
2nd supplement to part 1 of LIST OF DEFINITIONS OF ESSENTIAL TELECOMMUNICATION TERMS.
ITU - Geneva, 1961